Development of novel delivery technologies for vaccination through oral administration of farmed salmon

A thesis submitted to

University College London

For the degree of

Doctor of Philosophy

By

Zainab Ali

Department of Mechanical Engineering

University College London

April, 2018

Declaration

‘I, ZAINAB ALI confirm that the work presented in this thesis is my own.

Where information has been derived from other sources, I confirm that this has been indicated in the thesis.'

Abstract

In current times, the aquaculture industry has been faced with the dramatic on-set of various viral diseases specifically infectious pancreatic necrosis virus (IPNV) in Atlantic salmon *(Salmo salar)*. In order for the industry to persevere through and successfully meet a consistently growing demand, substantial measures need to be taken. The process of vaccination is known to reduce incidence of disease in addition to reducing intensity of infection as well. Even though vaccination has gradually become an essential part of disease control, there are still some challenges that need to be faced head on. Maintenance of antigen viability, incorporation of antigen in an appropriate delivery system and process of antigen delivery require further understanding as limited research has been reported on the development of oral delivery systems as far as vaccination in aquaculture is concerned.

This thesis explored three fundamental elements of oral drug delivery development; optimisation of microbead fabrication techniques, characterisation of microbeads through their unique mechanical and dissolution properties and finally the analysis of immune response following consumption of orally delivered antigen.

The first objective of this thesis was to demonstrate the potential of electrospraying (ES) and aerodynamically assisted jetting (AAJ) as fabrication methodologies for advanced orally deliverable systems. Micron-ranged delivery systems have previously been utilized for the long-term delivery of active biological compounds. However conventional methodologies pose significant challenges, particularly poor sample repeatability, lack of homogeneity and poor control, among other drawbacks. This thesis reports ES and AAJ as possessing the ability to produce highly monodisperse,

porous and reproducible polymeric microbeads at low cost. Operational maps obtained through an extensive sizing study established that ES possessed the ability to produce microbeads ranging from 250 – 2500 µm while AAJ produced beads ranging from 25 – 60 µm. The sizes of microbeads were seen to be primarily controlled through the fine tuning of process and solution parameters.

Since these polymeric microbeads offer protection of the active pharmaceutical ingredients (API), their own stability is crucial in order to achieve optimal performance. Effects of polymer concentration, type of cross-linking agent and fabrication methodologies on the mechanical stability of microbeads were studied. Polymeric microbeads also offer the imperative feature of safeguarding an API through proteolytic enzymes and harsh pH encountered in the digestive tract of fish. This prospect was studied by looking into the release characteristics of microbeads, using a model API and fabricated microbeads using various types of alginate. Microbead release kinetics were addressed through a custom tailored in vitro dissolution test representative of the environmental conditions faced by A. salmon.

To achieve the final objective of this thesis, A. salmon was exposed to a dose of viral antigen by using orally administered microbeads with encapsulated antigen. ELISA analysis indicated that at least some exposed fish had higher level of IgM antibodies targeting the specific IPNV antigen used for immunization. These results were also complemented by qPCR profiling in the head kidney, also including those encoding important immune transcription factors. Both treatments, with and without viral antigen showed an effect on a number of genes in head kidney. The most distinct expression profiles in the group of fish exposed to the viral antigen were seen at day 21 post exposure while at day 57 gene expression in both groups looked more similar.

STAT6, IL17A, Tbet and TCRy were found to be regulated at time points selected in this study.

The work presented in this thesis involves several stages in the process of development and optimization of the oral vaccine delivery system for an IPNV antigen in A. salmon. The system allows easy incorporation in fish feeds, however, it is not clear if the observed activation of the immune response will end up being protective against the disease. The hope is that the activation of the immune response by the studied antigen delivery system can be further optimized and tested in a challenge trial with live IPNV.

Impact Statement

Presently, aquaculture contributes towards 50% of the global seafood supply. Current reports suggest a substantially consistent increase in aquaculture demand. In order to meet this proposed demand, aquaculture production will have to almost double in the next ten years. The critical impediment standing in the way of achieving this goal is the startling ten-fold increase in the onset of viral diseases in fish farming operations. Disease prevention in aquaculture is usually handled through vaccination. Although vaccination through injection is highly effective, it is an arduous task especially during some of the later lifecycle stages, also being both time consuming and labour intensive. Oral delivery systems for vaccination have not been thoroughly explored yet as far as aquaculture is concerned.

This research puts forward two novel fabrication methodologies for the generation of oral drug delivery mechanisms; Electrospraying and Aerodynamically assisted jetting. The fabricated delivery mechanisms take the form of polymeric beads. The polymer acts as a superficial layer that surrounds a vaccine candidate protecting it from degradation. These methodologies have been rendered successful in producing perfectly spherical and monodispersed beads, capable of offering protection to sensitive biological compounds while the choice of polymer used can also offer biodegradability hence reducing any possible side-effects following consumption. Their micro/nano size range allows for them to be vacuum packed into fish feed pellets, so while farmed fish is being routinely fed it can also be vaccinated simultaneously.

These systems in combination with appropriate vaccine candidates present an immensely exciting prospect as far as curbing the rate of viral diseases is concerned. A decrease in disease onset is exceptionally advantageous for the aquaculture industry as it not only contributes to the improvement of the industry's economic sustainability but also enhances end product quality. Furthermore, these novel fabrication techniques possess the ability to generate delivery systems that can be of use across a wide range of disciplines such as materials science, the food industry, regenerative medicine as well as tissue engineering.

Acknowledgement

First and foremost, I would like to express my gratitude to my supervisor Professor Suwan Jayasinghe for providing me with this invaluable opportunity. He not only provided constant motivation but also helped me view the world of research with a much more holistic perspective. His continuous push for independence helped me find my own feet and stay positive in the face of adversity. I can proudly say that I will carry these life lessons with me from here on forward, and for that I thank him from the bottom of my heart.

Dr. Simon Wadsworth and Dr. Jose Troncoso helped direct this thesis in the right direction for which I am grateful. I would also specially like to thank Dr. Goran Klaric for being so reliable and providing consistent support. His ability to generate creative yet appropriate ideas has been inspirational. I would also like to extend my deepest gratitude towards Dr. Stanko Skugor for his contribution towards the ELISA and qPCR work and for his mentoring during interpretation of biological data. Your guidance has been extremely valuable and conducive to this thesis. My friends here at UCL, Muftau and Carolina, your support ensured my sanity remained intact in times of distress, and for that I am grateful.

Finally, I cannot thank my parents, Ahmad and Nabahat, enough for instilling the significance of acquiring knowledge in me, since childhood. They have been my pillars of strength and I thank you both for setting such an exceptional example. I look up to you. I would like to thank my brother, Pasha, for being an endless source of entertainment and also for his pick and drop services. You bring immense joy to my life. My husband, Naveel, for his unwavering support and motivational pep talks. I could not have done this without you.

My attendance here at UCL for this PhD programme would not have been possible if it wasn’t for the financial support of Cargill (EWOS Innovation, AS).

In memory of my Faru

forever in my heart

Contents

List of Figures

List of Tables

Nomenclature

C	concentration
C_t	cycle threshold
d	distance between electrodes
dph	days post hatch
dpi	days post inoculation
E	electric field
M_w	molecular weight
n	dynamic viscosity
n_r	relative viscosity
n_0	dynamic viscosity of the pure solvent
n_{intr}	intrinsic viscosity
R^2	coefficient of determination
V	voltage

Abbreviations

AAJ	Aerodynamically assisted jetting
AAPS	American association of pharmaceutical sciences
APC	Antigen presenting cell
API	Active pharmaceutical ingredient
BD	Blue Dextran
CMS	Cardiomyopathy syndrome
EE	Encapsulation efficiency
ES	Electrospraying
ELISA	Enzyme linked immunosorbent assay
FAO	Food and agriculture organisation (United Nations)
FDA	Food and drug administration
FIP	International Pharmaceutical Federation
GOAL	Global Aquaculture Alliance
HEMA	Hydroxyethyl methacrylate
HSMI	Heart and skeletal muscle inflammation
ILT	Inter-branchial lymphoid tissue
IPNV	Infectious pancreatic necrosis virus
ISA	Infectious salmon anaemia
ISAV	Infectious salmon anaemia virus
OD	Optical density
ODT	Orally disintegrating tablets

ORF	Open reading frame
PD	Pancreatic disease
PEG	Polyethylene glycol
PLA	Polylactide
PLGA	Poly(lactic-co-glycolic acid)
rpm	Revolutions per minute
SODF	Solid oral dosage form
SRS	Salmon rickettsial syndrome
UPS	United States Pharmacopeia
VP	Viral Protein

1. Introduction

1.1 Background and motivation

Being one of the fastest growing food production industries in the world, aquaculture plays a vital role in many countries by contributing to an increased income, improved nutrition and employment opportunities (Kannadhason et al., 2011). Aquaculture now provides approximately 50% of the global seafood supply. A recent newsletter published in 2015 by FAO (Food and agriculture association of the United Nations) suggests that aquaculture production should double by 2030 to meet the world's growing demands. Along with this development, however, there has also been a dramatic ten-fold increase in the incidence of viral diseases affecting in particular salmon farming operations (Norwegian Veterinary Institute., 2012). Diseases such as Infectious Pancreatic Necrosis (IPN) (Chen et al., 2014), Pancreas disease (PD) (Aunsmo et al., 2010) and Salmon Rickettsial Septicemia (SRS) (Cusack et al., 2002) are the most contagious diseases affecting salmon hence costing the fish farming industry millions annually. These diseases have a vast range of significant impacts namely; increased mortality, reduced final weight, increased transmission in wild stocks and finally, lower product quality.

Since disinfection is difficult to accomplish and pathogenic microorganisms can be transmitted through water more easily due to the increased number and density of fish in culture, disease prevention can become an issue when it comes to fish culture. Disease prevention established through stimulation of the immune system i.e. vaccination has now become a significant part of the development of the aquaculture

industry (Gudding and Muiswinkel, 2013). Currently, the most common preventative method in use for vaccination is through injection. Although, it is both time consuming and labour intensive, vaccination by injection remains highly effective. However, the efficacy of these vaccines tends to decline after a year in sea water. This is only made worse by the fact that re-vaccinating fish by injection is not an easy task (Ruma, 2006).

When salmon is in freshwater, its handling is easier, therefore, vaccination through injection takes place during this phase. However, when salmon is moved to seawater it becomes almost impossible to inject due to the great increase in salmon size as well as density present in each sea cage. A viable option for immunisation then is to incorporate a viral antigen into industrially available fish feed, so that A. salmon population develops protective immunity against IPN through diet.

1.2 Thesis objective

Over the years, research has delved into the development of oral vaccination in aquaculture but some hindering factors still remain, namely, encapsulation and protection of vaccine in the feed itself. Ultrasonic agitation and high speed mixing are perhaps the most common encapsulation methods being used currently. Even though these methodologies are able to produce a high yield of samples, these samples lack monodispersity. This stops the salmon population from receiving an equally distributed dose of vaccine.

As a response to the industrial need for novel encapsulation techniques that offer protection to sensitive biological compounds, this research aims to look into the encapsulation of specific vaccine candidates into an FDA (Food and Drug Administration) approved polymer through Electrospraying (ES) and Aerodynamically assisted jetting (AAJ), to be orally delivered via fish feed. This will allow the feed itself to be consumed, leaving behind the polymer to degrade inside the salmon's digestive tract without causing side-effects, while the vaccine itself passes intact into the blood stream, and further to immune organs where it initiates the development of adaptive immune responses.

Since the size and dissolution rates of particles play a paramount role in tuning adaptive immunity (Rice-Ficht et al., 2010), the short term objective is to assess and optimise the encapsulation methodologies; ES and AAJ for their ability to generate oral drug delivery systems capable of being incorporated within fish feed pellets. This means that when delivering a vast range of vaccine antigen candidates, encapsulated vaccine needs to have the ability to withstand acidic and proteolytic degradation along with shear mechanical forces. This will be achieved by determining their optimal size

distribution, morphology, dissolution characteristics and mechanical stability. The long term objective of this research project is the assessment of encapsulation efficiency of these drug delivery systems and antigen uptake.

1.3 Summary of contribution

The recognition of electrospraying and aerodynamically assisted jetting as novel fabrication methodologies for the production of alginate beads that can act as successful oral drug delivery mechanisms in aquaculture, puts forward a highly attractive prospect. These orally deliverable systems combined with specific vaccine candidates will not only help curb the rate of viral diseases affecting aquaculture but also improve the economic sustainability of the salmon farming industry by helping reduce mortality rates while also increasing product quality. Subsequently, these drug delivery systems can also be of use across various disciplines such as regenerative medicine and materials science.

1.4 Thesis Outline

This thesis is composed of 7 chapters, where the first chapter highlights the current obstacles faced by the aquaculture industry – the need for vaccination through oral delivery, specifically in Atlantic Salmon.

Chapter 2 consists of the literature review. It focuses on the significance of vaccination in aquaculture, the use of polymeric microbeads as drug delivery systems and drug encapsulation methodologies with an emphasis on electrospraying and aerodynamically assisted jetting.

Chapter 3 proceeds with a description of the materials that were used during the experimental procedures of this work. The production and optimization techniques, dissolution and mechanical testing protocols along with the IPNV trial specifications are detailed here.

The next three chapters contain the fundamental findings of this thesis. Chapter 4 looks into the fabrication, optimisation and characterisation of microbeads produced through electrospraying and aerodynamically assisted jetting. Factors such as the effect of governing process parameters as well as polymer characteristics were investigated. Furthermore, operational maps of microbead sizes were also produced and the mechanical properties of these microbeads were studied.

Chapter 5 investigates dissolution characteristics, employing both visual observation techniques as well as in vitro tests. Through microscopic observation, the effect of polymer concentration, cross-linking agent as well as fabrication methodologies was reported. Following which the encapsulation efficiencies and release profiles of microbeads - fabricated using five leading alginate types in industry currently - were

assessed. To further our understanding of these characteristics, their viscosities and molecular weights were also determined.

Chapter 6 delved into the biological effects of the encapsulated IPNV antigen into microbeads produced using aerodynamically assisted jetting; qPCR profiling of immune genes' expression was assessed at three time points, and was complemented with ELISA measurement in plasma of antibodies generated specifically against the used IPNV antigen. Measurement of biological responses at the molecular level can point out which specific treatments favour the most prominent immune response in the host, thus providing the basis for further refinement of the encapsulation technique.

Chapter 7 offers an overview and summary of the primary objectives established through the duration of this research, along with suggestions for further work.

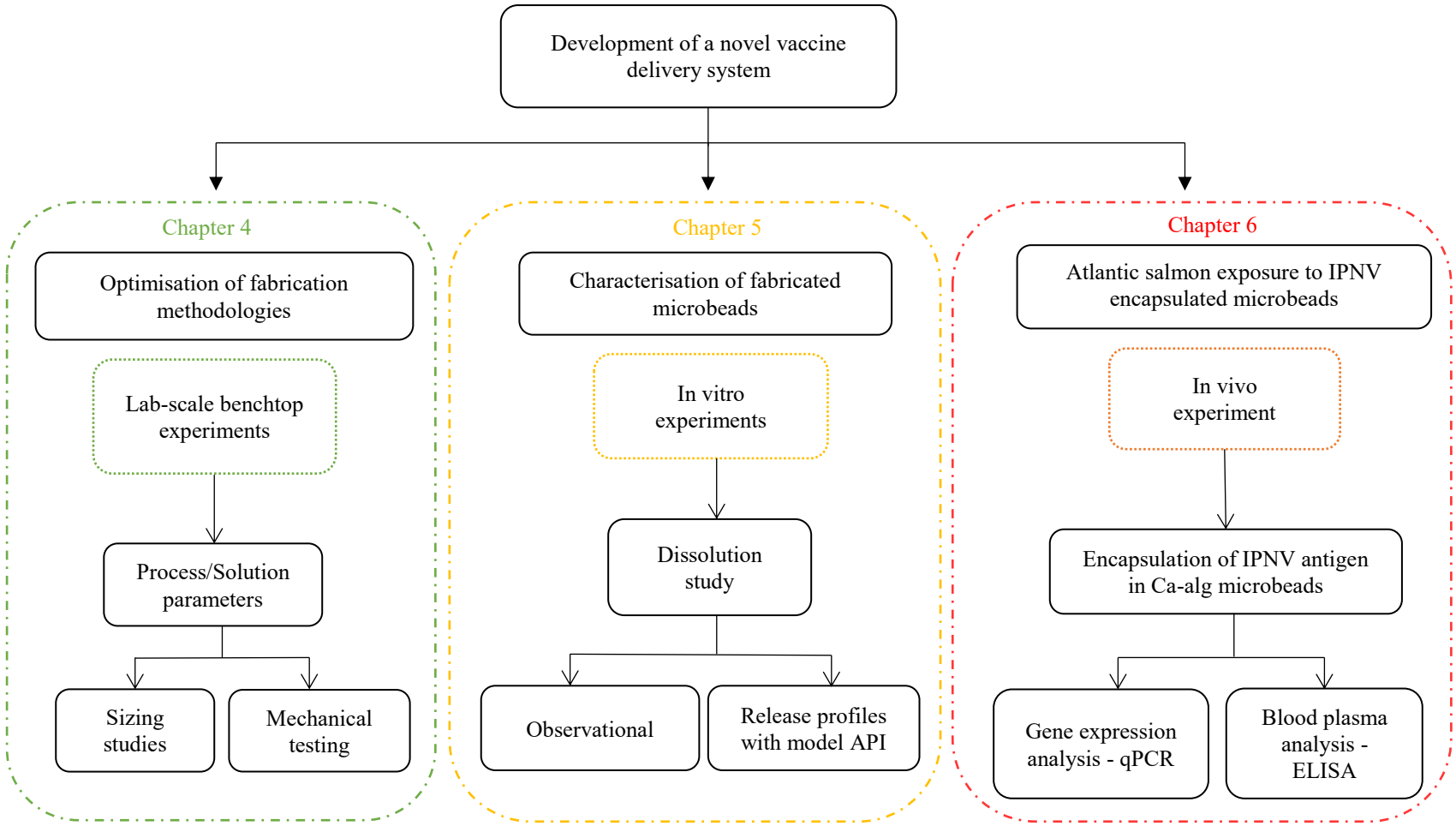

Figure 1-1: Overview of the primary objectives established through the duration of this work, in sequential order

2. Literature review

Overview

In order to preserve sustainable aquaculture, disease prevention and control are critical. Even though fish are the most primitive organisms to possess an adaptive immune system, it remains undifferentiated and less complex as compared to mammals. A fundamental difference between immune system of fish and that of higher vertebrates is that fish are poikilothermic, which means they adapt their body temperature to that of their surroundings. This is why their immune response is directly dependent upon the temperature of their aquatic environment. Hence, when an infectious agent is introduced, the response of the immune system will depend on whether it has experienced that specific infectious agent previously or not. Depending on the type of infectious agent, aspects of both innate and adaptive immunity will play their role in countering it (Ruma Guidelines 2006).

Vaccination is a method used for prevention of infectious diseases by increasing specific immunity (Ruma Guidelines 2006). Vaccines help produce immunity in the body, which provides protection against infection. It does so by introducing an antigen e.g. chemicals, viruses or bacteria to the body which then alerts the immune system to produce antibodies that have the ability to fight off that specific antigen. Antibody producing cells known as B lymphocytes will remain sensitised and ready to counter attack should the same agent enter the body again. However, before vaccines can be

successfully commercialised factors such as the production of effective and cheap antigens as well as adjuvants need to be taken care of, too.

In 1942, Duff published the first report highlighting disease prevention through the use of vaccines by presenting results showing protection against Aeromonas salmonicida in trout through immunisation (Duff 1942). However, it was only until the seventies that vaccines became commercially available to use in the aquaculture industry. The first vaccine licensed in aquaculture was to prevent 'yersiniosis' in salmonid fish in 1976, USA (Gudding and Van Muiswinkel 2013). In the eighties, a disease first known as 'Hitra disease' (Egidius, Wiik et al. 1986) had a serious effect on salmonid aquaculture in Norway. Since then most of Atlantic salmon as well as rainbow trout have been successfully vaccinated in Norway, originally through immersion but currently via injection.

The three most viable routes for the application of vaccines in aquaculture are; injection, immersion and oral. Application via the injection route is tedious and time consuming. Injecting vaccines may also induce stress-related effects such as immunosuppression, injection/handling related mortalities and reduction in feed uptake. Injection may also not be a practical choice for fish that are transported to open-sea cages for final grow-out, as they may require additional injections or booster vaccinations to sustain the heightened protective status all through the farming period. This can result in a significant loss of fish due to infection just before marketing, which can prove disastrous for fish farmers who have devoted significant time as well as resources (Caruffo, Maturana et al. 2016). However, the injection method remains highly suitable for fish of high unit value in order to counter the cost of this procedure.

The size of the fish also limits the use of this delivery method. For example, due to the small size of ‘fry’, its safe handling becomes an issue (Ruma Guidelines 2006). On the other hand, the volume of vaccine needed for injection is relatively lower and each fish is vaccinated with the accurate dose required. Professional vaccination teams or machines are normally used in industrial salmonid farming (Sommerset, Krossoy et al. 2005). However, most importantly antigen protection is commonly highest with injection-vaccination (Embregts and Forlenza 2016) .

Immersion vaccination is a safe and easy method which is less stress inducing as compared to injection. The process starts with dipping fish in a hyperosmotic salt solution for a short time (in order to enhance the uptake of antigen) followed by immersion in antigen solution (Nakanishi and Ototake 1997). The main advantage of the immersion technique is that a large number of fish can be vaccinated at the same time. However, this method is limited to only small fish and is impractical for larger sized fish in tanks or sea cages. This technique is also labour intensive along with being costly as both tanks and specialised equipment is required.

Due to the disadvantages associated with the immersion and injection techniques, a more practical approach was developed. Oral vaccination represents a massive advantage in aquaculture health management as it can be used for virtually any fish size. Not only is oral vaccination inexpensive and simple, it is also stress free. But in order to be deemed successful, oral vaccine delivery technology needs to address challenges such as shelf storage stability and prevention of leaching from feed upon contact with water (Caruffo, Maturana et al. 2016).

Other factors such as the adhering and persisting on the gut mucosal tissues, overcoming degradation in low and harsh pH digestive environment as well as

adequately eliciting innate and systemic immune responses also prove challenging for this method. However, these issues can be taken care of through the adoption of a viable vaccine encapsulation approach. Once the vaccine is encapsulated, the capsule itself tends to degrade in the lower gut, which in turn maximises the amount of antigen which reaches the intestine where it is eventually absorbed into the blood stream (Dunn 1989). It should be noted however that this method of delivery would also only be feasible for fish that are fed an artificial diet.

Over the years, several approaches to protect the antigen have been employed, such as entrapping in alginate beads (Maurice, Nussinovitch et al. 2004) or liposomes (Irie, Watarai et al. 2005), and neutralisation of gastric secretions or application of biofilm vaccines (Azad, Shankar et al. 2000). Currently, more than 40 million fish are orally vaccinated against ISA (Infectious salmon anemia) and SRS (Salmon rickettsial syndrome) annually, in Chile alone and due to the success of oral vaccination demand for more programmes is growing (Caruffo, Maturana et al. 2016).

2.1 Polymeric particles as drug delivery mechanisms

Drug delivery is a process where a pharmaceutical compound/drug is administered in order to achieve a therapeutic effect in humans or animals (Ward and Georgiou 2011). Though, achieving successful controlled drug delivery is not an easily accomplishable task. Environmental or enzymatic degradation, failure to cross the biological barrier and non-specific toxicity are just some of the crucial obstacles standing in the way of drug delivery success.

In the paradigm of tissue engineering, polymers have extensively been used as biomaterials for the development of scaffolds within which biological compounds can be incorporated (Dhandayuthapani, Yoshida et al. 2011) and used as delivery mechanisms. The polymer helps give the scaffold an appropriate three-dimensional structure so as to provide ample mechanical stability during the process of drug delivery (Morch, Donati et al. 2006). Polymeric scaffolds have gained intensive attention due to the rare properties they possess; biodegradation, mechanical strength, high surface to volume ratio and high porosity with small pore size. Furthermore, naturally occurring polymers such as polysaccharides (collagen, gelatin, actin, alginate), proteins (cellulose, dextran, chitin) or polynucleotides (DNA, RNA) (Yannas 2004) tend to have even better interactions with cells as they enhance cell performance, as compared to synthetic polymers (Dhandayuthapani, Yoshida et al. 2011).

The most significant qualities hydrogels possess are low levels of toxicity and biocompatibility (Bhattarai, Gunn et al. 2010). The three-dimensional structure of

tissues and other macromolecular based components in the body can also be mirrored in the gel (Elisseeff 2008). Hydrogels are formed when the polymer chains are cross-linked (either through covalent or non-covalent bonds), this means that hydrogels can simply be divided into two types; physical and chemical. Physical hydrogels are held together either by hydrophobic interactions, chain entanglements or electrostatic forces whereas chemical hydrogels will be connected through more permanent covalent bonds. Such a type of bond is characterised by shared pairs of electrons between atoms (Paleos 2012). Even though hydrogels have a high water content and water absorbing affinity, they demonstrate swelling instead of dissolving once present in an aqueous environment. This is attributed to the critical crosslinks present in the structure of the hydrogel (Hamidi, Azadi et al. 2008).

Considerable interest in hydrogels began after pioneering work was carried out on cross-linked HEMA (2-hydroxyethyl methacrylate) hydrogels in 1960 (Dreifus, Herben et al. 1960). Later, (Lim and Sun 1980) exhibited successful application of calcium alginate microcapsules for cell encapsulation. Since then, the use of polymeric hydrogel particles has gained rapid attention in the biomedical field particularly bio sensing, targeting and especially drug delivery. The interstitial spaces present in hydrogel structures provide a highly attractive prospect for the storage of a vast variety of biological compounds or drugs (Elisseeff 2008). Moreover, the high water content present in the hydrogel network provides a suitable environment for the diffusion of nutrients and oxygen as well as other empirical molecules that are critical for cell growth as well as proliferation (Canepa, Imperiale et al. 2017).

(Zhang, Ermann et al. 2015) studied an inflammation targeting hydrogel for local drug delivery in inflammatory bowel disease. It was reported that the inflammation targeting hydrogel preferentially adhered to mucosa from inflamed lesions as

compared to histologically normal sites. Hence, concluding that hydrogels act as a promising approach for targeted enema-based therapies specifically for patients with colonic inflammatory bowel disease.

PLGA (polylactic-co-glycolic acid) - PEG (polyethylene glycol) - PLGA copolymer hydrogels were assessed for sustained drug delivery in the ear (Feng, Ward et al. 2014). These copolymer hydrogels did not show any toxicity and also provided sustained release, which could also be controlled by using further additives for inner ear applications. Alginate hydrogels were investigated for the repair of the peripheral and central nerve systems. It was reported that alginate hydrogels introduced into the spinal cord parenchyma did not give rise to major inflammatory responses while also directing axonal regrowth (Prang, Muller et al. 2006).

2.1.1 Significance of particle size for delivery systems

Nanoparticles are solid particles ranging from 1 to 1000 nm in size while microparticles range from 1 to 1000 μm (Kreuter 1996) in size. Researchers are in agreement that where vaccine delivery is concerned, it is the size of the particles containing the antigen that is crucial to their adjuvant activities (Oyewumi, Kumar et al. 2010). However, conflicting data has been presented over time regarding the ideal size range of particle-based adjuvants depending on their resultant immune responses.

The success of carrier particles posing as drug delivery mechanisms by being taken up through target cells depends upon their size; particles ranging from 20 to 200 nm are taken up by endocytosis while those falling in the range of 500 nm to 5 microns are usually taken up through the process of phagocytosis (Coelho, Ferreira et al. 2010).

Since specific cells only have a certain size range for particles that they will tend to successfully take up the biggest advantage of polymeric particles is their ability to adapt in order to suit specific needs.

The popularity of particles being used as drug delivery mechanisms is simply due to two main advantages such carriers have to offer; adjustable drug release rates and drug protection (Nidhi, Rashid et al. 2016). Polymeric micro-particles act as reservoir systems since they are able to protect proteins from harsh environments thus boosting long term biological activity. They also allow for release rate control of the specific encapsulated drug anywhere from hours to months, while providing easy administration (Yang, Chung et al. 2000). These biodegradable particles are also of particular interest because of their high dissolution rates which in turn enhance drug bioavailability (Noyes and Whitney 1897, Horter and Dressman 2001). Therefore, possessing the ability to solubilise a concentrated drug while improving both drug stability and bioavailability. Coupled with the use of biodegradable and biocompatible polymers, they can help reduce the risk of toxicity and other such detrimental side effects.

Over the years, several studies have shown that not only the shape (Barua, Yoo et al. 2013), but also the size (Shang, Nienhaus et al. 2014) and surface functionalisation (Saha, Kim et al. 2013) of particles play critical roles where internalisation by cells is concerned. For example, Frohlich (2012) found out that nanoparticles with a cationic surface charge show higher cellular uptake and greater cytotoxicity in non-phagocytic cells whereas anionic nanoparticles showed more cytotoxicity towards phagocytic cells. This preference will indubitably affect the selectivity of these particles for drug delivery.

Even though smaller sized particles are more successful when it comes to permeating biological barriers, and hence are ideal as targeted delivery systems, but as far as vaccine delivery is concerned, microparticles are deemed more suitable. A primary reason being that the drug can be sustained for a longer time due to their decreased surface area therefore lowering the chance of abrupt drug release (Sinha, Bansal et al. 2004). However, when it comes to vaccine delivery there is no clear answer as to what is the ideal particle size range which produces the strongest and most long-standing immune response (Xiang, Scholzen et al. 2006). Another significant factor to note here is that their size might dictate the type of immune response induced. Research has shown that microparticles promote humoral immune responses while nanoparticles give rise to cellular immune responses instead (Caputo, Brocca-Cofano et al. 2008).

Yadav and Mote (2008) observed that Domperidone was released from starch microspheres in a sustained release manner. These microspheres were fabricated through emulsification and ranged from 22 – 103 microns in size and were used for the treatment of various kinds of emesis through intranasal administration. (Gawde and Agrawal 2012) prepared chitosan microspheres of Deflazacort for colon targeting, average bead size ranged from 1 – 1000 micron. (Savale 2016) presented the encapsulation of Aceclofenac (an anti-inflammatory drug used for the treatment of osteoarthiritis) in ethyl cellulose microbeads. Sustained release activity was noted.

Perhaps it can be said that employing a mixture of particles covering specific size ranges favouring either a strong humoral or cellular response can help produce the most desirable of an immune response that is well-balanced (Oyewumi, Kumar et al. 2010).

2.1.2 Vaccine entrapment/encapsulation in microbeads

Due to the use of micro and nano particles as successful vaccine delivery tools they have garnered rapid attention commercially. Vaccination acts as an effective measure to not only treat but also prevent diseases. This is achieved through the activation of innate defences and the consequent development of the adaptive immune responses in order to combat intruding pathogens (Oyewumi, Kumar et al. 2010).

Ideally, the immune system should be presented with antigens at the precise location and the appropriate time. However, some antigens tend to exhibit weak immunogenicity. The inclusion of an immune adjuvant helps overcome this by enhancing the immune response (Scheerlinck and Greenwood 2008). An immunologic adjuvant is a substance that acts to accelerate, prolong and intensify antigen-specific immune responses (Lowrie and Whalen 2000).

The entrapment/encapsulation of an antigen inside the polymer works like so: once the mixture is subjected to a cross-linking agent, a gel-like polymeric matrix is produced. Following this, the antigen becomes entrapped inside the matrix. This gives rise to a particle that contains an antigen, which is now safely protected by an outer layer of cross-linked polymer matrix as seen in figure 2 - 1. The antigen itself covalently bonds to the polymer carrier. It is this covalent bonding that helps prevent rapid release of the entrapped antigen. Therefore, once the crosslinking takes place, the particle with antigen/adjuvant acts as one single macromolecule that allows for ease of purification. Increased levels of purity are essential to analyse the prime mechanism of action with regards to immunogenic activation (Rijcken and Holthuis., 2016).

Previous research states that uptake of an antigen by antigen presenting cells (APCs) is preferred in particulate form rather than its soluble state. The particulate nature of the antigen delivery system can greatly affect activation of the immune response. Once the response has been induced, the specific type of immune response will then be dependent upon the chemical composition of the vaccine consumed (Storni, Kundig et al. 2005)

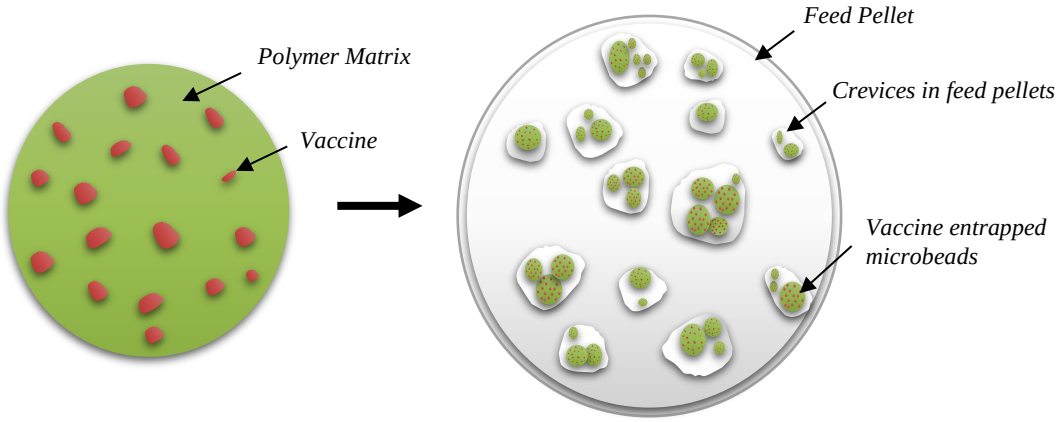

Figure 2-1: *Shows vaccine entrapped in a polymeric microbead and the same mirobead later being vaccum packed into the crevices present in feed pellets*

Not only do particles enhance immune response through stimulating antigen uptake, an antigen-loaded degradable particle will also act as a storage reservoir for the antigen. It will slowly help release the antigen in order to prolong antigen availability (Rice-Ficht, Arenas-Gamboa et al. 2010). Particulate vaccines also have the ability to cross-present antigens which is critical because cross-presentation contributes to the activation of CD8 T-cell responses against viral infections (Jain, Yap et al. 2005). Furthermore, cross-presentation is also required for the induction of cytotoxic immunity.

2.1.3 Role of oral vaccines in aquaculture

As previously mentioned, vaccination regimes are developed for various species consisting of a combination of injection, immersion and oral, in order to ensure protection throughout the entire production cycle (Embregts and Forlenza 2016).

Olesen and Jorgensen 1986 reported that antibody responses in salmonids are not always correlated with protection. Subsequently, Bootland, Dobos, and Stevenson 1990 reported that inactivated vaccines were in fact capable of reducing mortality but substantial evidence was still not put forward that suggested infection prevention. Much improvement has occurred in more recent times. De las Heras, Saint-Jean, and Perez-Prieto (2010) vaccinated rainbow trout and brown trout orally with microparticles containing DNA of VP2 protein of the infectious pancreatic necrosis virus (IPNV). The vaccine was reported to have induced innate immune responses by raising IFN expression more than ten-fold relative to fish vaccinated using an empty plasmid. It was reported that protection against IPNV was high with a 15% mortality rate for brown trout and 15 – 20% for rainbow trout.

Mucosal membranes make up the core barrier between the internal tissues and invading pathogens. Since injury at these sites normally result in the onset of infection, induction of an immune response at mucosal sites becomes a logical strategy for allowing specific immunity against viral microorganisms (Tobar, Jerez et al. 2011). With respect to fish welfare, it is now certain that the mucosal route of vaccination particularly oral is an ideal mechanism for vaccine delivery (Embregts and Forlenza 2016).

There are several reasons why the gut is the most attractive route for antigen delivery in fish. Not only is it a simpler way of administering antigens, the level of stress decreases considerably, a vast range of fish with different size ranges can be vaccinated with no associated side effects (Mutoloki, Munang'andu et al. 2015). However there are still very few oral vaccines registered for the purpose of treatment in the aquaculture industry. Out of the seventeen commercial vaccines available in 2014, only 2 were oral preparations (Dhar, Manna et al. 2014).

Oral vaccines that are currently commercially available for salmonid species include those against Infectious pancreatic virus (IPN), *Piscirickettsia salmonis* (P. salmonis) and infectious salmon anaemia virus (ISAV), for rainbow trout against IPN, *Y. ruckeri, P. salmonis* and for rainbow trout and sea bass against *V. anguillarum* (Embregts and Forlenza 2016). Leading regions where oral vaccination for fish is routinely practised are Norway, Chile and Scotland (Brudeseth, Wiulsrod et al. 2013).

The oral route taken by the encapsulated polymer-vaccine matrix works like so; the polymer possesses the ability to protect the microbe/antigen or plasmid encoding antigen, while transporting it through the digestive tract. It then diffuses through the gut mucus layer and reaches the enterocyte surface. From there, the polymer (especially alginate) can be actively taken up by antigen-sampling cells and deliver the microbe/antigen or DNA plasmid. Enteric pathogens are likely to possess the innate ability to activate local mucosal responses whereas DNA plasmids encoding antigen of interest can enter the nucleus, triggering antigen expression in the host cell, comparable to what happens during a viral infection. The substantial success of DNA vaccines in fish can be attributed to the aforementioned latter mechanism (Lorenzen and LaPatra 2005).

The potential of nano and/or microparticles for oral antigen delivery has been explored in various species of fish, utilising a variety of polymers. Even though, oral delivery in fish is highly preferred, lack of efficacy has been its main limitation. However, there is research present, which presents positive levels of uptake in the end gut, an increased specific antibody production and enhanced protection through the use of carrier particles (Gudding and Van Muiswinkel 2013).

In the world of aquaculture supporting evidence has been acquired for the use of polymeric micro-particles as oral drug delivery systems. Joosten, Tiemersma et al. (1997) were one of the first to assess the ability of antigen encapsulated micro-particles as oral vaccination for fish against *Vibrio anguillarum*. Their results indicated that antigen encapsulated alginate microparticles evoked systemic memory and induced mucosal immune responses in fish.

Also, it was observed that vaccinated carriers of IPNV were less able to spread the disease as compared to unvaccinated carriers (de las Heras, Saint-Jean et al. 2010). In a catfish study, (Thinh, Kuo et al. 2009) concluded that repeated oral boosting offers an attractive method to maintain immunity. Other significant results for orally administered vaccines in various aquaculture species have been summarised in figure 2 - 2.

Author/Year	Vaccine/Antigen/Adjuvant	Encapsulation methodology	Size	Polymer	Application
(Joosten et al. 1997)	*Vibrio anguillarum* bacterin using Artemia nauplii as the antigen carrier	Bioencapsulation	1 – 20 μm	Alginate	Vaccination of juvenile carp and gilthead seabream
(Maurice at al 2004)	A-layer protein (At-R) and At-MTS as antigen	Mixing	Microspheres (unspecified)	Alginate	Immunisation of goldfish
(Ramos, Relucio, and Torres-Villanueva 2005)	B-galactosidase DNA-vaccine	Coacervation	Nanospheres (unspecified)	Chitosan	DNA immunisation for transient gene expression in tilapia
(Rajeshkumar et al. 2009)	DNA construct containing VP28 gene of WSSV	Mixing	Nanoparticles (unspecified)	Chitosan	Immunisation of *Penaeus monodon* (black tiger shrimp) against WSSV (white spot syndrome virus)
(de las Heras, Saint-Jean, and Perez-Prieto 2010)	IPNV DNA-vaccine	Emulsification	Microspheres (unspecified)	Alginate	Vaccination of brown trout and rainbow trout
(Ballesteros et al. 2012)	VP2 IPNV DNA-vaccination	Emulsification	Microspheres (unspecified)	Alginate	Vaccination of Oncorhynchus mykiss (rainbow trout)
(Chen et al. 2014)	Infectious pancreatic necrosis vaccine	Electrospraying	Microparticles (unspecified)	Alginate	Vaccination of Atlantic salmon

Figure 2-2: *Summary of previous research carried out where vaccines were orally administered in aquaculture*

2.1.4 Vaccine types in aquaculture

As previously mentioned, fish are known to be the most primitive vertebrates that possess a developed immune system along with an adaptive immune response. It is this adaptive immune response, which leads to the expansion of B-lymphocytes – a population of antibody producing cells. B-lymphocytes produce antibodies, which are specialised proteins that have the ability to specifically bind to sites available on the antigen. Since the immune response is a complicated process that not only stimulates immune functions, homeostasis maintains memory of the infection and is also responsible for restoring functions that were perhaps lost during infection. The thymus, spleen, blood tissue and anterior (head) kidney are the major lymphoid organs of the fish. The head-kidney in particular is exclusive to teleost fish, consisting of cytokine producing lymphoid and endocrine cells (Geven and Klaren 2017).

Currently, in the aquaculture industry the most common virus vaccines are either based on inactivated viruses, recombinant subunit proteins or live attenuated vaccines. As far as inactivated vaccines are concerned, inactivating agents are normally used to connect pathogen proteins that combine with cellular receptors and block nucleic acid replication. However, a disadvantage of this type of vaccine is that toxic reactions may be caused by immune enhancing adjuvants and also a decreased level of immunogenicity due to denaturation of proteins and systemic reactions (USDA 2014). It is also important to note that inactivated viral vaccines are not quite efficacious unless delivered through injection. Cost-effectiveness also becomes an issue for inactivated viral vaccines as relatively high doses are required to achieve protection (Sommerset, Krossoy et al. 2005).

On the other hand, live viral vaccines are prepared from one or more viruses. The pathogens are attenuated with heat, serial passage in cell culture, culture under abnormal conditions or even genetic manipulation (Desmettre and Martinod 1997). Live viral vaccines have produced positive results in terms of efficacy and protection (Ronen, Perelberg et al. 2003). They also offer the advantage of good antigen presentation as the organism is growing in the host and delivery can be offered through various routes. The major drawbacks of this type of vaccine however are the safety issues that come with its usage. Hazards include virulence in immune-compromised vaccinates, residual virulence or reversion to virulence (USDA 2014).

Where salmonid farming is concerned, commercial vaccines are available for the majority of common viral diseases. For example, IPNV caused by the birnavirus has both types of vaccines available (based on inactivated cell culture-propagated virus or recombinant structural proteins). Mainly, IPNV vaccines exist as polyvalent oil-adjuvanted vaccines however. The IPNV antigen is mixed with one or more bacterins which appears to enhance the efficacy as compared to monovalent IPNV vaccines (Sommerset, Krossoy et al. 2005).

It should be noted that mucosal tolerance is driven by high local levels of anti-inflammatory cytokine expression that help sustain the generation and maintenance of tolerogenic regulatory T cells and dendritic cells (Weiner, da Cunha et al. 2011). Hence, for the development of oral vaccination in veterinary species, potent mucosal adjuvants along with targeted delivery strategies are being used. (Neutra and Kozlowski 2006) found that the use of live attenuated vaccine administered along with strong adjuvants show immense capacity to facilitate the induction of mucosal responses. (Zhang, Sun et al. 2008) produced an attenuated vaccine against E.tarda – a marine and freshwater pathogen – and was shown to be efficacious as well as safe

in Japanese flounder through injection, immersion and also oral delivery. Marana et al (2017) set out to test the efficacy of experimental subunit vaccines against A. salmonicida infection in rainbow trout. A significant immune response was seen in fish that were immunised using the subunit vaccines.

2.2 Atlantic Salmon (Salmo salar L.)

Among all the commercially cultivated species, Atlantic salmon (Salmo salar) is the highest per fish and total value fish species that is cultivated at an industrial scale (Dhar, Manna, and Thomas Allnutt 2014). Commercial farming of Atlantic salmon began in Norway in the late 1960s. Production gradually spread over the next three decades towards north-western Europe as well as Chile, currently standing at over 2.3 million tonnes of production worldwide as highlighted in figure 2-3 (FAO 2012). Due to advancement in diets, feeding, management and also genetic selection, there has been a continuous increase in their growth rate (Webster and Lim., 2002). According to the Norwegian Seafood Council the export value of salmon stood at an all-time high of NOK65.5b in 2016, cementing its position as one of the most significant species in the fish farming industry (Lokka., 2013).

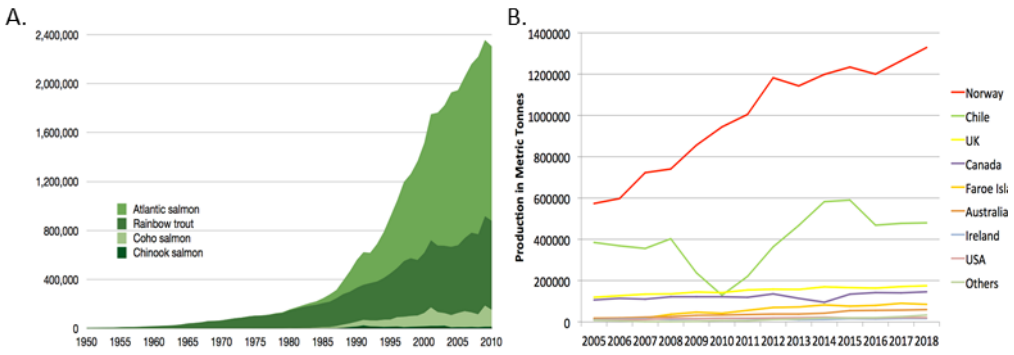

Figure 2-3: A. *Production of salmonids (in tonnes) as reported by the FAO for the time period spanning 1950 – 2010 (FAO., 2012),* B. *A.Salmon production by country highlighting Norway and Chile to be the lead suppliers worldwide 2005 – 2017 (GOAL., 2016) with production of almost 1.4 million and 0.6 million tonnes, respectively*

Salmon farming requires both freshwater as well as seawater operations. It starts by the roe/fish eggs being fertilised in fresh water, they hatch approximately after 60 days. Soon after hatching the salmon fry develops a sac on its stomach, which it uses to feed itself. 4 - 6 weeks after hatching the salmon fry becomes ready to eat feed and is transferred to freshwater tanks. After remaining in the freshwater tanks for 10 – 16 months, the salmon is moved to net pens in the sea to undergo smoltification which enables the salmon to live in saltwater. Smoltification is a series of physiological changes where juvenile salmonid fish adapt from living in fresh water to sea water.

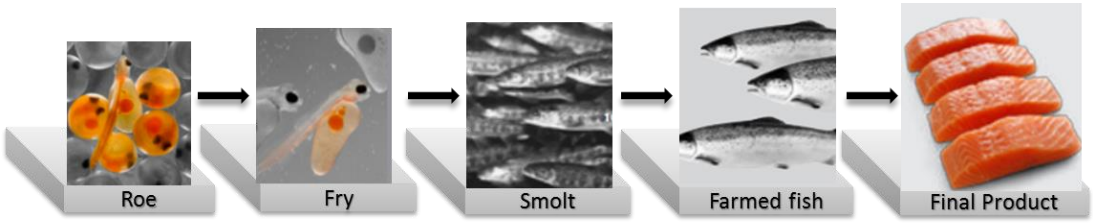

Figure 2-4: *Highlights the salmon farming process in its entirety - from roe to market. Images acquired and modified from Aquaculture in Norway, 2011*

Norwegian seawater temperatures can range from below 4℃ in winter to above 18℃ during the summer (Aldrin et al. 2013). After being in net pens for 14 – 22 months, the fish reaches a mature state where it weighs at an average of 4 – 6 kg and is ready to be processed (Norwegian Seafood Federation FHL and the Norwegian Seafood Council NSC., 2011).

2.2.1 Ontogeny

Till today there is only limited information present regarding Atlantic salmon gastrointestinal tract development. The functional development however of the digestive organs from hatch following the start of feeding has been known to follow the order; liver and pancreas followed by mouth and rectum then the oesophagus and intestine and finally the stomach and pyloric caeca (Sahlmann et al. 2015). Reports have suggested that digestive functions are detected as early as 7 dph (days post hatch). Moreover, Sahlmann's (2015) research also indicates that A.Salmon fry digestive functions are ready for the digestion of external feed much before the yolk sac is even internalised into the abdominal cavity. The newly hatched fry however has a yolk sac present in the stomach, which produces necessary nutrients until the digestive tract is fully functional, and equipped to take in exogenous food.

Atlantic salmon is indigenously carnivorous and is placed in the salmonid family in the teleost (ray-finned fish) division phylogenetically. It is to be noted that the teleost gastrointestinal system is different from that of mammals. The teleost tract displays a varying topography through the intestinal length, the number of pyloric caeca and the extent of looping (Kapoor, Smit, and Verighina 1975). Due to this, a general division of headgut, foregut, midgut and hindgut is used even if distinguishing between the precise borders of the regions is difficult (Harder 1975). The fore-gut consists of the mouth, oesophagus and stomach. The pyloric caeca and mid intestine are part of the mid-gut while the hind-gut consists of the distal intestine all the way to the rectum (Madsen et al. 2011).

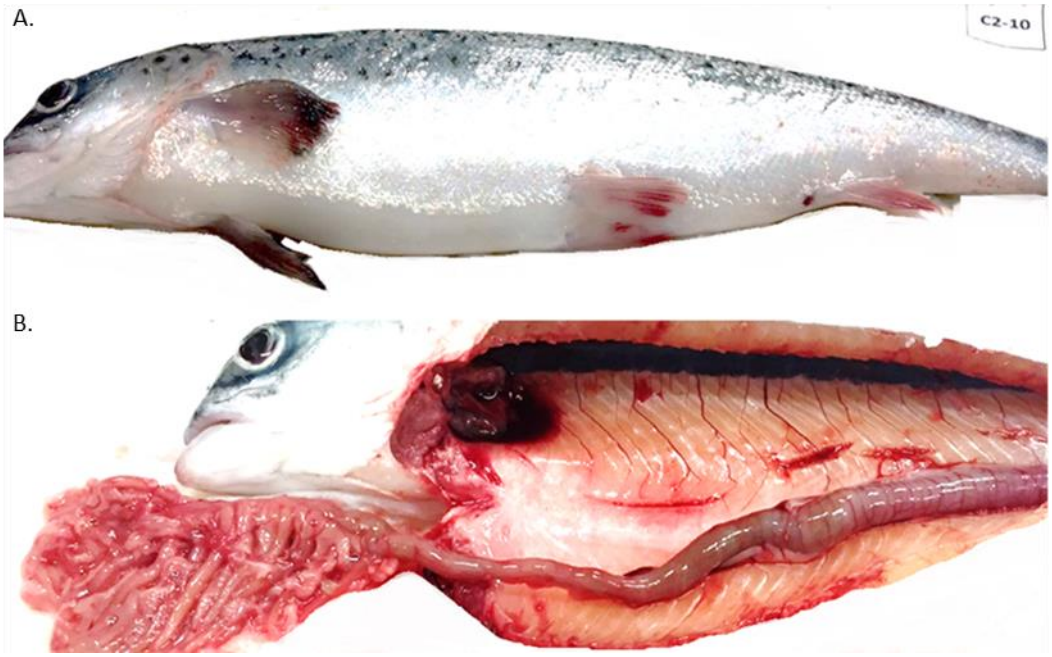

Figure 2-5: *Shows before and after images of a dissected A.Salmon. The second image shows the gastrointestinal tract displaced from the body cavity of a hemorratic salmon. This condition is attributed to the stress caused due to the living conditions present in a tank. As this fish is not completely healthy, this image shows a larger than normal intestine, more mucus, increased number of red lines on both the intestine and the fins and also more defined capillaries with filaments as compared to a healthy sample. This dissected sample has an overall larger capillary network due to swelling and haemorrhage. Dissection of sample shown took place at EWOS, Chile*

According to histological studies, mucus cells are present throughout the full length of the stomach (Sahlmann et al. 2015). Food is transported from the stomach – where digestion begins - into the midgut through the pylorus. The effectiveness of digestive enzymes present in the stomach is mainly controlled by two main factors; pH and temperature. A.Salmon has an adequate complement of digestive enzymes – proteases, lipases and glucosidases out of which pepsinogen and trypsinogen are key. These enzymes are secreted in the pyloric caeca and small intestine, both areas where nutrient absorption takes place. Since the pancreas is a diffuse organ in Atlantic salmon, it is

responsible for the synthesis of precursors of the main digestive enzymes necessary for luminal digestion (FAO 2017).

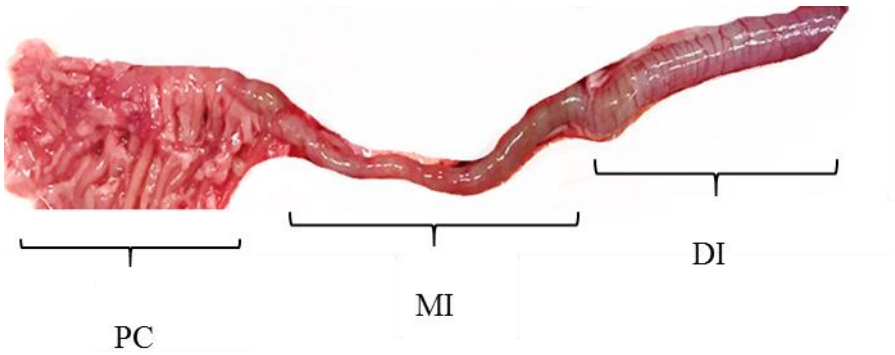

Figure 2-6: *A closer look into the intestinal tract of Atlantic salmon divided into; pyloric caeca (PC), mid intestine (MI) and distal intestine (DI) as visible. Dissection of sample shown took place at EWOS, Chile*

The intestine is a straight linear tube and the longest portion of the digestive tract as shown in figure 2-5. The proximal intestine is equipped with the pyloric caeca, which are blind-ended finger-like projections (FAO 2017). The pyloric caeca increases the mucosal surface area which in turn increases the digestive capacity too. Majority of digestion as well as absorption of nutrients takes place in this region, which is why this region's functional development can signify the level of development of the functional digestive system. Histological studies show that pancreatic tissue is present in the mesenterium adjacent to the pyloric caeca.

Usually, the distinguishing factor between distal and proximal intestine is the presence of mucosal folds in the former region (Sahlmann et al. 2015). Both are however lined by a simple layer of epithelium. The nervous system is rendered responsible for the regulation of the digestive function, secretion of digestive enzymes and the absorption of nutrients. While the distal intestine is in charge of osmoregulation and also the site

where electrolyte secretion takes place (FAO 2017). It has been reported that both the posterior and anterior intestine is important for the uptake of IPN virus. Live as well as inactivated IPNV has been reported to have been taken up by enterocytes present in the intestine through receptor-mediated mechanism (Chen, 2015).

The stomach of teleosts is presumed to be similar to mammals in that NaCl and H_2CO_3 react to produce $NaHCO_3$ and HCl. Along with acid and enzymes the stomach wall is also responsible for secreting mucus so as to keep the stomach from being digested. The midgut happens to be mildly alkaline as it contains not just enzymes but also bile. For teleosts such as rainbow trout research by (Bucking and Wood 2009) suggested that the average gastric pH of 2.7 increases to 4.9 as it goes from a state of being starved to fed. After the proteins are processed in the stomach, they are moved into the pyoloric caeca. It was reported that an average pH of 8.2 through the entire intestinal section before intake of feed, once the feeding state is over the pH decreases to around 7.5 in the proximal and mid intestine and remains unchanged in the distal section of the intestine.

Even though the proteolytic environment in the foregut and midgut is harsh, there are still some proteins that make their way to the distal intestine for absorption. Peptides which happen to be large in size or even antigens for oral delivery of vaccines have been reported to be absorbed in the distal intestine region (Dalla Valle et al. 2008).

2.2.2 Immune response following oral vaccination

Studies looking into host response to virus infections suggest that teleost fish and mammals are similar where vital mechanisms of both innate and adaptive immune

responses against viruses are concerned (Workenhe et al. 2010). A.Salmon's immune system possesses both non-specific (innate) immunity and acquired immune functions (adaptive/humoral and cell-mediated immunity) to tackle and eradicate invading pathogens. A satisfying response from an oral vaccine employed to aquatic species would be the successful induction of both humoral and mucosal antibody response.

Their first line of defence against foreign agents is mucus and skin, which contain immune-reactive molecules such as Ig (immunoglobulin). The biochemical composition of mucus in salmonid species has been found to contain molecules which are involved in immune response such as lysozyme, proteases, alkaline phosphatase etc. Moreover, antimicrobial peptides present in fish mucus have also been shown to inhibit viral replication (Collet 2014).

Non-specific humoral molecules in fish include transferrin, lectins and lytic enzymes while non-specific cells of the immune system include neutrophils, cytotoxic cells and macrophages. The activation of macrophages occurs through cytokines and beta-glycan, both of which help destroy invading foreign agents. In many cases, the innate immune system of salmonids will help limit viral replication until an adaptive response can be reinforced.

On the other hand, adaptive immunity in fish consists of both humoral and cell mediated responses. Adaptive immunity is associated with T and B cell activation which is followed by an immune response to specific pathogens (Hu and Pasare 2013). Immune responses characterised by cytokines, T-cell receptors, immunoglobulins and histocompatibility complex molecules (HSC) are displayed. If administered correctly, oral vaccination induces the production of cytokines that help regulate and also enhance the cellular response (Ruma 2006).

Once the oral vaccine has survived the gastric environment, it will also have to put up against attacks by proteases or nucleases. After which they have to penetrate through the thick mucus to finally reach the epithelial barrier. The vaccine will then be in contact with the apical epithelium, where it will be taken up and delivered to the basal side. It will then be processed by the lamina propria, innate immune cells and specifically APC's (antigen presenting cells) (Embergts and Forlenza., 2016).

After the APC's process the ingested antigens, their fragments are presented to T cells specially CD4+ T cells. These $CD4^+$ T cells play a significant role in immune protection by helping B cells produce antibodies, induce macrophages, employ eosinophils, neutrophils and basophils at the infection site. Moreover, through the production of cytokines they are also able to coordinate a whole array of immune responses (Zhu and Paul., 2008) as shown in figure 2-6.

Depending on the pattern of signals received by CD4+ T cells during their initial interaction with the antigen, they can differentiate into either of these populations; Th1, Th2, Th17 and also induced regulatory Treg cells. Th1 cells play a significant role for immunity towards intracellular microorganisms while Th2 cells for immunity to extracellular pathogens. It has been noted that the abnormal activation of Th1 cells led to autoimmune diseases whereas Th2 cells are held responsible for inflammatory diseases (Zhu and Paul., 2008). Th1 response induces the cell-mediated immune system while Th2 will induce humoral immunity (Collet., 2014).

Other than the Th1 and Th2 response pathways, there is a third mechanism too – Th3 – that occurs when Th1 and Th2 cytokines are balanced in order to prevent any inflammatory cell-mediated reactions, this mechanism is usually witnessed in the

mucosal tissue (Strober and Coffman 1997). Th3 cells happen to be an offset of Treg cells. The Th3 mechanism still remains unexplored for the most part.

Another novel T cell effector subset are Th17 cells. The induction of the Th17 pathway promotes autoimmunity and is highly pro-inflammatory characterised by quick induction of neutrophils (Skugor et al. 2008). Th17 cells are known to mediate immune responses against extracellular bacteria (Weaver et al. 2006).

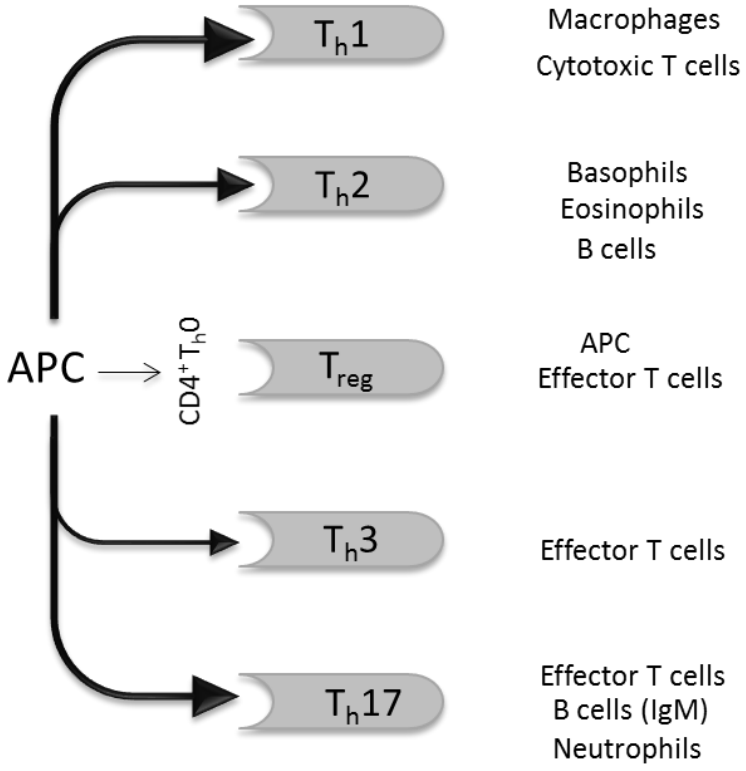

Figure 2-6: *Possible pathways taken by antigens following processing by APC's followed by their target cells. Th1 cells produce the cellular immune response while Th2 cells produce the humoral immune response. Major effectors of cellular immunity are macrophages and cytotoxic T cells. Humoral immunity effector cells happen to be basophils, eosinophils and B cells. Th3 cells help balance the Th1 and Th2 response. Treg cells are induced by the immune system in order to self-limit its response. On the other hand, the induction of Th17 pathway leads to autoimmunity.*

Transcription factors happen to be quite significantly involved in cytokine production upon stimulation. It should be noted that Th0 cells are activated and matured into effector Th1 cells against virus, intracellular bacteria and protozoa. This differentiation into Th1 cells is activated by IL-12 and IFN- γ cytokines (Wang and Husain 2014). Research concludes that T-bet and STAT4 are the transcription factors that control this rate of transcription (Whitmire 2014). (Sun et al. 2011) also suggested that IFN possesses the ability to offer protection to cells from IPNV infection either directly or indirectly through the production of type II IFN. T-bet on the other hand works as the Th1 master regulator and is up-regulated during Th1 differentiation. STAT1 also acts as a primary transducer of IFN- γ signalling plays an important role in the IFNy induction of T-bet (Lighvani et al. 2001).

There is also evidence to suggest the involvement of IFN in in vivo viral infections of fish. (Herath et al. 2012) found that Atlantic salmon infected by salmonid alphavirus had a potent IFN response in the head kidney as early as three days post infection. Moreover, IFN and IFN related genes are induced in the liver and head kidney of A.Salmon following ISAV infection (LeBlanc et al. 2012).

Parasitic infections are known to drive Th2 immune responses which happen to be characterised by production of IL-4 and IL-13, which in turn are capable of mediating elimination of multicellular parasites (Skugor et al. 2008).

Where the humoral response is concerned, T cells develop into effector T cells against pathogenic extracellular microorganisms. While the transcription is controlled by STAT6 and GATA-3 transcription factors, the development itself is activated by Interleukin (IL)-4 and IL-10. IL-17 is a pro-inflammatory cytokine that not only contributes to the pathology of various autoimmune conditions but also plays a

significant role in the clearance of extracellular bacteria. IL-17 is produced by T helper cells called Th17 (Moisan et al. 2007) thus far six IL-17 family ligands (IL-17A-F) and five receptors (IL-17RA-IL-17RD and SEF) have been identified (Shen and Gaffen 2008). Amongst these, $CD4^+$ T helper cells have been shown to primarily secrete IL-17A.

Once an infection is eliminated, induction is suppressed and proliferation of effector T cells takes place. This takes place due to Treg cells and happens to be a significant feature of the immune system. (Li and Flavell 2008) state that TGF-β and IL-6 cytokines help trigger the production of Treg cells which are responsible for limiting inflammatory responses while also preventing autoimmunity as described in further detail in section 2.2.3.

The rate of transcription is dealt by FoxP3 and STAT5 (Chen et al. 2003; Hori, Nomura, and Sakaguchi 2003). GATA-3 is known as the master regulator of Th2 and helps counteract proinflammatory responses (Takizawa et al. 2011). FoxP3 happens to be a T cell-specific transcription factor that plays a vital role in Treg cell development. Continous FoxP3 expression is needed to maintain the suppressive activity of Treg cells (Williams and Rudensky 2007). FoxP3 is highly expressed in the thymus however regulated expression can be seen in the head kidney, liver and spleen also (Zhang et al. 2011).

Th3 cells are a subset of Treg cells, even though Th3 cells are considered to be non-specific, their response is linked with microbial antigens (Weiner et al. 2011). With the influence of IL-10 and TGF- β, Treg cells can differentiate from Th0 cells therefore it can be concluded that these two cytokines are essentially apt markers for Th3

response (Sonmez et al. 2004). Previous research (Castro-Sanchez and Martin-Villa 2013) has also proposed that orally ingested antigens can commence the Th3 response.

B cells are one of the major effector cells of humoral immunity that are altered into antibodies or immunoglobulins (Ig). The three main Ig isotypes found in salmonids are: IgM, IgD and IgT which are determined by the heavy chain of the molecule μ, δ and τ respectively. Research carried out in 2011 (Tadiso, Lie, and Hordvik 2011) found out that in A.Salmon, the quantity of μ transcripts was 200 times that of δ while τ transcripts were 20 times more than δ. IgM is the major systemic antibody in teleost fish specially salmonids, whereas IgT and IgD are specialised to mucosal immune responses (Hordvik 2015).

2.2.3 Immune tolerance

Immunological tolerance is the non-reactivity of a body towards something that would normally be expected to elicit an immunological response. Even though immune suppression is a very significant factor that impacts oral vaccine efficiency, very few studies have looked into this phenomenon especially in aquaculture.

Research carried out by (Abad et al. 1987) reported that immune tolerance was seen to decrease specific antibody production against antigens in A.Salmon. In mammals, T cells control the differentiation and function of Tregs and are associated with immune tolerance. FOXP3 was also characterised in A.Salmon and its highest level of expression was observed in the thymus (Zhang et al. 2011). Furthermore, (Aas et al. 2017) found that the inter-branchial lymphoid tissue (ILT) present in A.Salmon, plays a significant role in immune tolerance as high levels of the transcription factor

FOXP3 were seen along with regulatory T cells (Tregs). It was also shown that mechanisms of central tolerance as found in mammals are also present in the thymus of A.Salmon. Therefore, identification of transcripts such as FOXP3, which is a marker for Tregs proves their involvement in maintaining tolerance in the ILT.

2.2.4 Current prevalent diseases

Infectious diseases pose a constant risk to industrial farming where a high density of farms and organisms within each farm are present (Aldrin et al. 2013). The substantial increase in aquaculture operations over the years has opened a new window for the transmission of aquatic viruses (Crane and Hyatt 2011). Due to the innate resistance present in wild populations of fish, periodic outbreaks of viral diseases have resulted in catastrophic losses hence threatening the long-term sustainability of the aquaculture industry (Dhar, Manna, and Thomas Allnutt 2014).

Some of the significant viral pathogens of finfish have been known since early 20^{th} century – aquabirnaviruses and infectious hematopoietic necrosis virus – while some have been discovered more recently – betanodaviruses. Aquabirnavirus is perhaps the largest and most distinct of the three genera that make up the Birnaviridae family. Examples of members belonging to the Aquabirnavirus family include the infectious pancreatic necrosis virus and yellowtail ascites virus. Aquabirnavirus particles are non-enveloped icosahedrons that contain a genome consisting of two segments: A and B, of dsRNA.

Segment A encodes a polyprotein that is separated post-translationally in order to form three viral proteins; VP2, VP3 and VP4. While segment B on the other hand encodes VP1 which is an RNA-dependent RNA polymerase (Crane and Hyatt 2011).

Betanodavirus on the other hand is one of the two genera making up the Nodaviridae family. Viral nervous necrosis is one of the biggest diseases caused by this etiological agent. This virus infects a vast range of host species, approximately 40 marine species and freshwater fish worldwide (Munday, Kwang, and Moody 2002).

The main causative agents of infectious diseases in aquaculture include bacteria – 54.9%, viruses – 22.6%, parasites – 19.4% and fungi – 3.1% (Taksdal et al. 2007). Even though bacterial diseases tend to be more prevalent in fish farming, it is the viral diseases that are more difficult to control mainly due to challenges in development of effective viral vaccines, natural resistance in wild populations of fish, lack of anti-viral therapeutics and a high susceptibility of fish during early stages of their life cycle (Dhar, Manna, and Thomas Allnutt 2014).

A few of the main viral diseases impacting Atlantic salmon are listed in figure 2-7.

Name of viral disease	Causal agent	Prevalence
Heart and skeletal muscle inflammation (HSMI)	Piscine reovirus (suspected)	Norway, Scotland
Cadiomyopathy syndrome (CMS)	Piscine myocarditis virus	Norway, Scotland
Infectious salmon anaemia (ISA)	Infectious salmon anaemia virus	Norway, Scotland, Canada, UK, USA, Chile
Pancreatic disease (PD)	Salmon alphavirus	Europe
Infectious pancreatic necrosis (IPN)	Infectious pancreatic necrosis virus	Europe, USA, Canada, India, Japan

Figure 2-7: *Viral diseases prevalent in the Atlantic salmon population, their causal agents and their regions of prevalence (Dhar, Manna, and Thomas Allnutt 2014)*

ISA was first detected in Chile in 1999 (Munir and Kibenge 2004). The estimated loss of salmon due to ISA from 2007 to 2011 was approximately US $1.0 billion. One of the major reasons contributing to such a devastating outbreak was the failure to vaccinate fish against ISA (Dhar, Manna, and Thomas Allnutt 2014). HSMI was also initially diagnosed in 1999, and there has been an annual increase in the number of outbreaks recorded. Affected fish exhibit anaemia and abnormal swimming behaviour. Atlantic salmon are commonly affected around 5 to 9 months after transfer to sea, even though mortality is variable, morbidity has been recorded to be very high (Kongtorp et al. 2004).

On the other hand, CMS is a recently identified disease and its aetiology currently remains uncertain. It primarily affects adult salmon after sea transfer. Fish suffering

from CMS may unexpectedly die without any clinical signs of disease and is usually diagnosed through histopathology, with severe inflammation and degeneration of the spongy part of the myocardium and similar changes in the atrium (Haugland et al. 2011). PD is caused by the highly contagious salmonid alphavirus, it is a disease that causes excessive damage to the exocrine pancreatic tissue combined with chronic myositis. The levels of PD associated mortalities during natural outbreaks have ranged from negligible up to 63% (Taksdal et al. 2007). On the other hand, IPN can cause up to 100% mortality in young salmonids if in its acute form, and it is highly likely that viral, environmental and host factor will only add to the severity of the outbreak (Snieszko 1975).

2.2.5 Infectious pancreatic necrosis virus (IPNV)

IPNV is a highly contagious disease that causes high mortality in juvenile salmonids. During the 1940's in North America this disease was first reported as catarrhal enteritis mainly affecting fingerlings (McGonigle 1941). However, it was not until 1960 that the virus was first isolated and characterised (Wolf et al. 1960). Currently, the virus has a worldwide distribution and has been isolated from more than 32 fish species, 4 crustacean species and 11 molluscs (DFO 2017). IPNV is a prototype member of the Aquabirnavirus in the Birnavridae family. It is an un-enveloped bi-segmented double stranded RNA virus.

As seen in figure 2-8, the two segments: A and B, contain ORFs (open reading frames). Segment A consists of two ORFs – the translatable part of DNA/RNA sequence. ORF1 encodes a VP5 protein, which has an anti-apoptopic effect while ORF2 consists of a

polyprotein which cleaves to produce three gene products: VP1, VP2 and VP3. VP2 is the major capsid protein, which is assumed to be a critical carrier of the virulence properties of IPN virus (Song et al. 2005). VP2 also plays a critical role where virus entry is concerned as it is responsible for receptor recognition (Bruslind and Reno 2000). VP3 is a minor structural protein with specific neutralising epitopes and VP4/NS is a non-structural protein with protease activity. On the other hand, segment B consists of one ORF which encodes VP1 – RNA dependent RNA polymerase which is involved in viral RNA synthesis (Dobos., 1995).

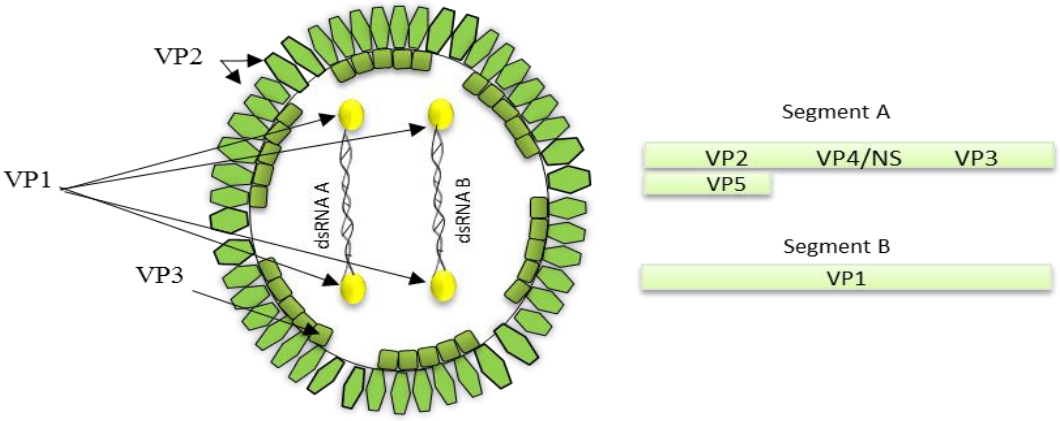

Figure 2-8: *A schematic representation of the IPNV virion and the segmented linear dsRA genome. The capsid itself is around 70 nm in diameter, consisting of 260 trimers of VP2 that are situated radially along the capsid. Image acquired and modified from Taghavian et al, 2013*

The virus can replicate in various types of continuous cell lines from teleost fishes at temperatures below 24°C. This virus has the ability to replicate in the cytoplasm. It

takes approximately 16 – 20 hours at 22°C for a single cycle of replication to take place, resulting in a characteristic cytopathic effect (CPE) (Dobos 1995).

The disease can be horizontally transmitted directly from fish to fish or vertically from the broodstock (Ruma., 2006). Infections mainly occur during the freshwater or fry first-feeding stages. However, with the expansion of aquaculture over time, IPNV outbreaks are now commonly witnessed in postmolts, too. Infected fish that overcome IPN remain asymptomatic carriers, these carrier fish are perhaps the key mechanism through which the virus is maintained and replicated in hematopoietic tissues (Holopainen et al. 2017).

IPNV remains one of the most economically critical viral pathogens of Atlantic salmon. In 2015, this viral agent was responsible for 30% of disease diagnoses reported by Chilean salmon farming centres (Manriquez et al. 2017).

A deeper understanding of the interferons (IFNs) and their path of action against viruses is imperative in order to develop new strategies to control this virus (Larsen et al. 2004).

2.3 Drug encapsulation methodologies

Various techniques have been identified for the production of polymeric nano and micro-particles over time. The most popular ones are based around the emulsion technique. In this process, specific therapeutic molecules are dissolved into a polymer solution and then emulsified to form micro-droplets that are then dried in order to remove the solvent. However, it is important to note that the use of solvents can cause denaturation of protein-based drugs hence giving rise to variability in encapsulation efficiencies and also loading capacities (Yang et al. 2000). The use of high shearing forces in this methodology can also contribute to the degradation of a sensitive antigen (Baras et al. 2000). Another major drawback of the emulsion technique is its production of inhomogeneous particles, which leads to their lack of reproducibility thus limiting their clinical use as monodispersity in terms of size of a sample is a critical factor as it gives better control of drug release profiles and bioavailability of the loaded drug (Valo et al. 2009).

Spray drying is another commonly used encapsulation method. It involves the atomization of liquid feed in order to form solid particles. However, this method uses high temperatures and therefore cannot be used for temperature sensitive compounds and mono-dispersity is again an issue (Murillo et al. 2002). Also, other physical stresses such as organic solvents, emulsion conditions and aqueous/organic interface can produce structural changes to the protein which can then contribute to loss of enzymatic activity (Baras et al. 2000). Similarly, for spray congealing, the drug being encapsulated needs to be stable at the temperature required to melt the matrix material. This method is also not favourable for viscous molten mixtures since it may cause clogging in the feed tube or atomiser (Oh et al. 2014).

Microfluidic techniques have also been used to fabricate microbeads. Such techniques offer simplicity and make use of robust devices however most reported microfluidic approaches involve emulsification hence possessing the disadvantages that come along with batch-wise emulsification techniques. Microfluidic devices have also reported to show low productivity unless a multichannel system is used (Kendall et al. 2012).

The development of various jetting processes has rapidly taken place over the last few years with electrospraying and aerodynamically assisted jetting leading as the main approaches that demonstrate versatile abilities in terms of fabricating an array of particle sizes using a range of materials – from nano and micro suspensions to biologically active cellular suspensions (Jayasinghe and Suter 2006). The flexibility, consistency and proficiency of producing micro or nanostructures with tailored shape, morphology and size make both these methodologies extremely promising especially in the pharmaceutical and biomedical fields. Both methodologies boost bioavailability of aqueous soluble drugs, offer control over drug release systems in order to deliver protein based drugs and also living cells along with producing targeted drug delivery systems. However, it should be noted that the multiple number of processing as well as formulation factors put forward some complexities (Nguyen, Clasen, and Van den Mooter 2016). These will need to be comprehended thoroughly for the success of encapsulated drug delivery systems.

2.3.1 Electrospraying (ES)

Electrospraying has emerged as a technology that overcomes the limitations related to most micro-particle fabrication techniques specifically the emulsion method. In 1600, William Gilbert noted that when a droplet of water and a piece of amber were held closely to each other, the interaction between them formed a conical shaped droplet. In the early 20th century Zeleny (1914) exhibited the formation of fine droplets from a conical shaped meniscus under an electric stress. Interest in the electrospraying process was increased by the Nobel Prize winning work of (Fenn 2002) on mass spectroscopy for the detection of macromolecules.

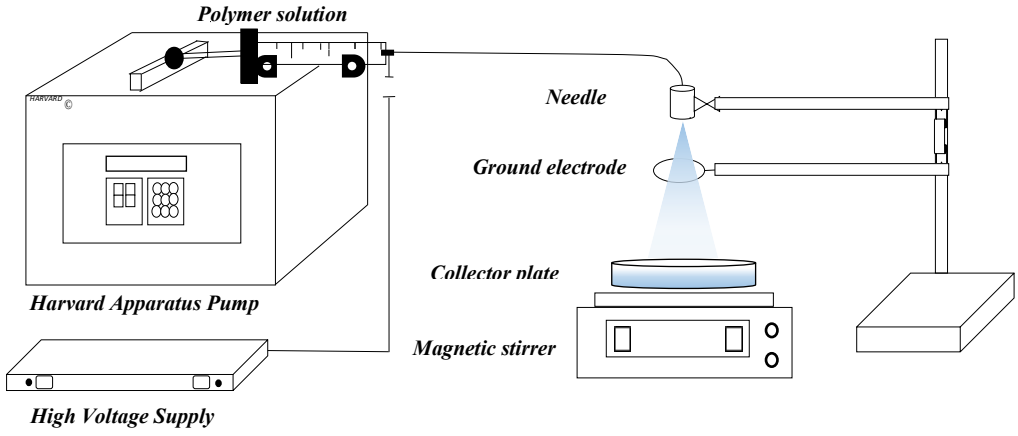

Figure 2-9: *Schematic image showing the electrospraying set-up. A high voltage supply is connected to a ground electrode. A syringe loaded with the liquid polymer solution is fixed onto a programmable syringe pump (PHD 4400, HARVARD Apparatus Ltd., Edenbridge, UK), which is connected to a needle through silicon tubing. The polymer solution flows through the syringe towards the charged needle, which acts as an outlet for the solution, exposing it to electric stress once pushed out of the needle tip. The jet breaks down into droplets, which due to simple gravitational pull compile onto the collector plate placed directly under the needle. A magnetic*

stirrer is present underneath the collector plate so as to avoid cross-linking solution from remaining stagnant, which in turn helps against aggregation of droplets

During the ES process, the liquid solution is pushed through a conducting needle as seen in figure 2-9. Once the liquid is pushed out of the charged needle it is exposed to an external electric field. The shear stress on the liquid surface due to the established electric field causes elongation of the jet. This jet then undergoes instabilities, which help disrupt the jet into charged droplets.

The jet break-up can be caused by axisymmetric or lateral instabilities. Axisymmetric instabilities are known as 'varicose'. With higher applied flow rates, the current flowing through the liquid will increase and with this the surface charge on the liquid will increase too. Lateral instabilities on the other hand are known as 'kink'. With the increasing influence of these kink instabilities, the size distribution of the main droplets becomes wider (Hartman et al. 2000).

There is however a limit present for the maximum charge allowed on the surface of a liquid, which is known as the Rayleigh limit. The Rayleigh limit being the magnitude of charge on a droplet which overcomes the surface tension of the droplet (Jaworek 2007). In simple terms, there are two forces acting in opposite directions in the charged droplet; surface tension of the charged droplet which tries to maintain the droplet's spherical shape and coulomb force of repulsion between the like charges on the surface due to which the droplet's spherical shape may or may not be broken down.

At the point where the surface tension can no longer retain the Coulomb force of repulsion, Coulomb fission will occur. Due to which the main/parent droplet will disintegrate into secondary/offspring droplets. Not only are the secondary droplets much smaller in size but also have a much higher charge to mass ratio (Banerjee and

Mazumdar 2012). Wang et al. (2012) concluded that Coulombic repulsion between induced charges is responsible for jet break-up. While, surface tension remains responsible for jet length. (Hartman et al. 2000) stated that charge in the liquid cone can be transported in two ways; through conduction in the liquid due to the electric fields or by charge convection.

ES is governed by processing conditions such as flow rate, needle diameter, distance between the needle tip and ground electrode and the voltage applied (Enayati et al. 2011) and also the properties of liquid solution itself such as its' conductivity, density, viscosity, surface tension and relative permittivity. A balance between all these factors promotes jet stability. An increased stability of jet gives rise to the production of a more homogenous sample of droplets (Irvine et al. 2007).

Once the liquid solution is accelerated at a specific flow rate, various morphologies can be observed exiting the needle. These are referred to as modes of jetting which are divided into two groups; the first comprising of modes where only fragments of liquid are ejected from the capillary i.e. dripping, spindle etc. The second group includes modes where a capillary in the form of a long and continuous jet is produced which eventually breaks off into droplets e.g. oscillating jet, multi-jet mode, cone-jet (Jaworek and Krupa 1999).

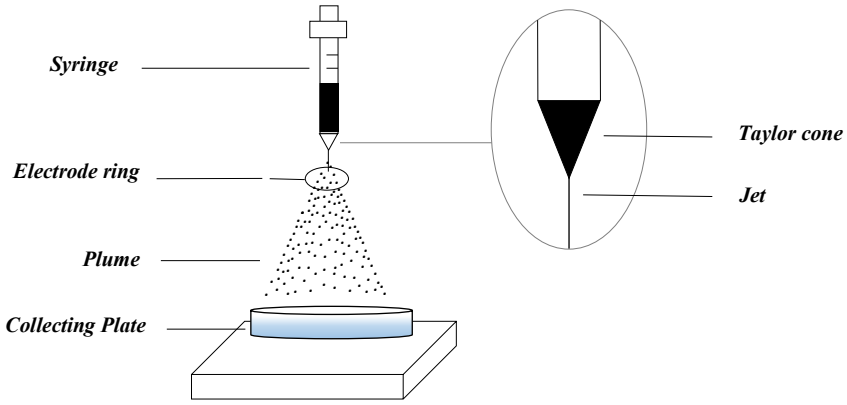

Figure 2-10: *Illustrating liquid solution electrosprayed in the stable cone-jet mode*

Due to its steady operation, the cone-jet mode, as illustrated in figure 2-10, has become the most researched mode of operation (Yurteri, Hartman, and Marijnissen 2010). Also known as the Taylor cone - as it was discovered by Sir Geoffrey Taylor in 1964 before the existence of electrospraying due to his interest in the behaviour of water in the presence of strong electric fields - this mode implies the formation of an almost conical shape of liquid at the meniscus, which is present at the needle tip.

The cone jet mode can go through three different processes; the first process is the acceleration of the liquid in the liquid cone, this acceleration and consequently the shape of the liquid cone are a result of the force balance of surface tension, gravity, inertia, electric stresses in the liquid surface and viscous stresses. The second process of electrospraying atomization in the cone-jet mode is the break-up of the jet into droplets. The third process is the development of the spray once droplets have been produced. Electrical interaction between highly charged droplets with various sizes (and therefore different inertia) causes a size segregation effect. Small droplets will be

found at the edge of the spray while the larger sizes will be found in the spray centre (Hartman et al. 1999).

It is significant to know that the shape of the liquid cone is a result of the balance of liquid pressure, liquid surface tension, electric stresses in the liquid surface, gravity, the liquid viscosity and inertia. On the other hand, the size distribution however is dependent upon the diameter of the jet and on the break-up of this jet into droplets (Hartman et al. 1999).

2.3.2 Aerodynamically assisted jetting (AAJ)

AAJ on the other hand is a pressure driven technology based on pneumatic atomisation technology. The laminar accelerating gas stream helps shape the steady liquid filament that then ultimately breaks up into a spray. It is capable of handling concentrated nano-suspensions for drop and placement of nanomaterials within droplet residues. Over time, various suspensions containing a vast array of nanomaterials – silicone, SiO_2, fullerenes, quantum dots, etc – have been processed using this approach (Jayasinghe and Suter 2006). (Irvine et al. 2007) demonstrated the ability of AAJ to handle living primary organisms, namely; porcine vascular and rabbit aorta smooth muscle cells.

Even though electrospraying has previously been shown to produce nanostructures from nanosuspensions, this approach relies heavily on the applied voltage, flow rate and suspension properties out of which the electrical conductivity and viscosity play an extremely significant role. As too high or too low a level can greatly hinder the generation of monodispersed droplets to form a jet.

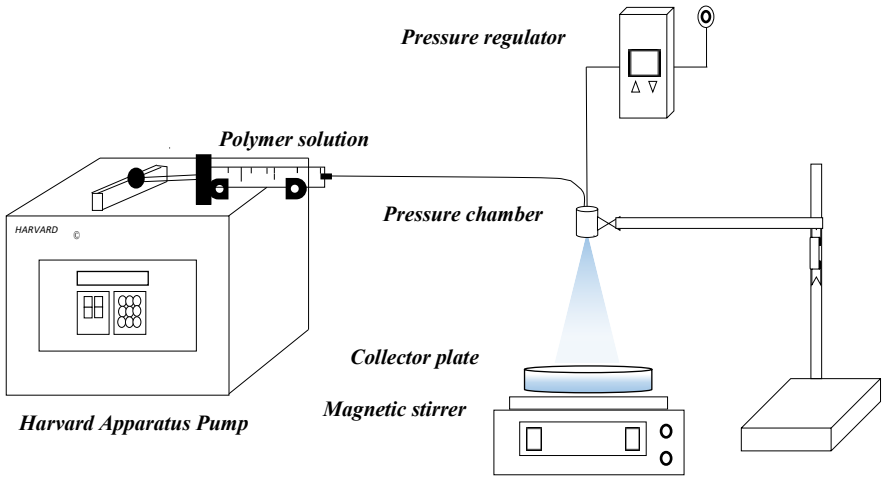

Figure 2-11: *Schematic image depicting the aerodynamically assisted jetting set-up. The main set up remains the same as electrospraying except the pressure chamber is put in place of the charged needle. The syringe pump holds the polymer solution in place which travels towards the pressure chamber with the help of silicone tubing attached at the inlet present at the top of the pressure chamber. The solution exits the chamber from the outlet present at the bottom directly facing the collector plate*

In the AAJ set-up, compressed air is used as a gas stream. If the applied pressure velocity is adjusted so that the liquid-gas surface tension stresses are larger than the gas pressure fluctuations, then the liquid filament will end up breaking into a nearly mono dispersed spray. As highlighted in figure 2-12 pressure is applied over an exit orifice within a chamber (further details on pressure chamber discussed ahead in section 3.2.1.2) that contains a needle holding the flow of the medium. Meanwhile, the gas flow is accommodated by the second inlet on the wall of the chamber that gives rise to a differential pressure within the chamber with respect to the surrounding atmosphere. The fluid medium gets drawn out of the needle due to the resulting pressure differential through the exit orifice, which is centrally in line with the exit of

the needle itself. The exit orifice is also counter sunk externally in order to let the jet have a smaller diameter as it passes through the exit orifice (Jayasinghe and Suter., 2006).

Therefore, the formation of a jet occurs which later undergoes Rayleigh's instabilities along with surface tension effects which will then help initiate the generation of droplets as well as droplet residues as seen in figure 2-11.

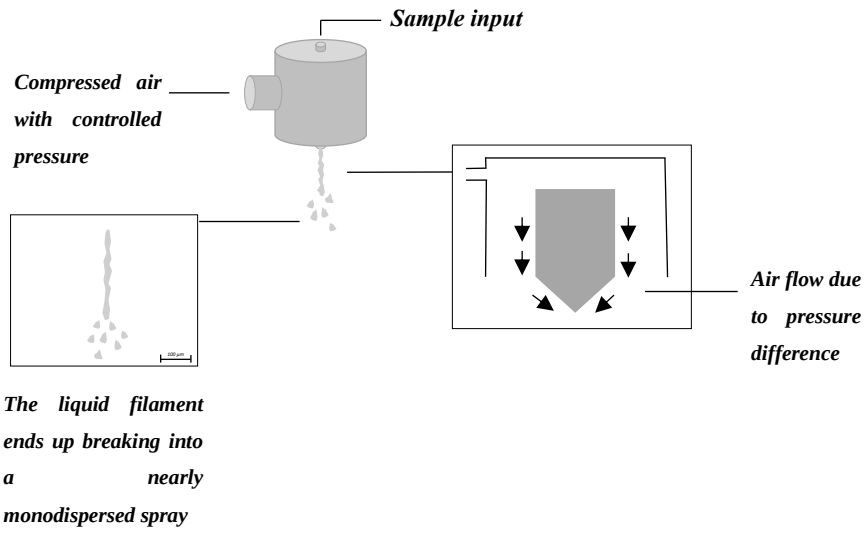

Figure 2-12: *Demonstrates the effect of applied pressure on the liquid filament exiting the orifice of the pressure chamber and then eventually breaking up into droplets. The pressure chamber contains three different orifices; one where the syringe containing media connects via silicone tubing (at the top), the other connecting the pressure regulator (sideways) and lastly an exit orifice (at the bottom)*

This jetting methodology and the various jet break up regimes are governed by the rheological properties of the liquid medium in combination with the applied flow rate. The only varying factor coming into play is the applied pressure unlike the applied

voltage in electrospraying. However, AAJ shares quite a few similarities with electrospraying in that they both have the ability to handle high viscosity suspensions containing a range of materials through which micro as well as nano structures can be generated. Another specific feature shared by both these technologies is their ability to switch from producing droplets to fibres with a simple change in the rheological properties of the liquid media being used (Jayasinghe and Sullivan 2006).

2.3.4 Encapsulation of bioactives by ES and AAJ

Many successful examples of bioactive compounds encapsulated within drug delivery mechanisms produced using these fabrication methodologies exist in literature today. (Martinez-Sanz, Lopez-Rubio, and Lagaron 2012) reported the successful encapsulation of whey protein concentrate in micro, submicro and nanocapsules through electrospraying. These capsules were also able to stabilise functional additives like antioxidant β-carotene making them suitable for applications in the food industry. Omega-3 fatty acid was encapsulated by (Torres-Giner et al. 2010) via electrospraying to offer protection from oxidative degradation. They reported that secondary oxidation products formed in encapsulated fatty acid were at a much lower level than the un-encapsulated products. (Valo et al. 2009) encapsulated two model drugs namely; beclomethasone dipropionate and salbutamol sulfate in PLA nanoparticles through electrospraying. They reported successful drug entrapment in these fabricated spherical polymeric delivery vehicles.

When it comes to the encapsulation/entrapment of antigens specifically, Preis and Langer were the first to present the ideology of a polymer construct encapsulating a protein antigen in (Preis and Langer 1979). Since then various polymers such as PLGA, PLA have been widely used as antigen encapsulating polymeric delivery mechanisms. (Gallovic et al. 2016) used the coaxial electrospraying methodology to formulate a micro particulate-based subunit anthrax vaccine. This study concluded an increased protection against the highly virulent B. anthracis ames strain in mice. (Furtmann et al. 2017) the ability of the electrospraying technique to produce PLGA nanoparticles that act as peptide based vaccine carriers. Klaric (2014) demonstrated the ability of electrospraying to encapsulate the IPNV antigen within alginate microbeads. It was concluded that this fabrication methodology was non-damaging towards the antigen.

AAJ has been known to not only safely handle biological materials but also produce encapsulated annular residue structures consisting of active primary cells (Arumuganathar et al. 2007). (Pakes, Jayasinghe, and Williams 2011) set out to examine the model eukaryotic Dictyostelium discoideum – a model for immune cell chemotaxis – under AAJ. It was concluded that the use of AAJ did not induce any stress to the cells neither did it affect cell development. Hence suggesting that the technique can be safely used in order to manipulate cells of this biological model. Furthermore, (Griessinger, Jayasinghe, and Bonnet 2012) also demonstrated the ability of AAJ to jet hematopoietic stem/progenitor cells directly while maintaining their viability. (Kwok et al. 2008) went one step further and combined both these fabrication methodologies to give rise to a hybrid bio-jetting approach. This was used to handle human embryonic kidney cells stably expressing eGFP (enhanced green fluorescent protein), it was found that post treatment these cells still remained viable.

3. Materials and methods

3.1 Materials

This chapter provides details of all the raw materials; chemicals and stock solutions, analytical instruments as well as the experimental methodologies/techniques used in this thesis.

3.1.1 Polymer selection

Alginate - an anionic, water soluble, linear polymer - is amongst one of the most versatile and readily available biopolymers at present as it has immense applications in the biomedical industry. Moreover, properties such as the alginate's mechanical strength, biodegradability, gelation and cell affinity can be attuned through its chemical and physical modification (Venkatesan et al. 2015).

The ability of alginates to protect the microbe and the plasmid while passing through the digestive tract and then diffuse through the gut mucus layer has been widely researched and supported. Following diffusion, alginate will reach the enterocyte surface. After the alginate comes in contact with the epithelium, the antigen sampling cells will take them up and deliver to the microbe or DNA plasmid. From thereon, DNA plasmids will enter the nucleus and trigger antigen expression in the host cell whereas enteric pathogens may possess the intrinsic ability to activate local mucosal responses (Embregts and Forlenza 2016).

Extensive research has supported the use of alginate microparticles as delivery vehicles for macromolecules such as proteins and DNA. A diverse range of biological compounds such as vitamins, vaccines etc can be incorporated into alginate matrices (Wee and Gombotz 1998) to avoid damage from low pH and interaction with proteolytic enzymes present in the digestive tract. An advantage of loading biomolecules into alginate micro-particles is that it helps retain their three-dimensional structure. Mandal et al (2001) suggests that porous alginate micro particles have a faster release rate as well as a higher loading content as compared to non-porous micro-particles.

Alginates are composed of homopolymeric regions; M (β-D-mannuronic acid) and G (α-*l*-guluronic acid) (MM- and GG- blocks) infused with segments of alternating heteropolymeric sequences; GM- or MG- block structures, making them true block copolymers (Grasdalen, Larsen, and Smidsrod 1981). It is the organism or tissue from which the alginates are isolated which dictate its molecular variability. The average molecular weight, the molecule-weight distribution of the polymer and the sequence of M and G residues dictates the physical properties of alginate (Ding et al., 2009).

The capacity of alginate to gel under benign conditions makes it attractive for encapsulation (Peppas et al. 2006). Divalent cations such as chloride salts have the ability to bind preferentially to the G-blocks present in alginate, therefore forming a gel. When sodium alginate is placed into a calcium based ion, the sodium ion in the polymer ends up being replaced by the calcium ion - with each calcium ion being cross-linked with two moieties of polymer stands (Venkatesan et al. 2015) as shown in figure 3 – 1.

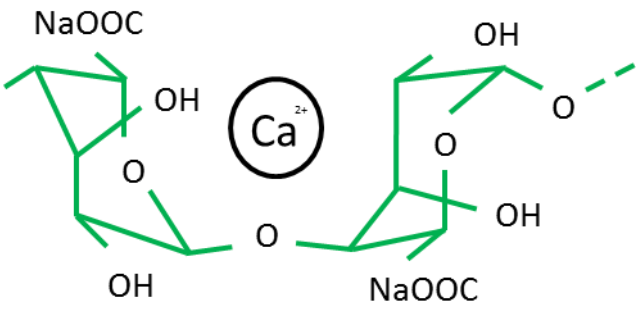

Figure 3-1: *Divalent ion binding site in G-blocks (Ca^{2+} in this case). Image acquired and modified from Venkatesan et al (2015)*

Once in solution, alginates tend to behave like flexible coils. They are however capable of forming ordered structures but only upon interaction with divalent metal ions. Therefore, divalent ions such as calcium, strontium and barium will bind to the G-blocks present in the alginate structure, preferentially but co-operatively, hence, resulting in the formation of a gel. For example, one Ca^{2+} binds to the G units in two alginate chains, following an 'egg-box model' (Smidsrod 1973) as shown in figure 3 - 2. The gelation tends to be instant and is an irreversible process.

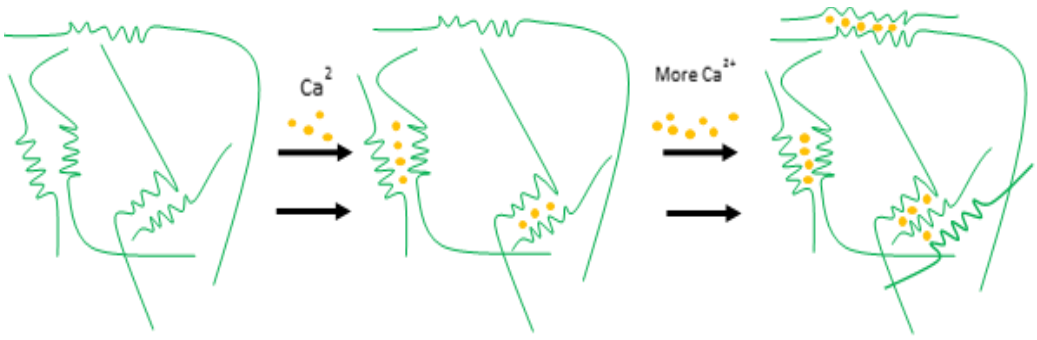

Figure 3-2: *The 'egg-box model' for alginate gel formation with divalent cations*

3.1.1.1 Sodium alginate

Alginate is found in seaweed and extracted from brown algae through treatment with aqueous alkali solutions, usually NaOH. In order to precipitate alginate, the extract is then filtered and calcium chloride is mixed with the filtrate. Treating it with dilute hydrochloric acid will help turn the alginate salt into alginic acid if needed. Once purification has taken place, water soluble sodium alginate is produced. Resilient gels tend to be formed when sodium alginate is in the presence of calcium and acid mediums.

Sodium salt is the most commonly used water soluble form of alginate. Over time, sodium alginate has found various applications mainly for the encapsulation and immobilisation of a range of cells since they can maintain their viability even within the cross-linked gel (Trivedi et al. 2001). Due to this, sodium alginate is typically used in an array of topical and oral pharmaceutical formulations and has specifically been used for the aqueous microencapsulation of drugs (Motwani et al. 2008).

Different grades of sodium alginate are commercially available and they all vary in their molecular weight, particle size and chemical composition (Liew et al. 2006). Sodium alginates are generally divided into two groups: M- and G- rich alginates. M-rich alginates are made up of approximately 60% mannuronic acid and 40% guluronic acid while the G-rich alginates consist of around 37% mannuronic acid and 63% guluronic acid (Lawson., 2003). M-rich alginates consist of various types of Keltone, Kelcosol, Kelvis whereas Manugels fall under G-rich alginates (Liew et al. 2006).

Types of Alginate	
Manugel GHB/GMB/DMB	All three types are generally used in fillings, structured foods and heat stable gels
Scogin MV/LDH	Scogin alginates are pre-eminent water retention agents and enhance rheology. Normally used as surface sizers and strengthen oil resistance, solvent handout possess greaseproof properties
Protanal (10/60FT)	Medical grade sodium alginate. Most common application is wound care

Table 3-1: *All sodium alginates are cold soluble gelling agents. Dry, free flowing powder form in nature and yellow to light brown in colour. All supplied and manufactured by FMC BioPolymer AS Norway. Reference: FMC Biopolymers – product specification*

The M:G ratio of these alginates is highlighted in the table below;

Alginate Type	M:G ratio
Manugel GMB	37:63
Manugel GHB	37:63
Manugel DMB	37:63
Scogin MV	61:39
Scogin LD	61:39
Protanal LF 10/60 FT	25:75

Table 3-2: *M:G ratios of different grades of alginates used in chapter five as provided by FMC Biopolymers*

Figure 3-3 shows a visual representation of the types of alginates used in the encapsulation efficiency and in vitro dissolution tests. The particle sizes of all five types were not rendered quite significant simply because the samples were not used in powder form, rather as solutions.

Figure 3-3: *Shows 1g each of Manugel GHB, Manugel GMB, Manugel DMB, Scogin LDH and Scogin MV respectively. The free-flowing powders are solubilised in DI water to produce alginate solutions which are then used to fabricate particles to be used in optimisation and characterisation tests. As seen in the image Manugels tend to have granules that are off-white in colour whereas Scogin alginates tend to possess more yellowish-brown coloured granule. This difference in colour is dependent on their extraction source*

3.1.2 Raw materials

Name	Description/Manufacturer
DI water	Analytic reagent grade, certified AR for analysis. Fisher Scientific, UK
Protanal	LF 10/60FT, Lot # GQ5501401, FMC Biopolymer, AS Norway
$CaCl_2$	Calcium chloride dehydrate, Mw 147.01, Lot # SLBB9179V
$SrCl_2$	Strontium chloride hexahydrate, Lot # 8253A, Sigma Aldrich, UK
$BaCl_2$	Barium chloride dehydrate ≥ 99%, Lot # MKBL4935V, Sigma Aldrich, UK
KPH	Potassium hydrogen Phthalate 99%, VWR, UK
HCl	Hydrochloric acid, 37%, VWR, UK
Glycine	Glycine ≥ 99%, Lot # SZBA357AV, Sigma Aldrich, UK
NaOH	Sodium hydroxide, flake, 98%, Lot # 10159374, Alfa Aesar, Fisher Scientific, UK
Blue dextran	Molecular weight 2,000,000, Sigma Aldrich, UK
Manugel GHB	Lot # G0600201, FMC Biopolymer, AS Norway
Manugel GMB	Lot # G1305601, FMC Biopolymer, AS Norway
Manugel DMB MGLDMB	Lot # G1011902, FMC Biopolymer, AS Norway
Scogin MV	Lot # G0903901, FMC Biopolymer, AS Norway

Scogin LDH	Lot # G9207802, FMC Biopolymer, AS Norway
TiO_2	Titanium (IV) dioxide 99.0 – 100.5%, Mw 79.88 g/mol, VWR, UK
Dye	Blue Food colouring, Super Cook, UK
96 well plate	Multiwall cell culture plates, VWR, UK
Plastic syringe	Sterile, disposable syringe, 1 ml, 10ml and 60 ml. VWR, UK
Needle	Hypodermic needle 19G, 1.1 x 50mm/21G, 0.8 x 50mm Terumo, VWR, UK
Silicone tubing	Silicone rubber tubing, platinum cured Wall thickness: 0.8 mm, Inner diameter: 0.8 mm, Outer diameter: 2.4 mm Silex Ltd, UK
Magnetic beads	PTFE coated spin bars, egg-shaped and polygon shaped. Spinbar, Sigma-Aldrich, UK
Filter	Cell strainer, 100 µm nylon, VWR, UK
Eppendorf tubes	1.5 ml, Sigma Aldrich, UK

Table 3-3: *Raw materials used during the experimentation stage of this research, including their type, grade and manufacturer details*

3.1.3 Stock solutions

Name	Description
$CaCl_2$	36.8g $CaCl_2$ dissolved in DI H_2O (1000ml)
$SrCl_2$	106g $SrCl_2$ dissolved in DI H_2O (100 ml)
$BaCl_2$	12g $BaCl_2$ dissolved in DI H_2O (100 ml)
KPH	0.4M Potassium hydrogen phthalate (KPH) prepared by dissolving 81.69g KPH in DI H_2O (1000 ml)
HCl	0.4M Hydrochloric acid (HCl) prepared by dissolving 33.33 ml in DI H_2O (1000 ml)
Buffer pH 3.0	Prepared by combining 0.4M KPH and 0.4M HCl (Hydrochloric acid). The resulting buffer is adjusted to pH 3.0 before replenishing with DI H_2O to give a total volume of 1000ml
Glycine	0.4M Glycine prepared by dissolving 30.03g in DI H_2O (1000ml)
NaOH	0.4M NaOH prepared by dissolving 16g in DI H_2O (1000 ml)
Buffer pH 8.6	Prepared by combining 500 ml of 0.4M Glycine with 40 ml of 0.4M NaOH. After fine tuning the pH to 8.6, the generated buffer solution is diluted to a volume of 2000 ml with DI H_2O

$NaHCO_3$ (saturated)	0.4M $NaHCO_3$ mixed with DI H_2O (1000 ml). Any undissolved $NaHCO_3$ crystals were filtered off prior to use
Blue Dextran (BD) solution	1g BD (powdered form) in 20ml DI H_2O

Table 3-4: *Stock solutions used during the experimental stage of this research*

3.1.4 Analytical Instruments

Name	**Description**
Modular stereomicroscope	MZ10 F, Leica microsystems
Microtec stereomicroscope	Infinity 1-1M, Lumenera, UK
Magnetic stirrer	Magnetic hot plate stirrer, Stuart®
Weighing scale	Plate size: 275mm x 225mm, Adam® CBK Bench scale
Weighing scale	Precision scale, Mettler Toledo, UK
High voltage DC unit	FP-30. Glassman Europe Ltd, UK
Texture Analyser	XT Plus, Stable Micro Systems, Godalming, UK
Dissolution tester	DT 626 series, ERWEKA, Heusenstamm, Germany

Microplate reader	Bio-tek Absorbance Platereader with Gen5 Data collection and Analysis software
qPCR	LightCycler 490 system (Roche) using the SYBR green RT-PCR Kit (Qiagen), Norway
ELISA plate reader	GENios, XFLUOR4 Version: V4.40, Tecan Group Ltd, Switzerland
Vacuum coater	VC-6, No, 1870, Halvor Forbeng AS, Norway
High performance disperser	T-25 IKA Werke GmbH & Co, Germany
pH meter	Oakton handheld pH meter. Oakton® instruments, Sigma Aldrich, UK
Rheometer	The Discovery Hybrid Rheometer series 3, TA Instruments, UK

Table 3-5: *Analytical instruments used during the experimental stage of this research*

3.2 Experimental Methodologies

3.2.1 Encapsulation Methodologies

The two alginate bead fabrication and encapsulation methodologies employed were namely electrospraying and aerodynamically assisted jetting.

3.2.1.1 Electrospraying

For the electrospraying process, microbeads were produced using the horizontal electrospraying configuration comprising of a high voltage supply which had the potential of reaching up to 30 kV. A 10 ml syringe was fixed onto a programmable syringe pump cradle (PHD 4400, HARVARD apparatus Ltd., Edenbridge, UK) as shown in schematic figure 2-9. The inner diameter of the stainless steel needle used was 15 mm, this needle was placed just above a copper ground electrode (10 mm external diameter and 8 mm internal diameter) which is connected to the syringe through silicone tubing. The microbeads produced were collected on a petri dish containing 35 ml of $CaCl_2$ (cross-linking solution). Each sample set was collected for 50 seconds. The same experimental set-up and procedure was used for microbead production by electrospraying throughout. Only the process variables were altered which will be highlighted in tables where needed.

In order to produce operational maps for alginate microbead sizes, a suitable polymer concentration needed to be determined first. This was assessed through experimentation where process variables highlighted in table 3 - 6 were used.

Process parameters	
Flow rate (ml/hr)	50
Voltage (kV)	5
Distance between electrode and collector (cm)	8
Distance between needle tip and electrode (cm)	2
Alginate concentration (%)	0.5, 1, 1.5, 2

Table 3-6: *Process variables used for experiment assessing the effect of polymer concentration on the size of electrosprayed microbeads*

3.2.1.1.1 Operational size maps

Once an appropriate polymer concentration was selected, the operational maps for microbead sizes were then produced using process variables shown in table 3 - 7

Process parameters	
Alginate concentration (%)	2
Distance between electrode and collector (cm)	8
Distance between needle tip and electrode (cm)	2
Molarity of cross linker (mol)	25
Sample collection time (sec)	50

Table 3-7: *Process variables used for producing microbead size operational maps using Electrospraying. Flow rate and voltage were changed over a range of 10 – 60 ml/hr and 0 – 12kV respectively*

3.2.1.1.2 Mechanical Testing

Alginate beads fabricated for mechanical testing were generated using the same parameters for the dissolution tests as seen in table 3 – 12, 3 – 13 and 3 – 14.

3.2.1.2 Aerodynamically Assisted Jetting (AAJ)

The Aerodynamically assisted jetting set-up consisted of a ‘pressure chamber’ which is a stainless steel container (DIN 1.4435). It consists of two inlets, one for compressed air and the other for a threaded needle and an exit orifice. The internal diameter of exit orifice is the same as the threaded needle i.e. 0.35 mm. Once the needle is fitted into the device, the distance between the needle tip and the exit orifice is 0.18 mm. The internal diameter of the chamber itself is 8.2 mm, while the height is 16.2 mm. Nozzle measurements are listed below in table 3-8.

Nozzle measurements	**Metric (mm)**
Top inlet diameter	8.5
Side inlet diameter	6.2
Needle length	4
Needle thread	9.9

Table 3-8: *AAJ nozzle/pressure chamber measurements*

The threaded needle helps accommodate the media flow into the device and is fitted vertically at the top of the chamber. The second inlet present on the chamber is to let compressed air flow in, this inlet is perpendicular to the threaded needle inlet. A

precision regulator connects to the compressed air inlet present at the pressure chamber through a silicone tube. The main air supply has a controllable on/off switch and a manual tuner to adjust the pressure with a resolution of +/- 0.01 bar. Similar to the electrospraying procedure, each sample was collected in a petri dish containing 35 ml of $CaCl_2$ for 50 seconds each.

Suitable polymer concentration for microbead fabrication using AAJ was chosen through an optimisation experiment for which there are process variables highlighted in table 3 - 9 below.

Process parameters	
Flow rate (ml/hr)	60
Pressure (bar)	0.03
Distance between exit orifice and collector (cm)	10
Alginate concentration (%)	0.5, 1, 1.5, 2

Table 3-9: *Process variables used for experiment assessing the effect of polymer concentration on the size of microbeads produced through AAJ*

3.2.1.2.1 Operational size maps

Operational maps for microbeads produced using AAJ were then produced using variables highlighted in table 3 - 10.

Process parameters	
Alginate concentration w/v (%)	2
Distance between exit orifice and collector (cm)	8
Molarity of cross-linker (mol)	25
Sample collection time (sec)	50

Table 3-10: *Process variables used for producing microbead size operational maps using AAJ. Flow rate and pressure was changed over a range of 10 – 60 ml/hr and 0.1 – 1 bar respectively*

3.2.2 Characterisation

3.2.2.1 Scanning electron microscopy (SEM)

Feed pellet morphology was determined with the help of SEM images. These were taken using the Hitachi S-3400 PC-based pressure scanning electron microscope – with a magnification range of 5x to 300,000x. It allowed for the porous surface of the pellets to be examined and helped determine the range of pore sizes present.

3.2.2.2 Environmental Scanning electron microscopy (ESEM)

ESEM has the ability to analyse hydrated samples without causing any physical alteration to them (Stabentheiner, Zankel, and Polt 2010). The Philips XL30 ESEM was used to examine the external structure of alginate microbeads as they were only partially dried.

3.2.2.3 Transmission Electron microscopy (TEM)

As the success or failure of TiO_2 encapsulation was based upon the size of their particles, TEM was used to determine their size range. This was done using the 2x JOEL 1010 transmission electron microscope with digital image capture and magnification up to 660,000.

3.2.3 Mechanical Testing

The mechanical properties of microbeads were quantified using a Texture Analyser XT Plus (Stable Micro Systems, Godalming, UK) a schematic diagram for which can be seen in figure 3-4. This equipment has the ability to measure up to 50 kg in force and can also be used to measure a range of properties including adhesiveness, tensile strength, fracturability, viscoelasticity etc.

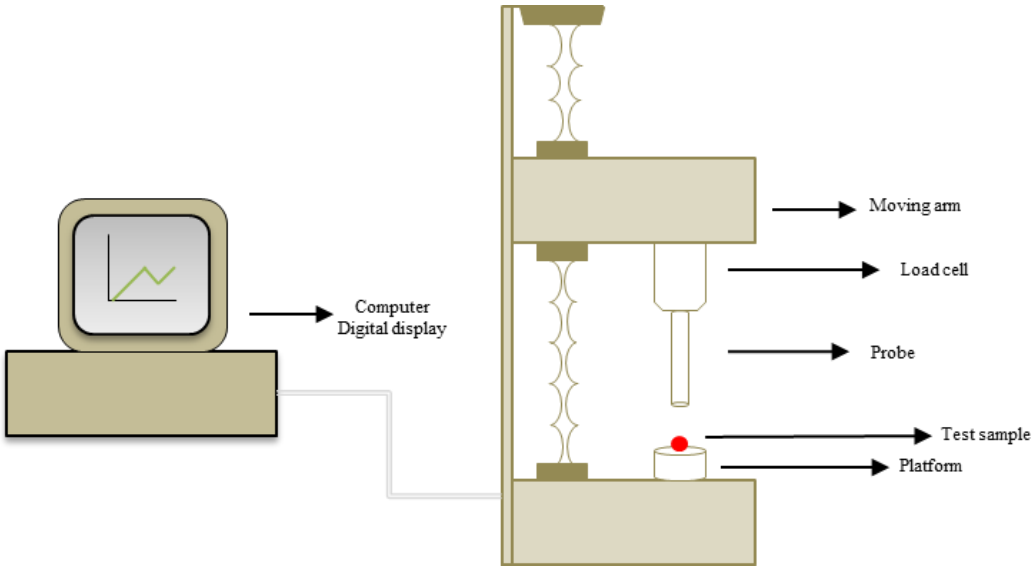

Figure 3-4: *Shows the TA.XT Plus Texture Analyser set-up including the texture exponent software version 6.0 for data recording, the probe used for compression testing; Perspex cylinder (diameter: 8mm), the platform where the test sample is*

placed and the moving arm that pushes the load cell vertically once the compression test starts

The base table is such that it provides easy and quick height adjustment in order to accommodate various sized samples. The selection of probe is dependent upon the type of test being carried out along with the surface area of the sample to be tested. Compression probes are usually cylindrical in shape. In order to maintain the applied compression forces it is important for the probe being used to have a larger area than that of the sample being tested (Test Cells Fixtures, Food Technology Corporation). The mechanical stability of samples was measured by compressing each individual microbead (n = 5 for each sampling point assessed). After a microbead was sized under an optical microscope, it was then placed on a plate and the probe was moved towards the microbead. The parameters highlighted in table 3 - 11 were set on the Analyser before starting the compression test;

Process parameters	
Pretest speed (mm/s)	0.5
Test speed (mm/s)	0.01
Postest speed (mm/s)	2
Trigger force (g)	2
Compression (%)	60

Table 3-11: *Test parameters used for compression testing*

3.2.5 Dissolution Testing

These tests were divided into two sets; observational and in vitro. Evidently, the testing requirements and experimental methodologies for both differed from each other as described in sections 3.2.5.1 and 3.2.5.2 below.

3.2.5.1 Dissolution – Observational

Ten different alginate concentrations were produced; 0.2%, 0.4%, 0.6%, 0.8%, 1%, 1.2%, 1.4%, 1.6%, 1.8% and 2%. Cross-linking solutions; $CaCl_2$, $SrCl_2$ and $BaCl_2$ were also produced at the same molarity i.e. 0.25 M. While the dissolving solution $NaHCO_3$ was produced at a molarity of 1 M.

Manual microbead production was carried out by simply loading the test solution into a 5 ml syringe (21G x 2/0.8 x 50mm). Microbeads produced through ES and AAJ for this test used the same set up as described in section 3.2.1.1 for ES and 3.2.1.2 for AAJ using the parameters in table 3 – 12 and 3 – 13 respectively.

The experimental set-up for the fabrication procedure combining both ES and AAJ aims to combine both the electrospraying processes successfully. To achieve this, the applied voltage is connected to the pressure chamber, so now the liquid drawn out of the exit orifice is dependent upon two factors; applied pressure and applied voltage. Similar to the aforementioned experimental set-ups, a 10ml syringe is fixed onto a syringe pump and the pressure chamber is placed just above a copper ground electrode which is connected to the syringe through silicone tubing. The voltage supply is connected to the needle present on top of the pressure chamber. The precision regulator is connected to the compressed air inlet which is attached to the pressure

chamber. Once, the flow rate, voltage and pressure were set to the values listed in table 3 - 14, microbeads were produced.

Process parameters	
Flow rate (ml/hr)	50
Voltage (kV)	2.5
Distance between electrode and collector (cm)	8
Distance between needle tip and electrode (cm)	2
Alginate concentration (%)	0.6, 1, 1.6, 2

Table 3-12: *Process variables used for experiment assessing the effect of fabrication methodology on the dissolution rate of electrosprayed microbeads*

Process parameters	
Flow rate (ml/hr)	40
Pressure (bar)	0.01
Distance between exit orifice and collector (cm)	10
Alginate concentration (%)	0.6, 1, 1.6, 2

Table 3-13: *Process variables used for experiment assessing the effect of fabrication methodology on the dissolution rate of microbeads produced through aerodynamically assisted jetting*

Process parameters	
Flow rate (ml/hr)	40
Voltage (kV)	2.5
Pressure (bar)	8
Distance between exit orifice and electrode (cm)	2
Distance between electrode and collector (cm)	8
Alginate concentration (%)	0.6, 1, 1.6, 2

Table 3-14: *Process variables used for experiment assessing the effect of fabrication methodology on the dissolution rate of microbeads produced through ES and AAJ in conjunction*

Once the microbeads were produced they were sized using an optical microscope (Leica MZ10F). The L4078 stage micrometre (1 mm scale, 0.01 mm sub-divisions, line width 2 µm, accuracy +/- 2 µm overall) was used as a simple and reliable means of precisely calibrating the optical microscope (Leica DFC280). A single bead was then moved into a single well of a 24 well plate containing 1 ml $NaHCO_3$ acting as the dissolving solution. The well plate was then placed under an optical microscope and images were taken at various time intervals while the process of dissolution was timed and recorded. Five replicates were carried out for each sample point being assessed.

3.2.5.2 Dissolution – In vitro

Dissolution tester ERWEKA DT 626 series (6x 1000ml semi-hemispherical bottomed glass vessel) in accordance with the USP 1 and 2 general method – rotating basket and paddle - was used. The apparatus consists of a metallic shaft attached to a rotating

cylindrical basket that is positioned in a cylindrical glass vessel, which holds the test media. According to FIP/AAPS guidelines to dissolution (2003) the volume capacity of the six vessels present in the dissolution tester is up to 1000 ml each. The six vessels themselves are placed in a rectangular glass water bath. The temperature probe helps regulate the temperature at which the test takes place as seen in schematic figure 3-5.

Figure 3-6 shows a closer look of the mesh basket placed in the glass vessel while being attached to the shaft which helps move the rotating basket in a vertical direction before or after the test as well as rotating it during the test. The mesh basket itself is made of stainless steel with 40 openings per linear inch of mesh. An opening at the top of the basket allows for the test sample to be placed inside.

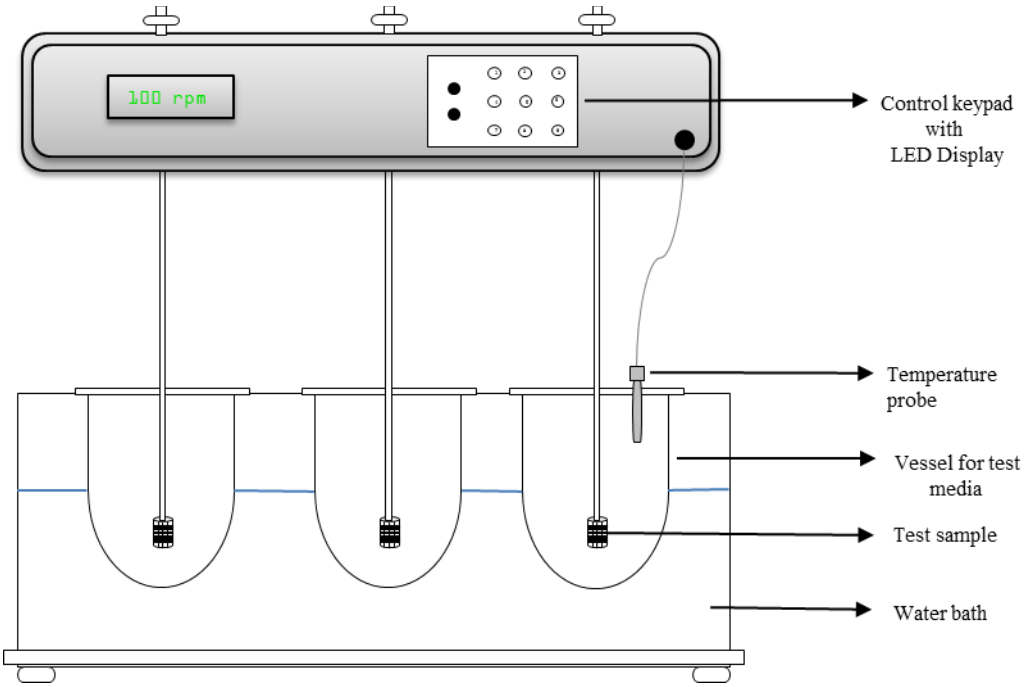

Figure 3-5: *Schematic showing dissolution tester- frontal view. The ERWEKA DT 626 series. Equipped with six test stations, with centering rings for the shafts, covers for each vessel along with a distance ball for height adjustment of the paddles*

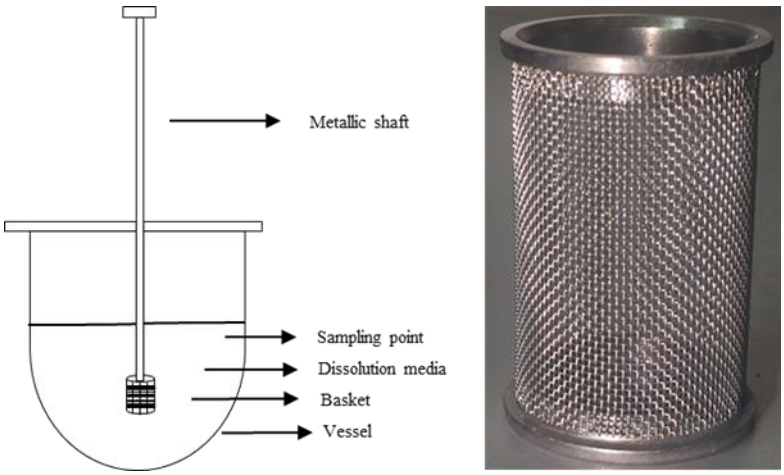

Figure 3-6: *A schematic representation of the USP rotating basket connected to a mettalic shaft that is placed in a semi-hemispherical glass vessel. Image on the right shows the 40 size mesh basket in which the test sample is placed*

For the in vitro dissolution tests, alginate beads were produced using 1.5 ml alginate solution for each vessel. Once bead fabrication took place, the beads were removed from the cross-linking solution – 25 ml $CaCl_2$ - after 10 minutes of the last bead being formed. They were then washed with DI water thoroughly in order to remove any excess cross-linking solution. Meanwhile, it was made sure that the rotation speed was set to 100 rpm in accordance with the UPS 1 apparatus set up. The temperature of the water bath was set to 11°C. 380ml of buffer 3.0 added to each of the five vessels. Timer was set to 15 minutes. The beads were then placed into their assigned mesh baskets and submerged into the respective vessel to begin the test. According to FIP/AAPS guidelines, the submergence of the rotating basket in the dissolution medium is necessary. Test started within approximately 30 minutes of alginate bead production.

After 15 minutes of the test start time, the tester was paused and 1 ml of dissolution media was pipetted out into an eppendorf tube for analysis later. The baskets were

then lifted out of the vessels and washed with DI water to get rid of excess buffer media that might be present on the mesh. The beakers were washed and reloaded with 380 ml of buffer 8.6. The baskets containing the same sample of beads was now submerged in the new dissolution media and the test was started once again.

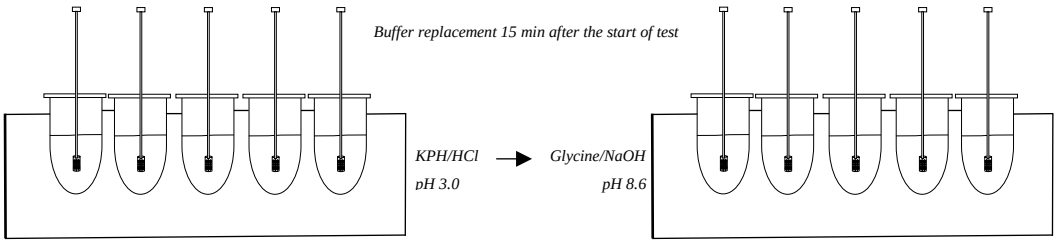

Figure 3-7: *The test was paused fifteen minutes after the starting point in order to replace media; KPH/HCl (Potassium hydrogen phthalate/hydrochloric acid) was used to represent acidic medium present in the stomach while Glycine/NaOH represented alkaline conditions present along the intestinal tract of Salmon*

Test was paused at five minute intervals in order to collect samples – 1ml each time - in eppendorff tubes. With each sample removal an equivalent amount of media was replaced back into each vessel so as to keep total volume constant throughout the test. A total of twelve sampling points were used for sample collection - from 0 to 55 minutes. The test conditions were set as summarised in table 3-15.

100 µl aliquots were taken from collected samples to prepare a 96 well polystyrene well plate. An endpoint assay was carried out using the microplate reader.

Parameters	
Alginate Type	Manugel GMB, GHB, DMB, Scogin LDH, MV
Dissolution media 1	KPH-HCl
pH	3.0 and 8.6
Sampling time point (mins)	15
Total number of sampling point (s)	1
Dissolution media 2	Glycine-NaOH
pH	8.6
Sampling time points (mins)	0, 5, 10, 15, 20, 25, 30....55
Total number of sampling points	12
Volume of media (ml)	380
Sample volume (ml)	1.0
Temperature (°C)	11
Rotation speed (rpm)	100
Apparatus	UPS 1
Number of vessels	5

Table 3-15: *Conditions set for the in vitro dissolution tests carried out using UPS Apparatus 1*

3.2.5.3 Standardised in vitro test strategy

The United States Pharmacopoeia (USP) have set out numerous standardised dissolution apparatus; USP apparatus 1 also known as the 'stirred beaker method' positions the test sample and a fixed volume of fluid in a vessel while stirring acts as

mechanical agitation. USP apparatus 2 is the ‘rotating basket and paddle’ whereas apparatus 3 is the ‘reciprocating cylinder’. USP apparatus 4 is the ‘flow through cell’ where the sample is placed in a column that is flushed with fluid continuously. USP apparatus 5 is ‘paddle-over-disk’ while apparatus 6 is a cylinder and apparatus 7 consists of ‘reciprocating holders’ (Siewert, Dressman et al. 2003).

It should be noted that the chosen test method may not necessarily be able to completely imitate the in vivo environment as long as it is able to test the pivotal performance indicators of the test formulation. As far as ODTs (orally disintegrating tablets) are concerned, apparatus 1 and 2 are the test method of choice. The rotating basket and paddle devices are robust yet simple and are therefore supported widely for experimental use. However, it should be noted that due to the single container nature of apparatus 2, change in pH or any kind of test medium leads to experimental difficulties. Even though the USP 1 set up may cause the formulation to clog the screen this apparatus offers the ability to change pH through media addition/replacement (US Pharmacopeia., 2011).

The in vitro dissolution test in this study was carried out in quintuplicates following the method described in Section 3.2.5.2. Conditions set for the in vitro dissolution test are summarised in Table 3-15. The reasoning behind dissolution test parameters being set as such is detailed in the following sections.

3.2.5.4 Temperature

The temperature of the water bath was carefully monitored at 11°C since Atlantic salmon is exposed to a temperature range of 4 – 18°C (Jensen, Wahli et al. 2015). It has been previously reported that low temperatures tend to have an adverse effect on

both cellular and humoral specific immune response. Moreover, 4°C has been established as the non-permissive lower water temperature in salmonids (Szalai, Bly et al. 1992). Therefore, an optimum temperature between 4 and 18°C was deemed ideal to assess dissolution rates - a point where salmonids are best able to induce an immune response.

3.2.5.5 pH

The pH conditions found in A.Salmon stomach are acidic. The major digestive components in the stomach happen to be pepsin and HCl (Volkoff, 2010). The optimum pH for pepsin is 3.0. After being processed in the stomach, the mixture of dissolved nutrients and partially digested feed pass into the pyloric caeca. This is where trypsin, chymotrypsin and aminopeptidase complete peptide hydrolysis (Krogdahl and Bakke-McKellep, 2005). When the acidic chyme reaches the proximal intestine it becomes rapidly neutralised by bicarbonate (HCO_3) in bile and pancreatic juice. Before feed intake the average pH through entire intestinal section is 8.2, after feed intake it decreases to 7.5 and the pH increases again during the period after feeding and can be slightly above 8.5 along the intestinal tract (Bucking and Wood, 2009).

For the microbeads to mimic a reasonably accurate passage through the A.Salmon GI tract, the dissolution medium needs to be kept acidic for the first fifteen minutes, so as to simulate gastric conditions. Following which, the dissolution medium then needs to be replaced with alkaline media to simulate the intestinal conditions present in A.Salmon. Additionally, for gastrointestinal formulations where one pH level is not capable of producing bio pharmaceutically relevant results, a change of pH during the

dissolution test is rendered appropriate. Therefore, buffer pH 3.0 (KPH and HCl) and buffer pH 8.6 (Glycine and NaOH) were used as the dissolution media.

Almost all alginate dissolution test studies have been carried out under conditions viable for the human digestive system. The only data available for the dissolution of alginate microbeads under simulated A. Salmon digestive conditions (Goran, 2015) used the following buffers; pH 3.0 and pH 8.6

3.2.5.6 Agitation rate

In accordance with USP apparatus test method 1 and 2, agitation should be obtained in the basket and paddle device is by stirring at 50 to 100 rpm and should not exceed 150 rpm. The agitation rate for the entire length of the test was set at 100 rpm.

3.2.5.7 Sampling points

Selecting dissolution test time points is based upon the type of formulation being tested. For delayed release formulations, dissolution requirements consist of at least three points, where the first sample is taken after 1 – 2 hours and the third sample is taken when the API is completely released. On the other hand, immediate release SODF's will have a test time of approximately 30 minutes to an hour.

Samples were taken at intervals of five minutes for an overall test duration of fifty-five minutes. The first sampling point 0 was taken 15 minutes after the test was started. 1 ml was pipetted out of each vessel and replaced by another 1 ml of the original dissolution media to keep total volume constant. After sampling point 0, every

following sampling point was after five minute intervals. All the samples were collected in 1.5 ml eppendorf tubes for analysis later.

3.2.5.8 Dissolution media

Each vessel was filled with volume of 380 ml buffer 3.0 at the start of the test. After sample 0 was taken at 15 minutes, the test media was then changed to pH 8.6, in order to keep in accordance with the simulated environment of A.Salmon's digestive system.

At the end of the test, aliquots of 100 µl were taken from the epindorffs to prepare the 96-well plate for microplate reader analysis. An endpoint assay was performed using the BioTek microplate reader at 630 nm at 27 ºC

3.2.6 Encapsulation Efficiency (EE)

The Bio-tek Absorbance Plate reader with Gen5 Data collection and Analysis software was used to detect absorbance in order to produce a standard curve. The in vitro tests used Blue Dextran (BD) – a water soluble model macromolecular drug with an average molecular weight of 2,000,000 as a suitable model API.

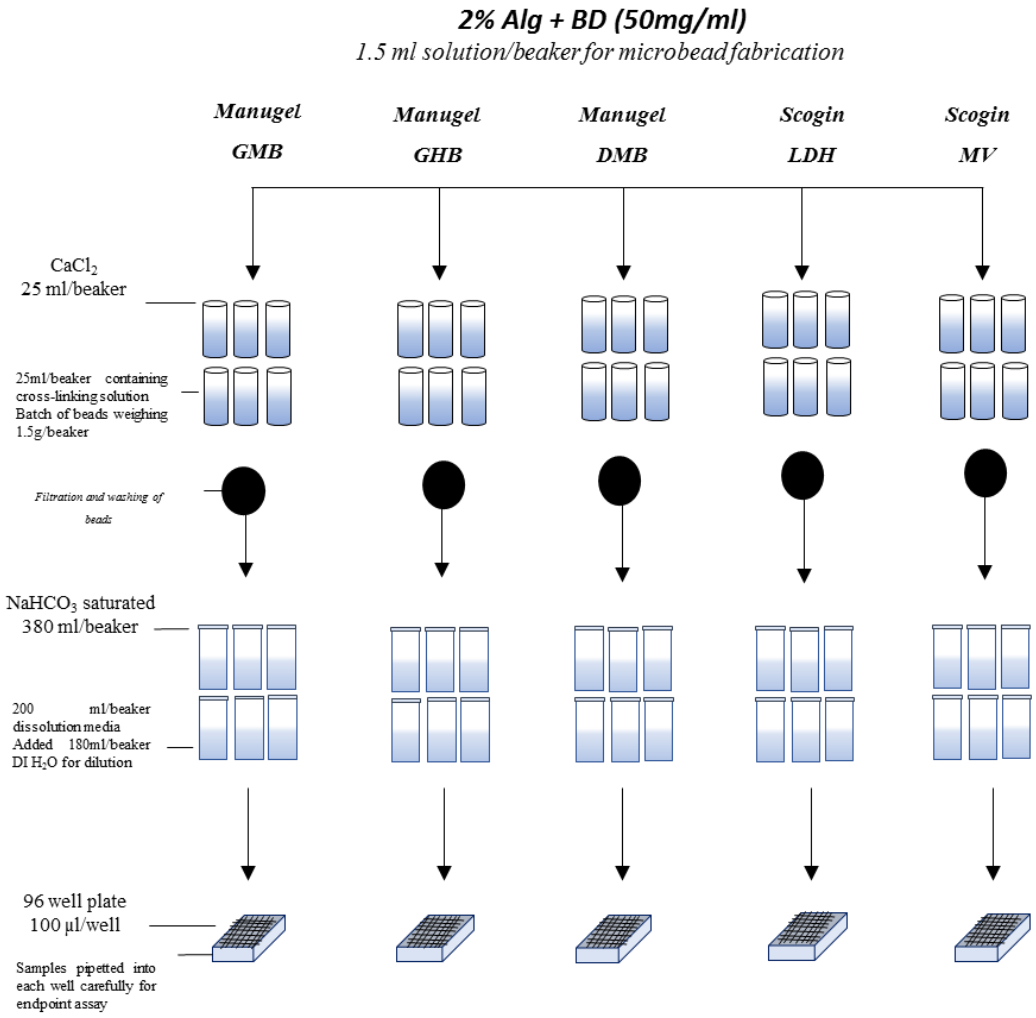

Figure 3-8: *Test strategy for the encapsulation efficiency experiment. Five sets of 1.5ml batches were produced for each type of alginate tested*

1.5 ml of alginate and BD solution were used to produce microbeads in 25 ml of $CaCl_2$ which played the role of a cross-linker in this test. Beads were then filtered to remove the cross-linker and washed with DI water in order to get rid of excess cross-linker. Beads were then added to a beaker filled with 200ml saturated $NaHCO_3$. After a period of 24 hours when the beads were completely dissolved, 180ml of DI water is added to the beaker for dilution – this is done to avoid crystallisation and hence the need for further filtration. An aliquot of 100 µl is finally taken from the beaker and placed into an eppendorf tube to be prepared for the plate reader. Absorbance of BD was measured at 630 nm and 24°C. All measurements for this test were replicated five times and averaged.

Process parameters	
Flow rate (ml/hr)	50
Volume (ml)	1.5
Diameter (µm)	23.2
Distance between exit orifice and collector (cm)	10

Table 3-16: *Microbead fabrication process variables for encapsulation efficiency testing for all five types of alginates*

3.2.7 Viscosity Testing

Discovery Hybrid Rheometer series 3 was used for this experiment. The rheometer consisted of cone and plate set up with measuring geometry as follows; 60 mm cone, angle of 1º and a 27 µm gap – which was used along with the TRIOS software to

obtain viscosity measurements of all samples. Five different types of alginate products provided by FMC polymers were measured at the following constant parameters;

Process parameters	
Solution concentration (w/v %)	2
Temperature (℃)	25
Volume of solution tested (ml)	5
Shear rate (1/s)	101
Alginate type	Manugel GMB, Scogin MV, Scogin LDH, Manugel GHB, Manugel DMB

Table 3-17: *Process variables used for the viscosity measurements of all five alginate types*

Each sample was placed on the bottom plate with the help of a syringe. The experiment was carried out in quintuplicates with the plates cleaned by a dry napkin carefully before a new sample was loaded for testing. For each sample, the strain was measured as the sample itself was subjected to a stress gradually increasing from 0 to almost 180 Pa for the time duration of 2 minutes/sample.

3.2.8 Trial

3.2.8.1 Production of encapsulated IPNV microbeads

The following process parameters were set for the encapsulation process;

Process parameters	
Alginate type	Protanal 10/60FT
Concentration (%)	2
Pressure (bar)	3.0
Flow rate (ml/hr)	60.5
Distance between exit orifice and collector (cm)	10

Table 3-18: *Process parameters used for IPNV antigen encapsulation using AAJ*

Two sets of microbeads were produced; empty alginate beads to act as the control group and the experimental group which consisted of IPNV antigen encapsulated microbeads

3.2.8.2 qPCR

Real-time PCR is currently the most accurate and sensitive detection/quantification method for nucleic acids (Dorak 2007). Quantitative PCR was performed by using the SYBR green RT-PCR Kit (Qiagen) and the LightCycler 490 system (Roche).

Quantitative polymerase chain reaction (qPCR) also known as real-time PCR is a molecular biology technique based on the polymerase chain reaction (PCR). PCR is driven by a thermostable polymerase enzyme which will synthesize a complementary

sequence of bases to any single strand of DNA. This means that a specific gene can be chosen which the polymerase will amplify in a mixed DNA sample through the addition of DNA complimentary to the gene of interest. Small pieces of DNA called 'primers' prime the DNA sample at the right location in order for the polymerase to bind and copy only the gene of interest. The binding of primers is highly specific but the activity of the polymerase is controlled through temperature.

The same principle of amplification is employed during a real-time quantitative PCR (qPCR) reaction, where the amplification of a targeted DNA molecule is quantified in real-time, and not at the end as the conventional PCR, which reduces accuracy of quantification. Since qPCR allows for the reaction to be witnessed while it takes place (in real life), the acquired measurements are much more accurate, and qPCR therefore has become the workhorse of targeted quantitative analysis of gene expression.

For the qPCR test carried out in this research, the SYBRgreen® dye was used as the real-time detection technology. It is the most commonly used intercalating fluorescent dye, which in the presence of a double stranded DNA will bind to the DNA helix. This ends up altering the structure of the dye hence activating its fluorescence. Every time a PCR reaction results in the double stranded DNA, the SYBRgreen® dye will bind to it and emit fluorescent signal which will be read off in real-time by the instrument as seen in figure 3 - 9. SYBRgreen® absorbs light at 497nm and is able to emit light at 520nm (Dorak 2007).

During the denaturation phase of the DNA, the SYBRgreen® dye is present in the mixture but these molecules have less affinity towards single-stranded DNA. Once annealing or polymerisation takes place, the level of fluorescence increases. This is because as more and more DNA is created by PCR, more dye is able to bind with the

DNA double helix thus increasing the fluorescence intensity. When the two separate genes of interest have been produced, the DNA present in the mixture becomes double-stranded and SYBRgreen molecules bind to this dsDNA. Figure 3-9 offers a schematic description of the process.

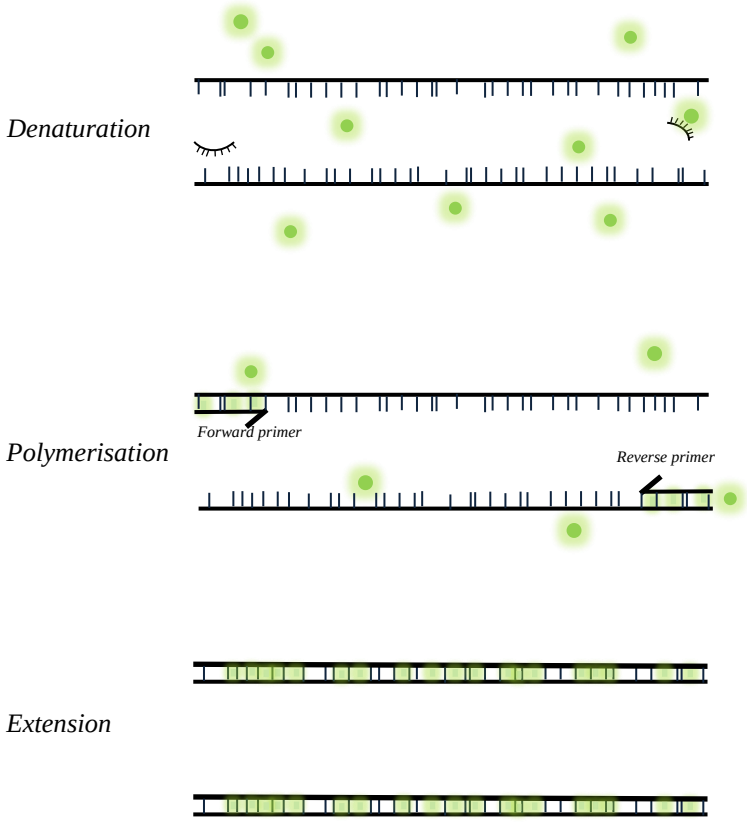

Figure 3-9: *Highlights the process where SYBRgreen dye binds to the dsDNA product resulting in fluorescence*

The samples were all subjected to qPCR and the individual Ct values were determined. Ct data was then normalised for the expression of the house-keeping gene. House-keeping genes are control genes used in qPCR as they are constitutive genes vital for the maintenance of basic cellular function and are expressed in all cells of an organism under normal and also patho-physiological conditions (Eisenberg and Levanon 2003).

Once normalised, they are then processed by the Delta Delta Ct method as described previously by (Livak and Schmittgen 2001). Final results are presented as delta delta Ct values, and expression of each gene in control fish (not exposed to beads or antigen) was set to zero.

For each gene, 50 ng of RNA was used as a template in a mixture of primers – 250 μm and SYBR Green RT-PCR master mix giving a total volume of 20 μl. The mixtures were incubated at 50 °C for ten minutes, followed by 95 °C for five minutes after which forty amplification cycles took place.

3.2.8.3 ELISA (Enzyme-linked immunosorbent assay)

The enzyme linked immunosorbent assay (ELISA) is a detecting/quantifying technique normally used to measure substances such as proteins, antibodies, peptides and hormones. This immunological assay technique is considered to be strongly specific and highly sensitive (Xiao and Isaacs 2012).

Prior to sampling, the fish were anaesthetised with tricain mesilate (100 mg/l). Blood was collected from the caudal artery with a heparinised blood collection tube (V = 4 ml) fitted with 0.8×38 mm disposable needles. The pooled blood samples were centrifuged at 4000 rpm for 10 min immediately after sampling. The plasma was then removed and kept frozen at -80^{o}C prior to ELISA test.

ELISA was performed following the method previously described by (Munang'andu et al. 2012) with minor modifications.

ELISA plate wells were coated with 100 µl polyclonal anti-IPNV diluted 1:2000 in coating buffer pH 9.6 (0.1M Carbonate buffer) and then incubated overnight at 4^{o}C. The plates were washed before the incubation of 200 µl of 5% dry milk per well for the duration of 2 hours at room temperature. The washing steps were done in triplicate with 200 µl PBST/well, the dilutions were carried out with 1% dry milk. Once washed, the wells were incubated for 2 hours with 100 µl of IPNV supernatant 10^{8} TCID50/ml. After another wash, the serum samples were diluted 1:40, added to the wells and incubated at 4^{o}C overnight. Following another wash, 100 µl of mouse antibody against rainbow trout IgM diluted in 1:5000 was incubated for 2 hours. After this 100 µl of 1:1000 dilution of peroxidase conjugated antimouse Ig (DAKO, Denmark) was incubated in each well for 1 hour. After washing 100 µl of O-phenylenediamine dihydrochloride substrate diluted in water was added to each well. The reaction was incubated for a duration of 15 minutes, after which the recation was stopped by adding 50 µl of 1 M H_2SO_4 per well. An ELISA plate reader (TECAN, Genios) was used to analyse the samples at 492 nm.

4. Fabrication, optimization & characterisation

4.1 Introduction and aims

The mechanism of drug delivery has a significant effect on both the likelihood for commercialization of the drug as well as its efficacy. This is why more effective methods for drug delivery need to be explored and analysed. Ideal drug delivery systems need to administer the correct amount of a specific therapeutic agent at the appropriate time, at the right location in a way that not only boosts compliance but simultaneously reduces side effects. Microbeads are one such mechanism that offer controlled drug release for extended periods of time. These microbeads provide protection for the drug itself and have the ability to offer controlled release which also increases patient comfort (Kim and Pack 2006). Moreover, the vaccine formulation itself should be stable with respect to carrier size, size distribution and surface morphology throughout the process of fabrication, storage as well as administration (Oyewumi et al., 2011).

The bioactive compound itself is encapsulated into a polymeric matrix so as to protect it from degradation; proteolytic or acidic. The main aim of the first results chapter is to assess two novel microbead fabrication methodologies; Electrospraying and Aerodynamically assisted jetting. In order to initiate the optimisation of both ES and AAJ, firstly, polymeric parameters such as concentration of the alginate solution were

assessed. Following which, the governing process parameters such as flow rate, applied voltage, pressure and collecting distance were also studied.

As there are a wide variety (especially in terms of size range) of feed pellets available, a similarly appropriate range of microbeads is also needed in order to fit into the pellet pores. The next objective was to carry out an extensive sizing study - for microbeads produced using both fabrication methodologies – in order to produce operational size maps for appropriate combinations of flow rate and applied voltage/pressure.

Since these encapsulated microbeads are vacuum packed into industrially available functionalized feed pellets ready to be orally fed to the fish, it is imperative to gain a clearer understanding of the porous nature of these feed pellets. Hence, another aim of this research chapter was to analyse their surface morphology through SEM.

Since biological compounds are neither cheap nor readily available, a secondary objective of this study was to gauge the effects of encapsulation on the sizes of alginate microbeads fabricated using ES and AAJ. TiO_2 particles were used as a stand-in for potential API's in this sizing study.

Hydrogel microbeads used for drug delivery can be highly deformable specially the ones ranging from 1 µm to 100 µm. It is the mechanical properties of these microbeads that will determine whether they will be able to withstand the stress and shear forces applied upon them in the microenvironment they may be exposed to (Thanos, Bintz, and Emerich 2007) such as the feed coating stage or in capillaries in vivo, once inside the body. The maintenance of microbead integrity is also crucial in order to prevent immune response, dose dumping and achieving successful optimal performance (Kim et al. 2009). Hence, the final aim of this chapter was to study their mechanical

stability, specifically; the effect of polymer concentration, varying cross-linking agents and fabrication methodologies on the strength of alginate microbeads.

4.2 Optimal Size distribution

Smaller sized particles promote stability in blood circulation, as they possess the ability to permeate through biological barriers more efficiently by passing through capillaries following injection (Manfordini and Veronese., 1998) suggesting that nanoparticles tend to be a superior choice when it comes to targeted drug delivery. On the other hand, larger sized particles are deemed preferential when it comes to vaccine delivery as they produce stronger and more lasting immune responses (Mody et al., 2017).

Once, polymeric microbeads are fabricated the next step is to incorporate them within fish feed pellets for successful oral delivery. There are two methods currently in use for the addition of microbeads into extruded feed pellets; through the pre-extrusion addition with water and meal mix or through vacuum infusion coating, which is the post-extrusion addition with oil. The former method requires a typically high temperature, which can put the biological compound at risk of denaturing, whereas the latter requires low temperatures. Even though, the temperature requirement for vacuum infusion is rather suitable, the process can only be effectively carried out if the microbead is able to fit into the pores present in the feed pellet.

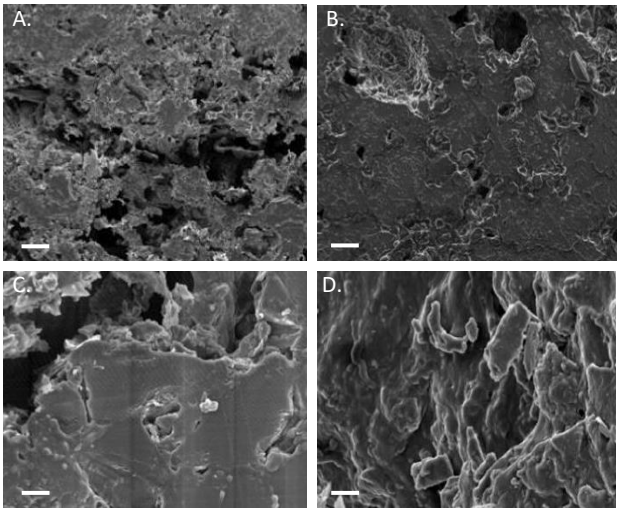

Figure 4-1: *SEM micrographs showing the superficial irregular porous nature of a typical fish feed pellet. The scale bar represents 20 µm. Magnification x 10 (A and B), x 100 (C and D)*

As seen in Figure 4-1, the pores present in feed pellets are not necessarily uniform. The idea is to fit as many microbeads in these pores as possible in order to attain maximum packing efficiency. Depending on the type, size and stage of growth span the fish is in, it will be fed using a specific feed pellet. Thus, depending upon the size of pellet being fed, the size of alginate microbeads able to fit into the irregularly shaped pores will change too.

The functionalised feed pellets consumed in the IPNV trial study are the Commercial Starter feed produced by EWOS. These pellets have a uniform size distribution, roughly 1.3 mm in size. SEM carried out on these feed pellets highlights their porous morphology (Figure 4-1) it was also seen that the sizes of pores present on these pellets ranged from 22 – 47 µm approximately (Figure 4-2). Due to this, it was noted that

successful vacuum packing of microbeads would only be possible if the microbeads themselves are less than 47 µm in size.

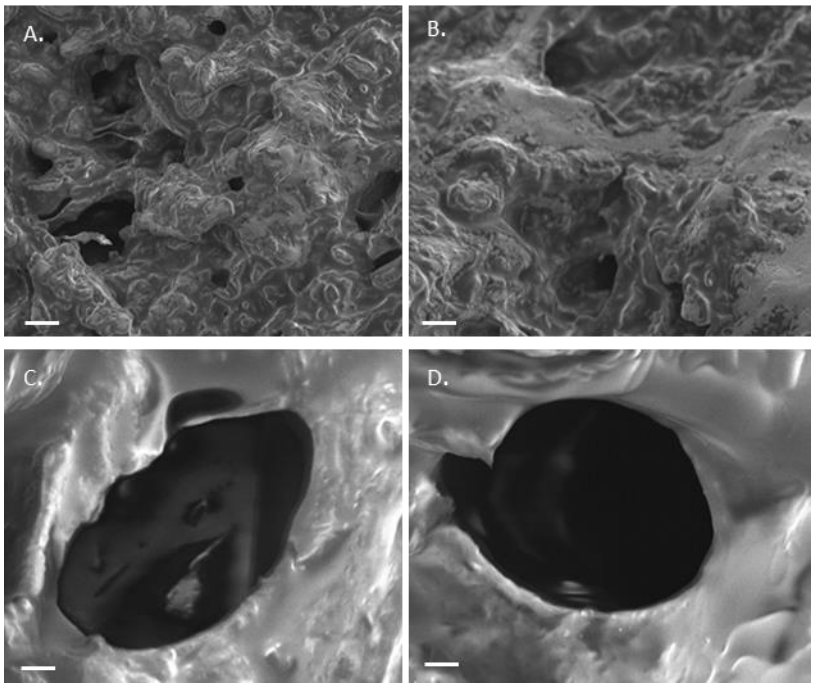

Figure 4-2: *SEM micrographs showing a closer look into the morphology of a 1.3 mm fish feed pellet used in the IPNV fish trials. The scale bar represents 5 µm. Magnification x 10 (A and B), x 100 (C and D)*

4.2.1 Effect of polymer concentration on microbeads produced through electrospraying and aerodynamically assisted jetting

Concentration (%)	Microscopic Images	Observations
0.5	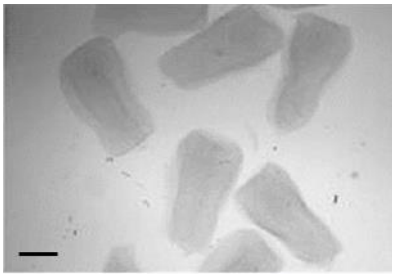	Irregular structures that tend to take a more elongated/cylindrical shape
1	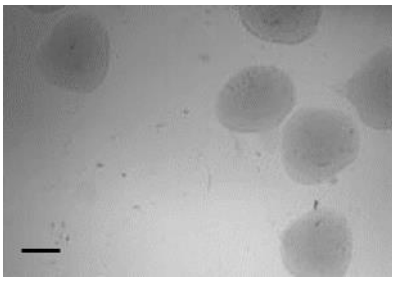	Slightly more spherical beads with tails
1.5	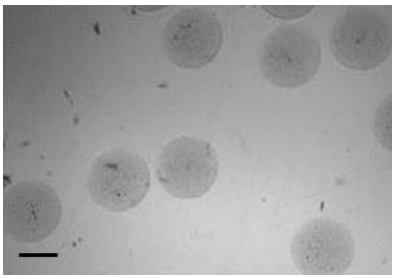	Spherical beads with smaller tails
2	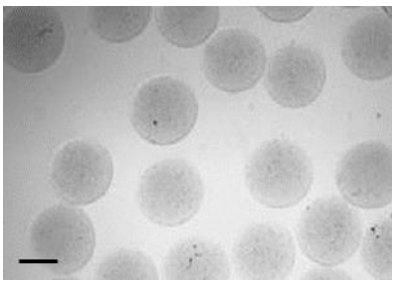	Spherical beads with no tails

Table 4-1: *Comparison of four different alginate concentrations – 0.5, 1, 1.5 and 2%, the corresponding visual representation of microbeads produced (magnification x 8, Leica MZ10F) via ES and observations noted. Scale bar represents 50 µm*

The difference in morphology for microbeads produced using 0.5% concentration is quite visibly different to the sample produced using 2%. This observation is in accordance to previous research where polymer concentration was highlighted as one of the main parameters as far as morphology of electrosprayed particles was concerned (Wu, Kennedy, and Clark 2009).

Two main mechanisms that control the morphology of electrosprayed beads are; 'polymer diffusion' during evaporation and 'solvent evaporation' from droplets when they move from the needle tip to the collector (Almeria et al. 2010). The polymer solution, namely its molecular weight and concentration, will dictate both these mechanisms. A flattened irregular structure was seen for microbeads produced using 0.5% concentration suggesting that a lower polymer concentration favours the production of flat particles rather than take a spherical morphology as shown for microbeads produced using 2% concentration. This can be a direct effect of incomplete solvent evaporation as the solvent contents are comparatively higher for the decreased polymer contents in samples produced using a lower polymer concentration. Hence, particles produced using a lower polymer concentration are moderately dissolved and not completely dried when they touch the collector therefore leading to irregular or semi-solid, flat particles that solidify fully only after deposition (Bock et al. 2011).

Moreover, chain entanglements also have an effect on the physical properties of particles produced. Solutions with lower concentrations contain less entanglement possibilities for polymer chains. However, at higher solution concentrations, the same available hydrodynamic volume will contain more polymer chains thus increasing chain entanglements. It has been shown previously that if the evaporating droplets have an adequately entangled network before reaching Rayleigh's limit, the particles produced will be spherical in nature and also monodispersed. Since the entangled

network will help stabilise the droplet against rupture therefore also reducing the possibility of smaller and more irregular offspring particles being produced (Almeria et al. 2010).

A similar trend was witnessed for microbeads produced using AAJ. Particles produced with 0.5% and 1% concentration solution took the form of irregular structures. Whereas, particles produced using 1.5% and 2% concentration solution started taking up a spherical shape. This again can be explained using the aforementioned mechanisms; polymer diffusion during evaporation, solvent evaporation during droplet moving from exit orifice to the collector and finally the number of chain entanglements increasing with increasing polymer concentration. Hence, spherical particles are generated when a sufficiently entangled network is present before the Rayleigh's limit is achieved by the droplets (Almeria et al. 2010). Another observation that was noted during the use of 0.5% and 1% alginate concentration was the consistent spitting at the exit orifice. This suggested that the jet produced was not stable as the entangled network was not adequate enough to stabilise the droplet against rupture due to the applied pressure force, hence giving rise to many secondary (offspring) particles, too. Research by Xie and Wang (2007) also concluded that the morphology of particles tends to become worse with a decrease in polymer solution concentration.

The results gained through this experiment as highlighted in Table 4-2, supported this research as the standard deviation for samples produced using 2% (w/v) concentration was the smallest, suggesting that this sample produced was in fact the most homogenous and monodispersed. Due to this, it was decided to produce the operational maps for microbead sizes (Section 4.2.2) using this concentration.

Concentration (%)	Microscopic Images	Observations
0.5	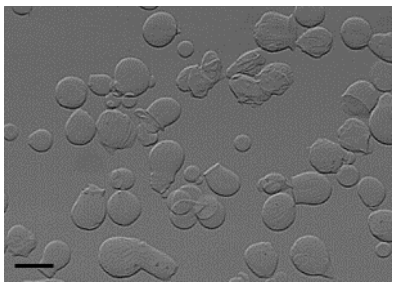	Constant spitting observed at the exit orifice. Multiple jetting witnessed and irregular shaped structures produced
1	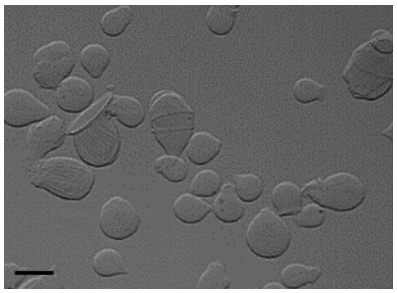	Unstable aerodynamic conditions such as constant spitting at the exit orifice. Irregular shaped structures produced
1.5	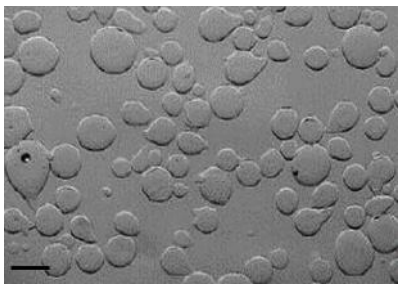	Beads take a slightly more spherical shape but possess tails
2	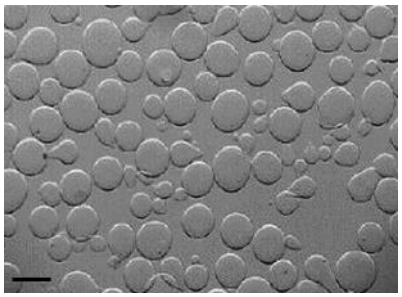	Beads much more spherical in shape however some beads with tails still present

Table 4-2: *Comparison of microbeads produced using four different alginate concentrations – 0,5, 1, 1.5 and 2%. The corresponding visual representation of microbeads produced (magnification x40, Leica MZ10F) via AAJ and observations noted. Scale bar represents 40 µm*

4.2.2 Effect of process parameters on the size of microbeads produced using electrospraying and aerodynamically assisted jetting

The first and main process parameter analysed was flow rate. For both processing methodologies it was seen that an increase in flow rate showed an increase in the microbead size, too (Figure 4-3 and 4-4). This can be owed to the fact that at lower flow rates, a smaller volume of solution is ejected from the needle tip and therefore electrohydrodynamic forces have insufficient solution to act on (Pancholi, Stride, and Edirisinghe 2008). It was also seen that with a gradual increase in the flow rate at a constant voltage, only a slight increase in microbead size is seen due to the electric field strength not being capable of breaking the jet formed by the constantly increasing ejected solution as there is an insufficient amount of charged ions present (Zargham et al. 2012).

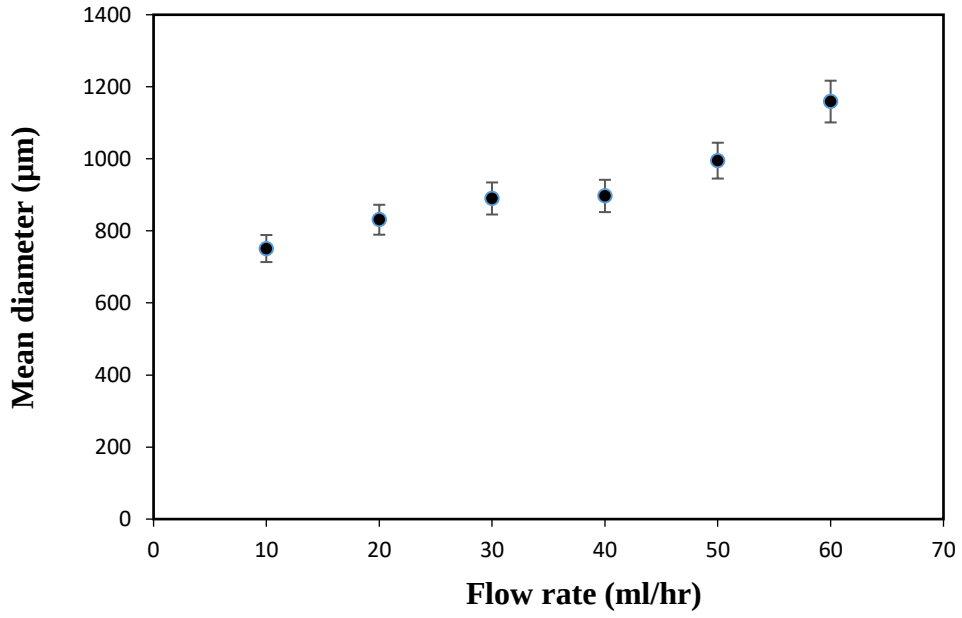

Figure 4-3: *The effect of flow rate (ml/hr) on the mean diameter (**µ**m) of beads produced using ES (n=5). While flow rate was varied from the range 10 – 60 ml/hr, the voltage was kept constant at 4 kV*

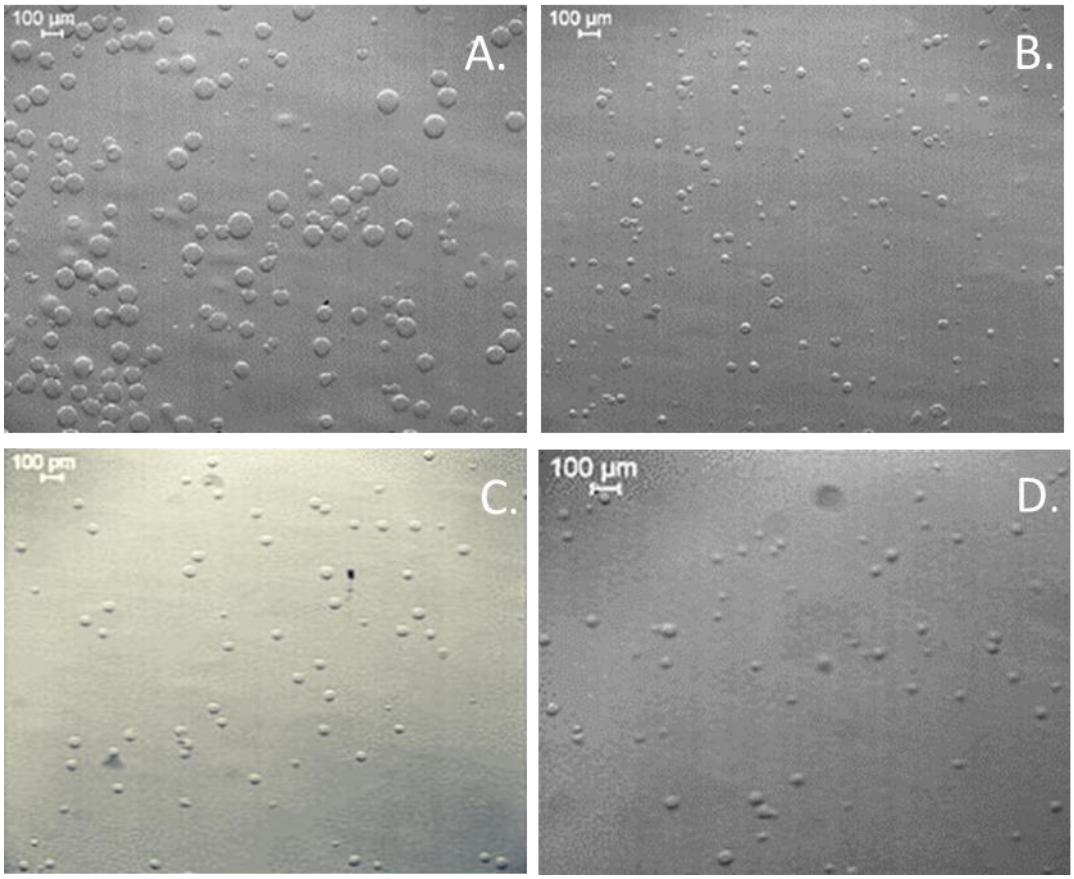

Figure 4-4: *A visual representation of microbeads produced using AAJ at the following parameters A) flow rate: 60ml/hr, pressure: 0.1 bar B) flow rate: 60ml/hr, pressure: 0.5bar C) flow rate: 20ml/hr, pressure: 0.1 bar D) flow rate: 20ml/hr, pressure: 0.5bar (n=5). Images taken using optical microscopy (MZ10 F, Leica microsystems) at magnification x 80*

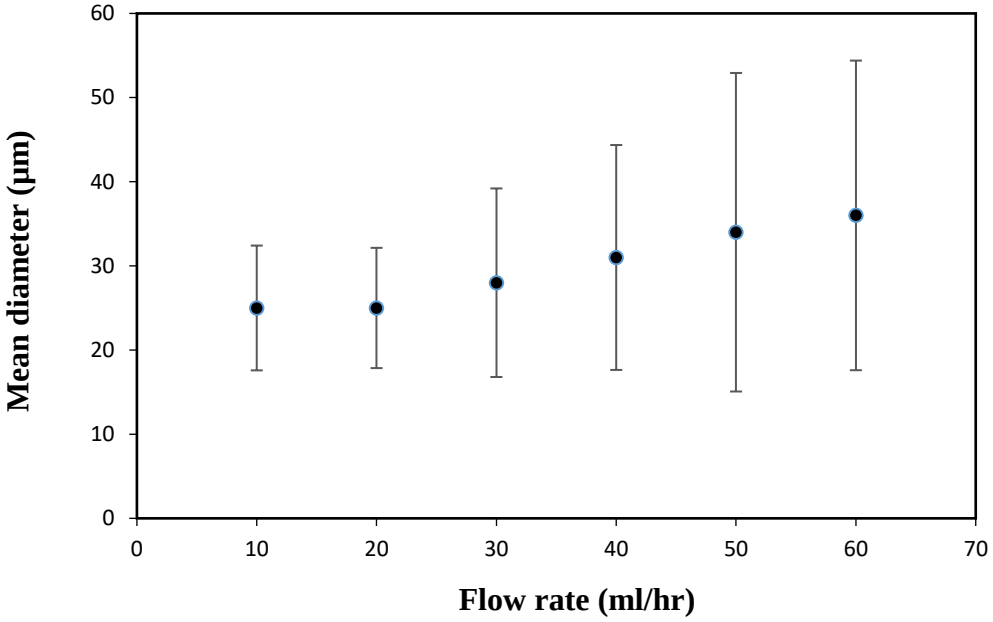

Figure 4-5: *Graph showing the effect of flow rate (ml/hr) on the mean diameter (**µ**m) of beads produced using AAJ (n=5). Flow rate varied from the range 10 – 60 ml/hr while the pressure was kept constant at 0.8bar*

As clear from the trend witnessed in Figure 4-5, flow rate had the same effect on microbeads fabricated using AAJ as it did on ES fabricated ones. An increase in flow rate showed an increase in the mean size of microbeads. This is because for the same amount of aerodynamic forces, there is now more solution present. Hence, the same mechanism that applies for electrospraying and flow rate, can be applied here too. This trend is supported by previous research (Xie, Marijnissen, and Wang 2006) which also suggests that the solution flow rate is one of the dominant factors which contribute to particle size, and also observed the trend of particle size decreasing with decreasing flow rate.

It was also noted that below 10 ml/hr, backflow was observed. Due to the low flow rate, the corresponding low applied pressure did not allow for jetting to take place. The pressure instead gave rise to the formation of bubbles in the silicone tubing holding the flow of the polymer media thus resulting in back flow.

On the other hand, the second process parameter affecting microbead size for electrospraying; *'applied voltage'* had the opposite effect on size of microbeads fabricated. The microbead size decreased with an increase in voltage (kV) as seen in Figure 4-6. The effect of applied voltage on the flowing liquid is the induction of charge on the surface of the droplet generated. The charge is accelerated towards the apex of the droplet which helps the formation of a jet which eventually (depending on the level of voltage applied) breaks up into main, secondary and/or satellite droplets (Gomez and Tang 1994). Hence, as the voltage increases the meniscus formed at the needle tip elongates further due to the electrostatic forces present, causing smaller droplets to detach from the meniscus.

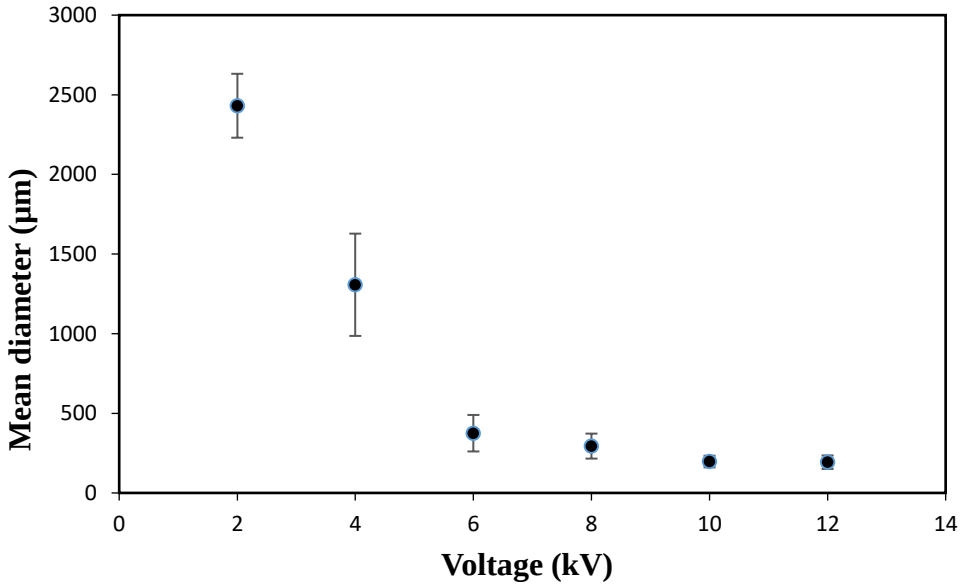

Figure 4-6: *The effect of voltage (kV) on the mean diameter (µm) of beads produced using electrospraying (n=5). Voltage varied from the range 2 – 12 kV while flow rate kept constant at 40 ml/hr*

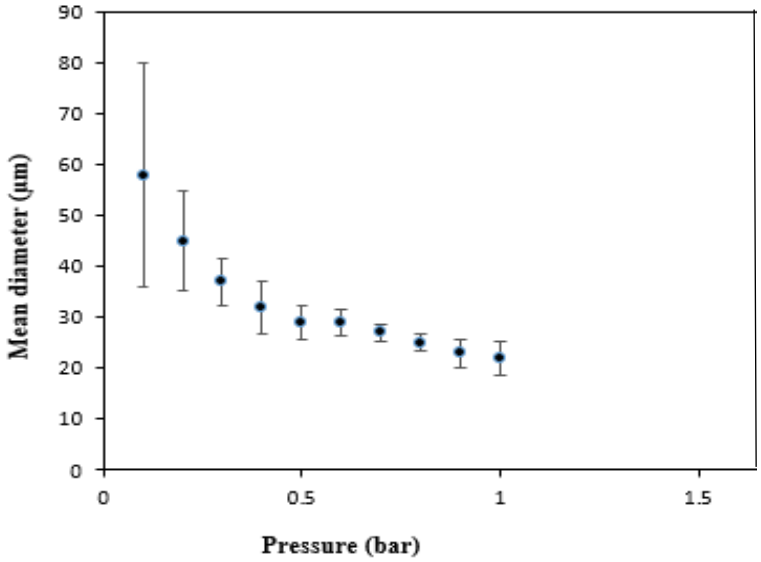

Figure 4-7: *The effect of pressure (bar) on the mean diameter (µm) of beads produced using aerodynamically assisted jetting (n=5). Applied pressure varied from the range0.1 – 1bar while flow rate was kept constant at 40 ml/hr*

The second process parameter known to have an effect on microbead size produced using AAJ is *applied pressure*. It was seen that an increase in applied pressure also showed a decrease in the size of microbeads produced. Hence, for a constant flow rate but an increasing external applied pressure, the pressure gradient becomes higher which eventually breaks the jet up into smaller and smaller droplets. Once the liquid jet leaves the exit orifice, the pressure gradient - which at this point is acting as the main accelerating force in the axial direction - will vanish and the jet evolves under the influence of the viscous shear stresses exerted by the gas flow on the jet surface and the capillary stress (Ganan-Calvo and Barrero 1999). The standard deviation seen in figure 4 -7 is due to the pressure gradient not being enough to break the jet up into monodispersed particles, which means more offspring particles are present now due

to the liquid being jetted under unstable conditions. Arumuganathar et al. (2007) concluded that for a constant flow rate, if the pressure was too low, the medium flowing through the needle will be drawn out but not be jetted under stable conditions due to varied aerodynamic force flows. This tends to give rise to a more polydispersed sample with unwanted residues as seen in Figure 4-8.

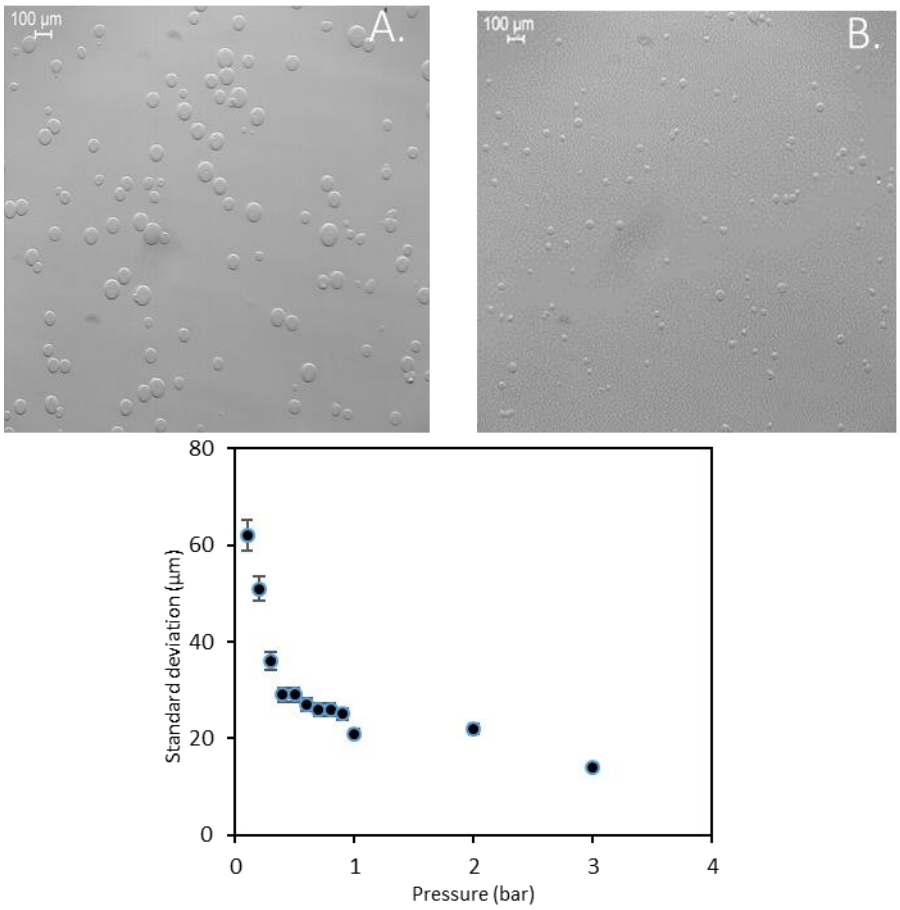

Figure 4-8: *Microscopic images (A – B) showing samples produced using a constant flow rate of 40 ml/hr but varying applied pressure A) pressure: 0.1 bar B) 0.4 bar. Graph showing the relationship between pressure and standard deviation of samples produced. The standard deviation very clearly decreases with an increase in pressure showing the formation of a more monodispersed sample (n=5). The flow rate was kept constant at 40 ml/hr while the pressure varied from 0.1 – 3 bar*

Lastly, the effect of collecting distance was assessed to see if it had any consequences on the size of microbeads produced. It was seen that an increase in distance also increased the particle size. This can be owed to the decreased strength of the electric field at larger distances. The strength of electric field is dependent upon the applied voltage divided by the distance of collection. Therefore, at these smaller distances the role of solvent evaporation becomes negligible when compared with that of the electric field. However, it was also noticed that with an increase in distance, the morphology of particles started changing too. As seen in figure 4-9 below, the particles started becoming less and less spherical. This can be attributed to solvent evaporation before the droplet reaches the collector plate.

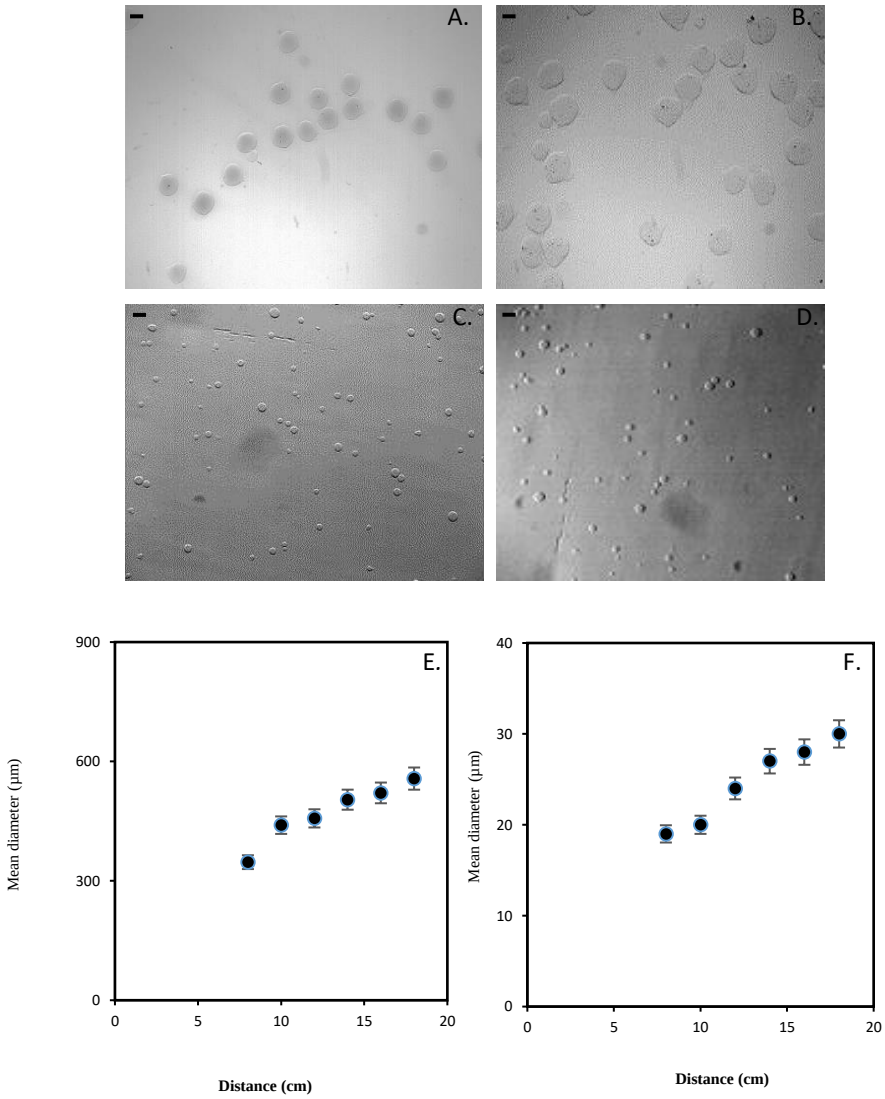

Figure 4-9: *Optical images of samples produced using ES with collecting distance A) 8 cm B) 18 cm, and AAJ with collecting distance C) 8 cm D) 18 cm D) AAJ. The scale bar represents 200 µm. Graphs E and F showing the relationship between mean size and distance between needle and collector - ES and AAJ respectively). Both the graph's show a positive correlation as an increase in distance also increases the mean diameter of microbeads produced (n=5)*

4.3 Operational size maps

An intensive sizing study was carried out and operational maps were created which will be able to highlight alginate microbead size produced for every appropriate combination of flow rate (ml/hr) and applied voltage (kV)/applied pressure (bar).

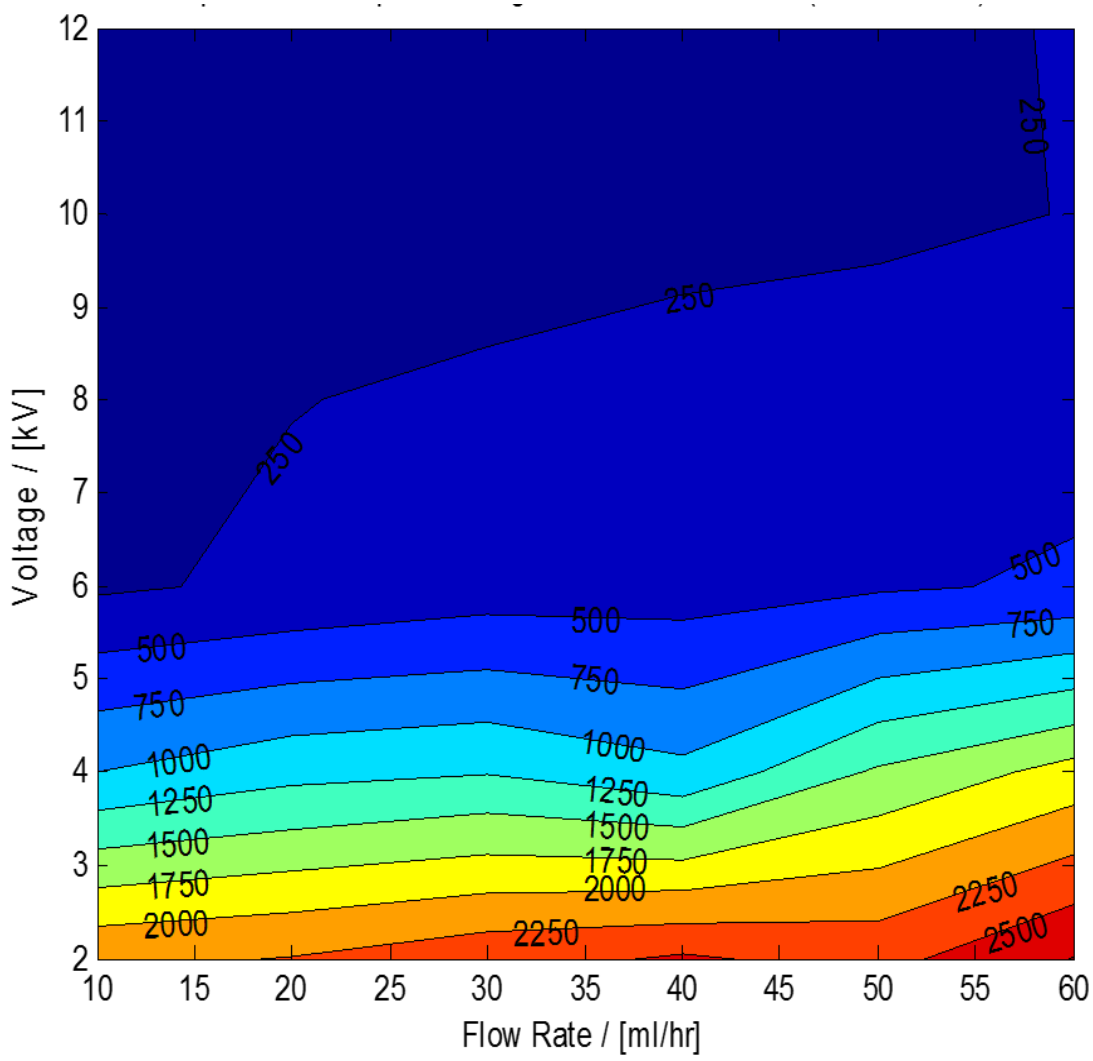

Figure 4-3: *Operational size map of 2% alginate microbead sizes (μm) produced using ES, created for each appropriate combination of flow rate (ml/hr) and applied voltage (kV)(n = 5)*

Parameter selection was carefully carried out. For the ES process, it was not deemed suitable to go further than 60 ml/hr since beyond that, microbeads with tails were being generated which are not suitable for vacuum packing in the crevices of feed pellets. Voltage was not assessed beyond 12 kV simply because characteristics of discharge became apparent through electric sparking. This was due to a sufficiently high electric field being created. Electric field being a function of voltage and distance;

$$E = {}^{V}/_{d}$$

where E is the electric field, V is the applied voltage and d is the distance between the two electrodes. This could not have been avoided since it was critical to keep all other parameters constant e.g. distance between needle and electrode and distance between needle and collector while only altering the flow rate and voltage.

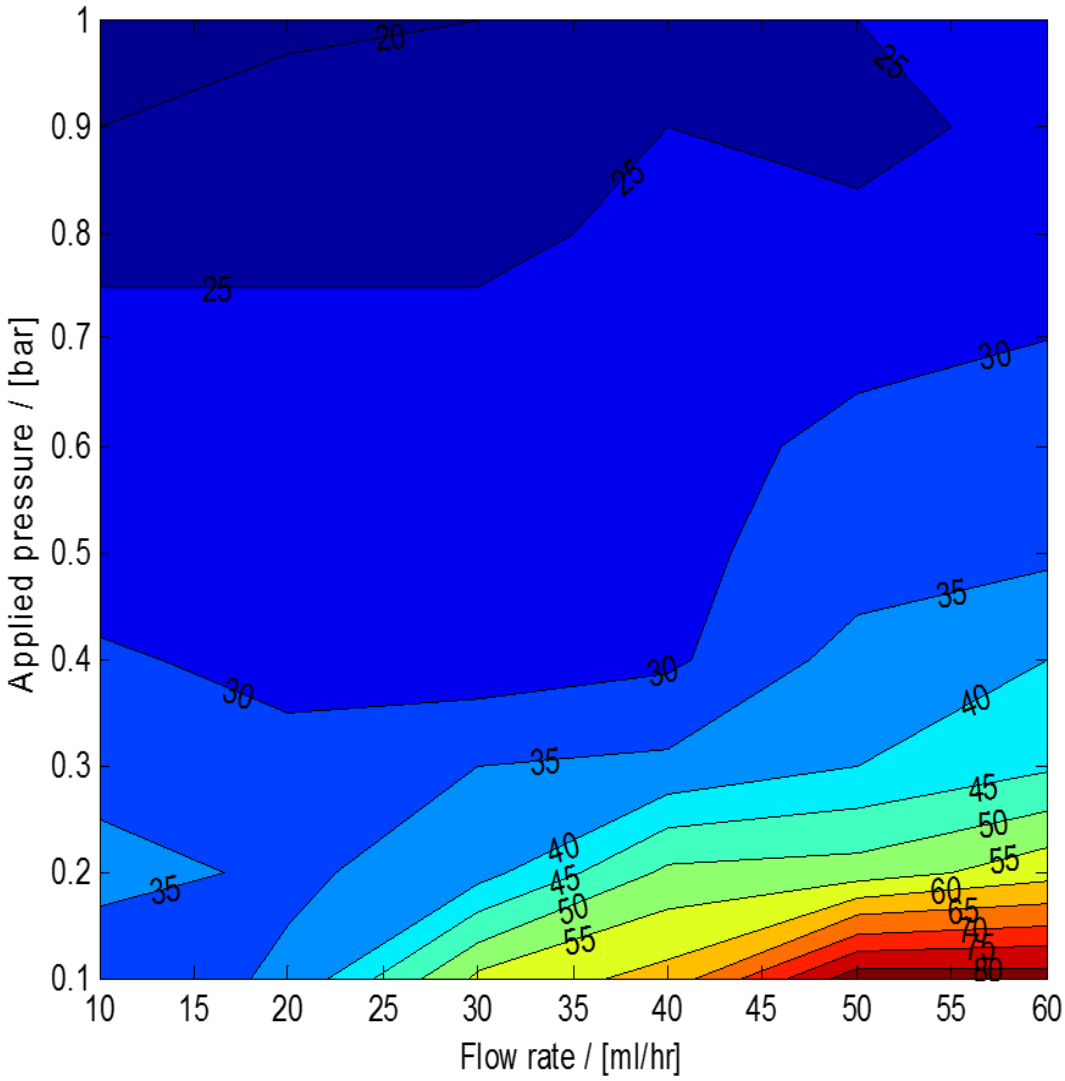

Figure 4-4: *Operational size map of 2% alginate microbead sizes (µm) produced using AAJ, created for every appropriate combination of flow rate (ml/hr) and applied pressure (bar) (n = 5)*

The parameter selection of the operational map created for microbeads produced using AAJ was as follows; flow rate was assessed till 60 ml/hr to keep in accordance with the ES operational map. Pressure was not assessed beyond 3 bar as beads sized 10 µm were achieved at that point and most pore sizes in industrial feed pellets range from 10 µm to 500 µm (Klaric, 2015).

The range of microbead sizes produced through ES using the chosen parameters was 250 – 2500 µm (Figure 4-3). Whereas microbeads produced using AAJ ranged from 20 – 80 µm (Figure 4-4). This is not to say that ES and AAJ can only produce alginate microbeads within these specified size ranges as this range is solely specific for the chosen parameters in this study.

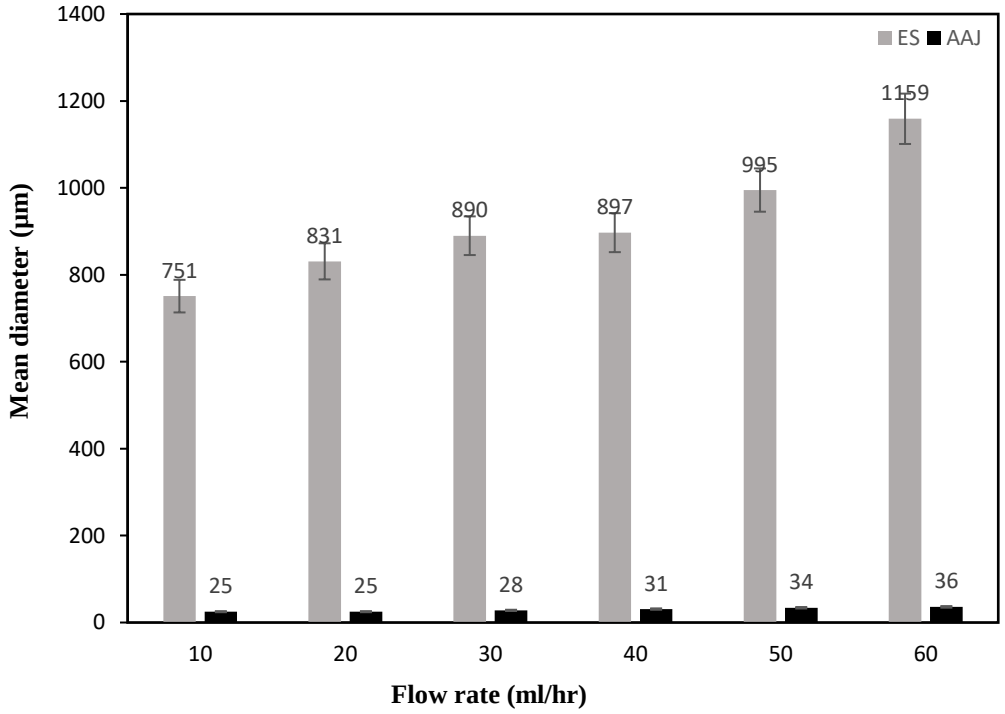

Figure 4-5: *Bar chart comparing the mean sizes of microbeads produced using ES and AAJ at a given flow rate (ml/hr) (n=3)*

4.3.1 Inclusion of TiO_2 in microbeads to act as a stand in for potential API's

The operational maps shown in Figure 4 - 3 and 4 - 4 were of empty alginate microbeads. The final objective of this project however is to have biological

components (mainly vaccines) encapsulated within these microbeads. Since vaccines are quite an expensive biological component, it was deemed suitable to use an appropriate marker that would perhaps act as a stand in for a vaccine in order to see if and how the encapsulation of a material may affect the size of microbeads produced using the two fabrication methodologies; ES and AAJ.

TiO_2 is an inert and indigestible marker that has been used in various studies to assess the digestibility of diets, mostly in ruminants (Titgemeyer et al. 2001). In order for encapsulation to successfully occur, the marker had to be smaller than the micron range. TiO_2 particles were sized using Transmission Electron Microscopy (TEM) and as seen in Figure 4-6 the particles were found to be in the nano range.

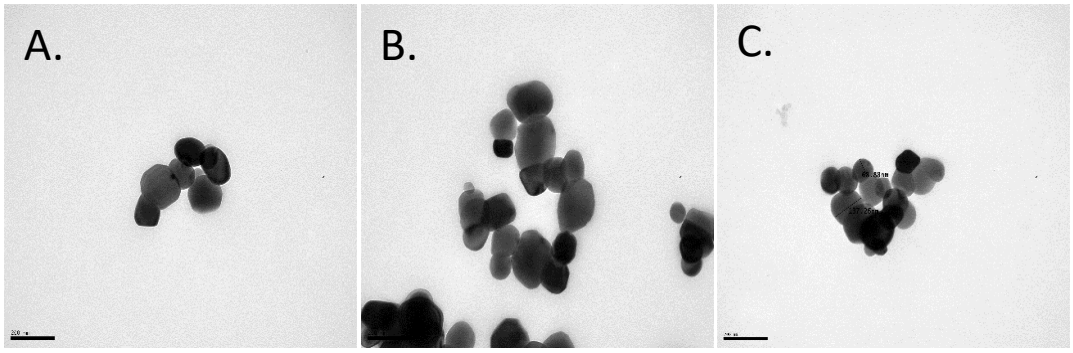

Figure 4-6: *TEM images obtained of TiO_2 particles showed that their sizes ranged from 50nm – 200 nm (Magnification x 100,000). Scale bars represent 200 nm*

Different concentrations of TiO_2 in 2% alginate were then assessed; 0.5%, 1%, 1.5% and 2%. It was seen that stable jetting was only achieved with the use of 2% TiO_2 in 2% alginate. Stable jetting is significant since it allows for a monodispersed sample to be produced. Hence, the use of 2% TiO_2 in 2% alginate was seen appropriate for the production of microbead size operational maps. The same parameters that were used

for only 2% alginate microbeads were used for the TiO_2 inclusive maps, too. Since TiO_2 was in powdered form, a concern was the onset of 'sedimentation' once incorporated into alginate solution. However, a sedimentation test was carried out where 2% alginate solution + 2% TiO_2 was observed for 48 hours. No visible sedimentation of TiO_2 particles was observed during this period of time.

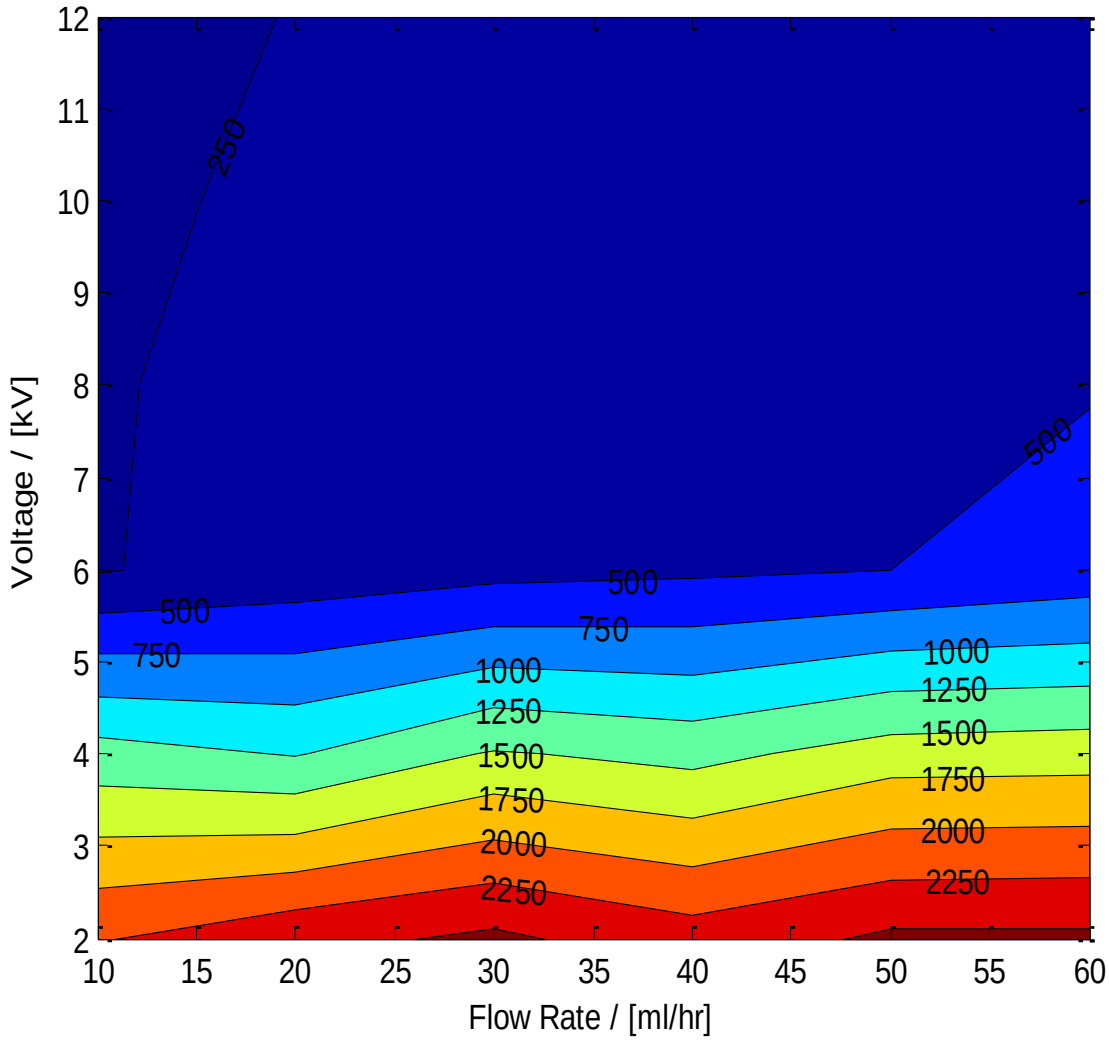

Figure 4-7: *Operational map of 2% alginate and 2% TiO_2 microbead sizes(μm) produced using ES, created for each combination of flow rate (ml/hr) and applied voltage (kV) (n=5)*

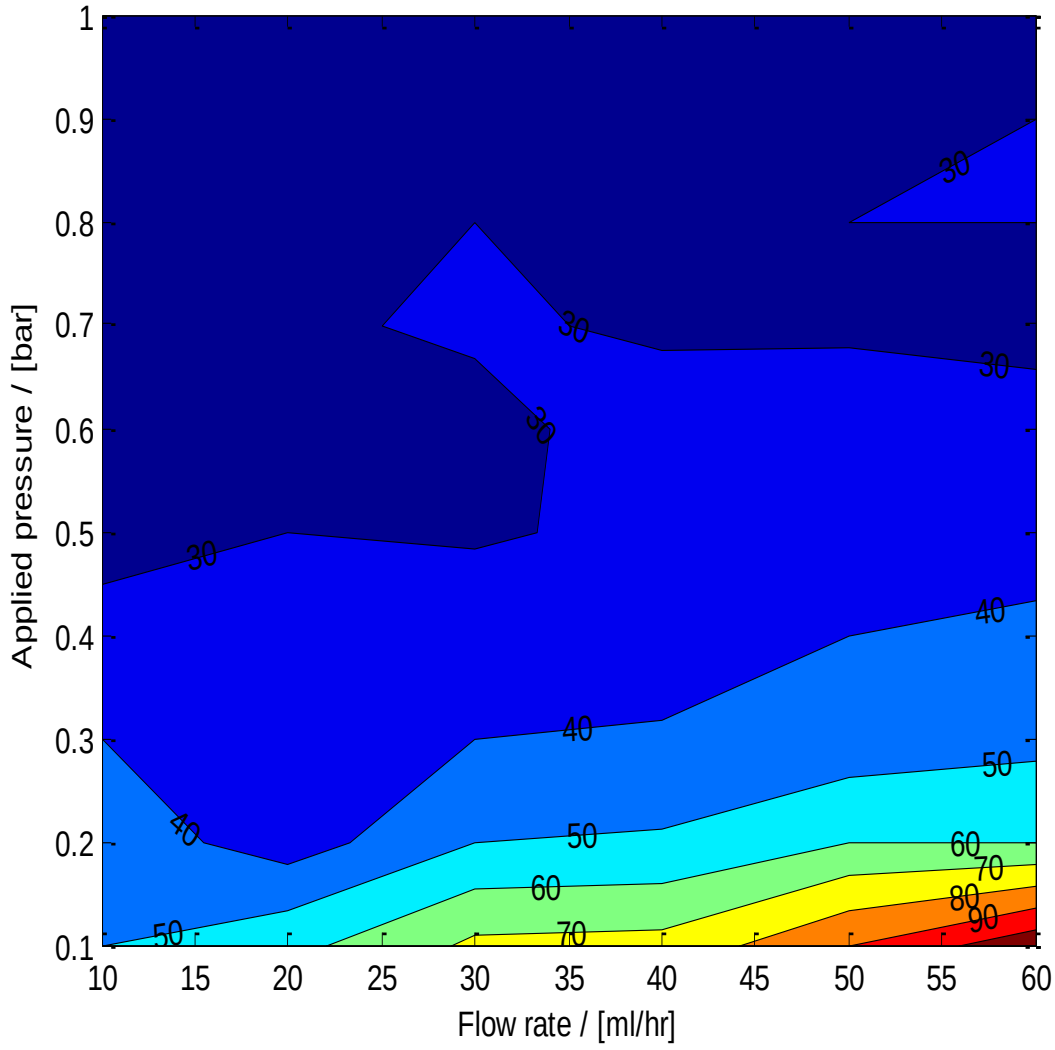

Figure 4-8: *Operational map of 2% alginate and 2% TiO_2 microbead sizes (μm) produced using AAJ, created for each combination of flow rate (ml/hr) and applied pressure (bar) (n=5)*

A slight increase in microbead size ranges was witnessed for beads produced using both fabrication methodologies as seen in Figures 4 - 7 and 4 - 8. However, the effects of process parameters followed the same trend. An increase in flow rate increased the size of microbeads produced (at constant applied voltage or pressure) while an increase in either voltage or pressure decreased the size of microbeads produced (at a constant flow rate).

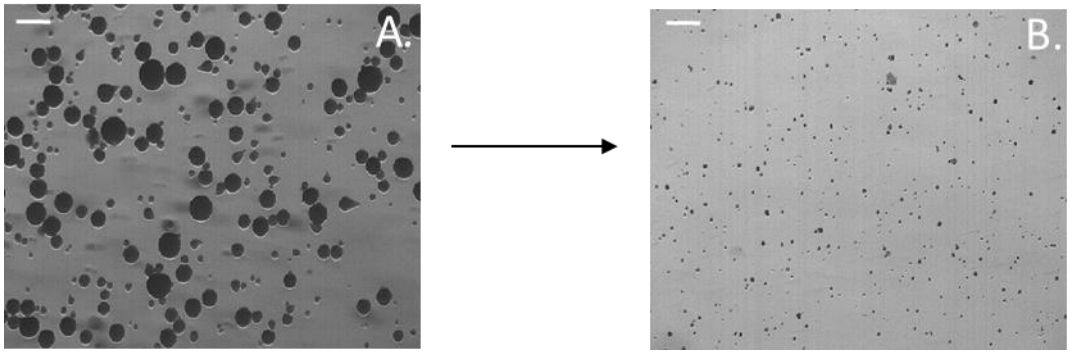

Figure 4-9: *2% Alginate + TiO_2 microbead samples fabricated through AAJ using flow rate: 60 ml/hr at varying pressures A) Pressure: 0.1 bar B) 3 bar. It can clearly be seen that bead size drastically decreased with increasing pressure. Further supported by microbead sizing which revealed the mean diameter of sample A) 1232 µm and B) 334 µm. Both images taken at x10 magnification (n=5). Scale bar represents 250 (µm)*

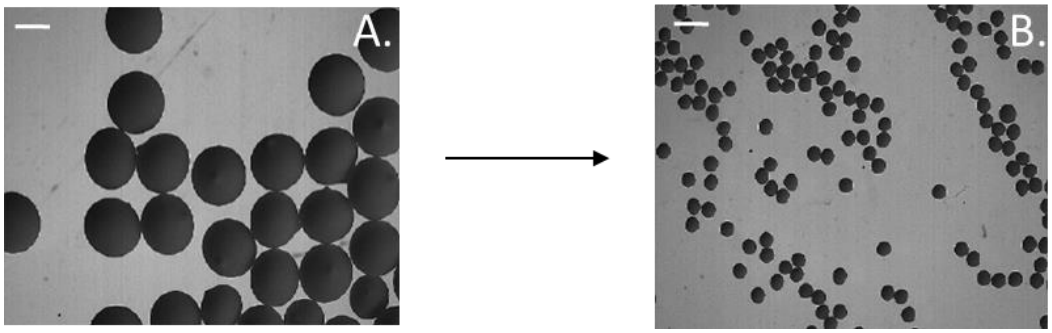

Figure 4-10: *2% Alginate + TiO_2 microbead samples fabricated through ES using flow rate 20 ml/hr at varying voltages A) Voltage: 4 kV B) 8 kV. It can clearly be seen that bead size drastically decreased with increasing voltage. Further supported by microbead sizing which revealed the mean diameter of sample A) 1232 µm and B) 334 µm. Both images taken at x10 magnification (n=5). Scale bar represents 250 (µm)*

These results will be further supported by data gained in Section 6.2.1 where 2% alginate + TiO_2 microbead sizes will be compared with 2% alginate + IPNV antigen,

to see whether the changes in size ranges remain constant to support the use of TiO_2 as a cheap and readily available stand in for vaccine for size distribution studies.

4.4 Morphological characterisation

As mentioned earlier, irregular shapes have been associated with protrusion of any type of encapsulated component. Therefore, the ideal shape of microbeads needs to be spherical. Optical microscopic images of alginate microbeads generated using four different fabrication methodologies were obtained. Even though the microbead shapes were quite clearly etched out, and showed a perfectly spherical shape - as can be seen in Figure 4-11 - the optical microscopy technology offers a fairly low resolution along with a smaller depth of field.

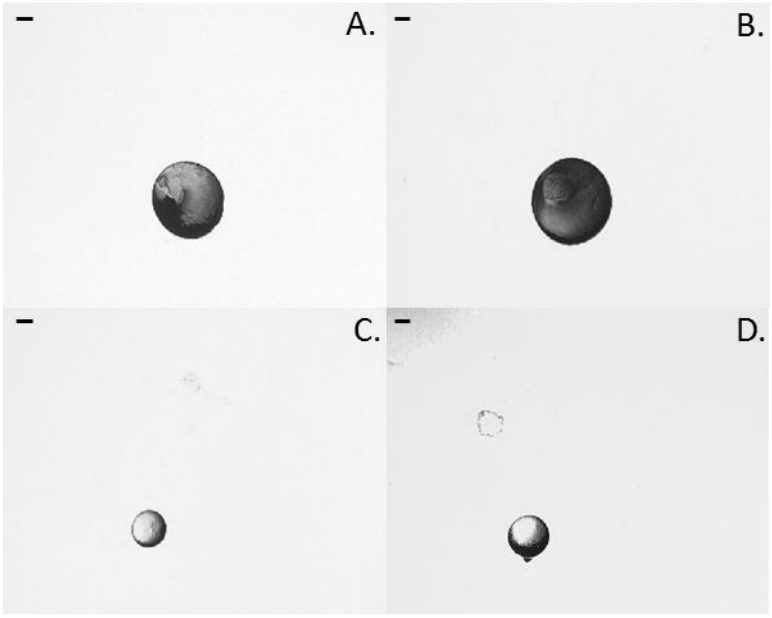

Figure 4-11: *Optical microscopic images of 2% alginate microbeads fabricated using A) ES B) Manual deposition C) AAJ D) ES in combination with AAJ. Microbeads were seen to be spherical in shape regardless of the processing methodology used. Scale bar represents 200µm*

The most commonly used technologies to assess the morphological characteristics of particles are AFM and SEM. However, both come with their own drawbacks.

Atomic Force Microscopy (AFM) is a technology that is known to image almost any type of surface, both conducting and semiconducting. This is done by using a cantilever with a sharp probe (diamond or gold coated tip) that scans the sample's surface. However, since the cantilever drags across the sample surface in order to operate, it is not a viable option to assess alginate microbeads that are gel-like and therefore extremely vulnerable to damage and rupture.

Scanning Electron Microscopy (SEM) is another commonly used process to obtain insight on surface morphology. However, this technology requires surface stain coating (usually with an ultrathin coating of an electrically conducting material, normally gold) in order to avoid scanning faults and image artefacts. Therefore, SEM is limited to solid, inorganic samples which are capable of handling vacuum pressure (Anderson., 2012). Surface coating of alginate microbeads is hence not a possibility since that process will undeniably alter the bead's surface morphology. Since alginate is a hydrogel, its hydrophilic structure means they have the capability of holding large amounts of water in their three-dimensional networks (Ahmed 2015).

This means that taking a microbead out of the cross-linking solution for a long period of time for the surface morphology assessment procedure (including coating) may cause distortions such as shrinkage. Freeze-drying is a process that helps reduce shrinkage which occurs when a wet specimen dries through evaporation. This is because freeze-drying causes fast sublimation of frozen water from the alginate matrix thus resulting in the production of pores in areas where ice crystals were formally situated, without any time for shrinkage. This was observed when SEM was carried

out on electrosprayed alginate microbeads. The samples were clearly not able to withstand the vacuum pressure present as the microbeads severely dried out as seen in figure 4 - 2.

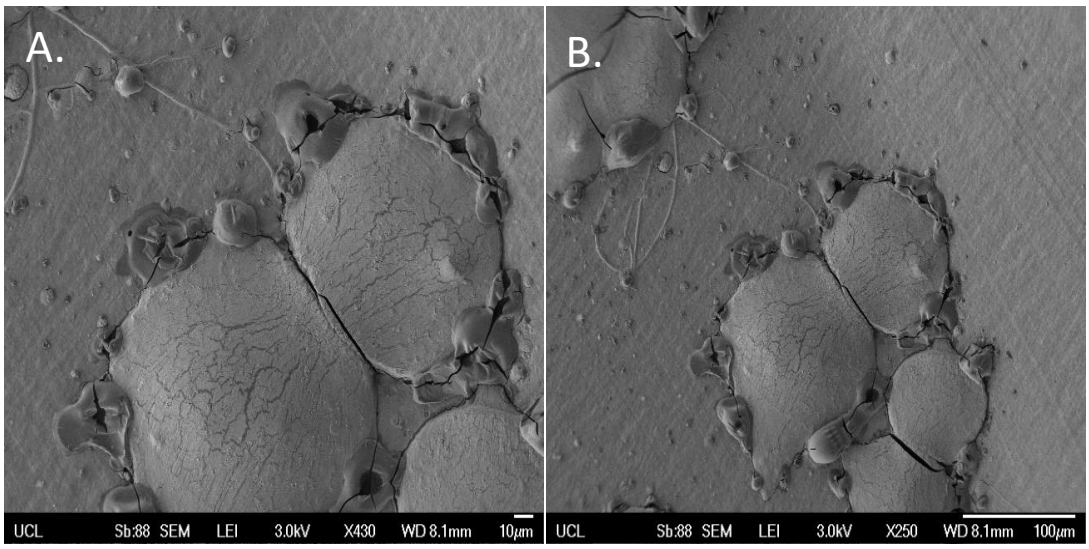

Figure 4-12: *SEM images of 2% alginate microbeads produced using electrospraying Scale bar represents A) 10 µm and B) 100 µm*

However, non-conducting samples can be imaged without coating using specialised SEM instrumentation known as the 'Environmental SEM' which operates at a much lower vacuum.

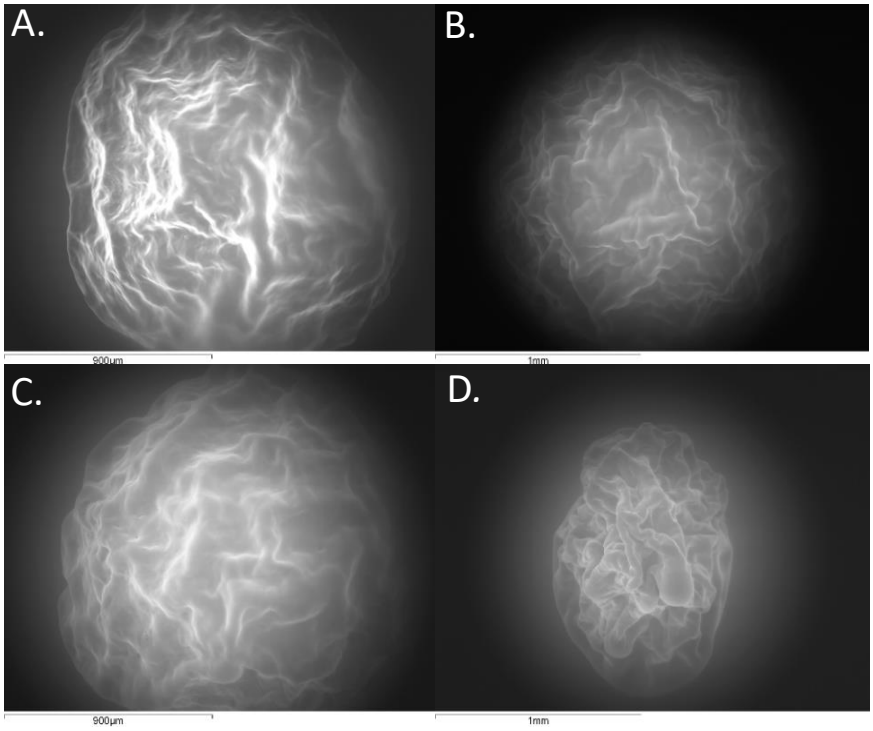

Figure 4-13: *ESEM images of 2% alginate microbeads produced using A) ES B) Manual deposition C) AAJ D) ES in combination with AAJ. Each microbead was mounted onto a stub, individually and observed under ESEM operated at 10kV. 2 different magnifications used; x160 (A and C) x125 (B and D)*

Due to constant shrinking of the specimen and also desiccation and rupture in some cases, it wasn't possible to obtain absolutely accurate images of the original surface morphology of the microbeads using ESEM and a wrinkled morphology was observed on the surface of all specimen. However, it is clear that ESEM images show similar topographical variations present on each specimen's surface. The same irregular surface morphology for all four microbeads was observed even though they were produced using four different fabrication methodologies. Hence, it can be suggested that microbeads produced using ES and AAJ had the same morphological traits as those produced through manual deposition.

4.5 Mechanical Testing

Alginate gels are known to degrade slowly as the mechanical properties of these gels are altered with time (Langer et al., 2006). Tablets, beads and capsules are usually assessed for strength/deformation through a compression test, as illustrated in figure 4-14, this test determines the behaviour of a material under a crushing load. Therefore, it was deemed feasible to define mechanical stability of microbeads through two parameters; strength and elasticity. The strength will be measured by quantifying the force required to compress a microbead while elasticity being dependent upon the time required to compress the specific bead to a set value. The combination of these values will be able to determine the success or failure of these microbeads in vivo.

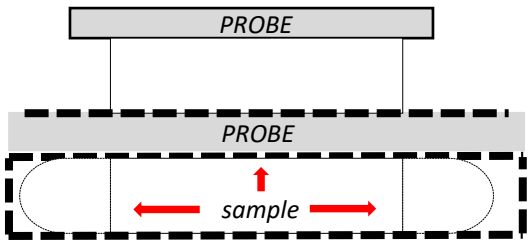

Figure 4-14: The geometry of a sample tends to change as friction is produced at the test interface. During the compression test a sample will get crushed/squashed in one direction while remaining unrestrained in the other two directions

Previous research states that both strength and elasticity are significant factors for the functional survival of cells as far as in vivo application is concerned (Stabler et al. 2001). According to (Morch et al. 2006) the mechanical stability of beads is determined by alginate concentration and the type of gelling cation applied. Hence the

mechanical testing study was divided into three main objectives; to assess the effect of alginate concentration on the strength of microbeads, to see the effect of varying cross-linking agents and lastly to determine the effect of microbead fabrication methodologies on the strength of these microbeads.

Microbeads tested were all spherical in shape since irregular shapes have been associated with protrusion, which is unsuitable for cell encapsulation for immunoprotection (DeVos et al. 1996). This can be applied to other biological compounds as well such as vaccines in this particular case.

4.5.1 Effect of alginate concentration on mechanical stability

Results gained in this study show that compression is influenced by the concentration of alginate solution used. Figure 4-15 (A) shows a positive correlation between solution concentration and force applied. This means that a microbead produced using a more concentrated solution e.g. 2% will also need a higher amount of force to be applied for the microbead to reach 60% deformation i.e. 10.7g as compared to a bead produced using 0.6% alginate solution which will require less than half the force i.e. 3.7g to reach the same level of deformation. The time required to compress the microbeads was also seen to increase linearly with the concentration of alginate used to produce the microbead. For example, 0.6% concentration solution reached the 60% deformation limit at 63 seconds while a bead produced using 2% alginate solution reached the same amount of deformation in 121 seconds. Hence suggesting that a microbead produced with a more concentrated solution is more mechanically stable.

A.

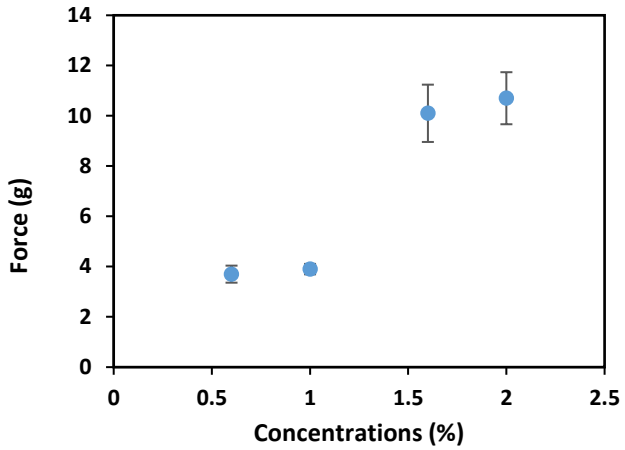

B.

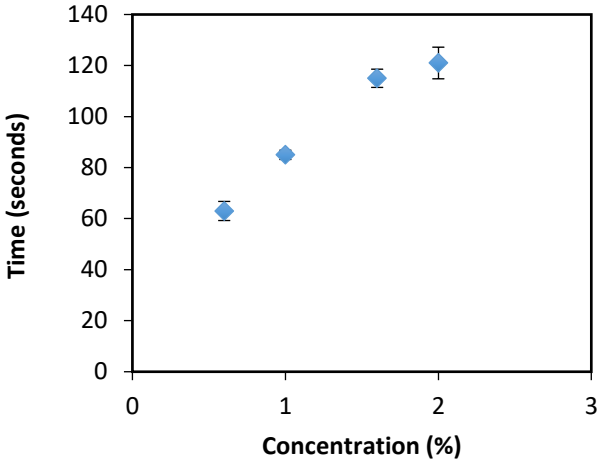

Figure 4-15: *Graph presenting the relationship between alginate concentration (%) and A) the force required to compress the microbead till it reaches 60% deformation and B) time required to compress the microbead to 60% deformation. Size of microbead and time of gelation were kept constant throughout (n=5)*

The viscosity of an alginate solution increases with higher concentrations of alginate (Chan et al. 2009). A more concentrated and viscous bead will contain more polymer chain entanglements within itself, which will therefore require a higher amount of force to overcome in order to reach a given level of deformation. These results were

also supported by previous research, namely Devi et al. (2010) who also reported an increase in bead strength with increased concentration of alginate solution. This trend was observed for alginate microbeads cross-linked using $SrCl_2$ and $BaCl_2$, as well.

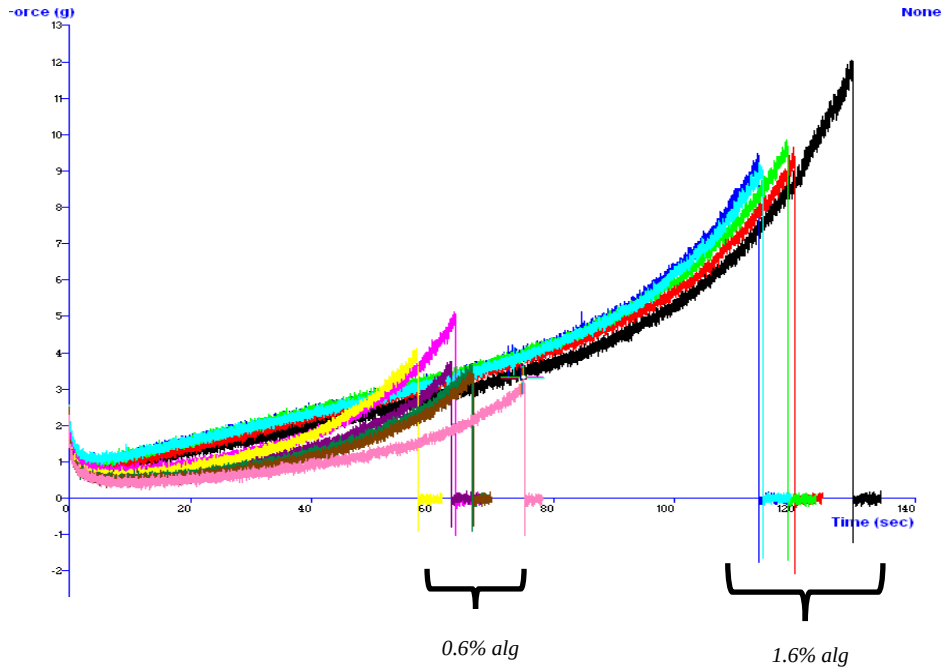

Figure 4-16: Representation of raw data acquired using the TA.XT Plus Texture analyser software version 6.0. Force (g) against time (sec) graph. The 2 sets of data represent the mechanical strength of microbeads produced using 0.6% alginate and 1.6% alginate (n=5)

To make sure it was only the varying concentration affecting the strength of microbeads and not other variables, it was made sure that all the microbeads produced were kept at a consistent size and also kept in the cross-linking solution for a set time, each. Research suggests that both these factors will otherwise have an effect on the mechanical stability of beads (Vaithilingam et al. 2011). While the effect of size will

be discussed later in this thesis, the consequence of altering the time an alginate microbead is kept in contact with cross-linking solution (also referred to as gelling time) can be explained as follows; alginate creates junction zones when it comes in contact with a cross-linking agent, an increase in gelling time will also increase the number of junction zones until a saturation point is achieved. Since unzipping these junction zones is a co-operative process, when gelling time increases, more and more cations take part in the formation of junction zones. This also increases the susceptibility for uncoupling in the junction zones (Zhang, Daubert, and Foegeding 2007). Bhujbal et al. (2014) also supported this mechanism by reporting that an increase in gelling time decreases the mechanical strength of beads.

4.5.2 Effect of varying cross-linking agent on mechanical stability

Since alginate has an affinity towards positive cations, cross-linking agents usually used in order to form alginate gel's are; $CaCl_2$, $SrCl_2$ and $BaCl_2$. Figure 4-17 showed that microbeads cross-linked using $BaCl_2$ required the most amount of force to compress (average force = 25g), while $SrCl_2$ required the least (average force = 10g). However, the time required to compress $SrCl_2$ beads was found to be a little higher (average time = 125 seconds) compared to the beads cross-linked with calcium (average time = 115 seconds) or barium (average time = 110 seconds). Therefore, microbeads cross-linked with $BaCl_2$ appeared to be stronger with decreased elasticity while one's cross-linked with $SrCl_2$ showed the highest elasticity with a decrease in strength.

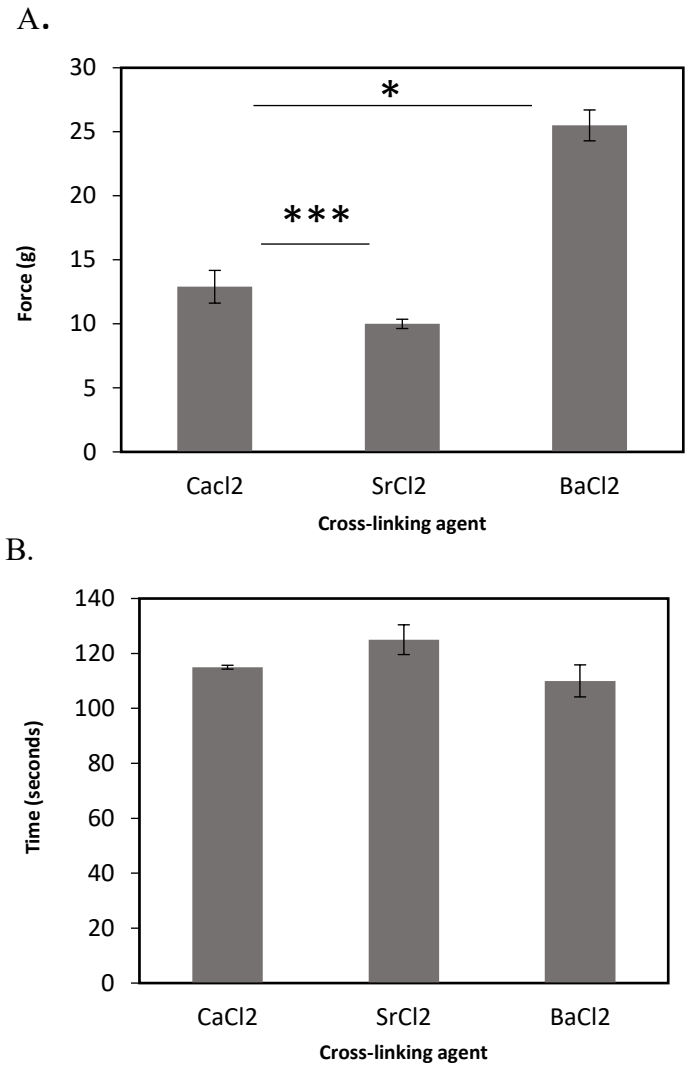

Figure 4-17: *Bar chart showing relationship between the type of cross-linking solution used and A) the force required to compress beads to 60% deformation (***p<0.001, *p<0.05, n = 5) and B) the time it takes for the beads to reach 60% deformation once compression is applied (n = 5). Time for gelling with cross-linking solution as well as the size of microbead was kept constant. Microbeads fabricated manually and average bead size was 2 mm*

These results show that mechanical stability of microbeads is in fact affected by the kind of cross-linking solution used. In the case of divalent cations, the 'egg box' model shows that the cations bond with the blocks of alginate polymers in a two-dimensional planar fashion. The extent of binding increases with an increasing ionic radius. It has been reported that Ba^{2+} cations with larger ionic radius can form a tighter structure compared to Ca^{2+} cations with a smaller ionic radius since Ba^{2+} cations are expected to take up a larger space between the blocks of alginate polymers resulting in a tighter arrangement of cross-linked alginate polymers (Kaklamani et al. 2014).

The minimum length of G-G blocks needed for cross-linking decreases with increasing affinity of cations for alginate. As mentioned before, Sr^{2+} binds to G-G blocks only, Ba^{2+} binds to G-G and M-M blocks while Ca^{2+} binds to G-G and M-G blocks. This binding pattern lets Ca^{2+} and Ba^{2+} cross-linked beads form two times as many junctions as compared to Sr^{2+}.

The stability of beads is heavily dependent upon the type of cation applied for cross-linking. This effect is caused by the varying chemical properties of the applied cations such as their atomic number, association constant, ionic radius, ionic strength and chemical affinity towards alginate (Juarez et al., 2014). This probability and specificity of binding patterns explains why it takes less force to compress Sr^{2+} cross-linked beads. However, the time required to compress these beads till they reached 60% deformation was slightly more for Sr^{2+} cross-linked microbeads which shows the elastic nature of Sr^{2+} beads while highlighting the more brittle nature of Ba^{2+} microbeads.

4.5.3 Effect of microbeads fabrication methodologies on their strength

Figure 4 - 18 shows that beads deposited manually were the most mechanically stable since they required the highest amount of force to reach 60% deformation (mean force applied = 10g). While beads fabricated through AAJ required the least amount of force to reach the same level of deformation (mean force applied = 3.8g). It also took manually deposited beads the longest to reach 60% deformation (average time = 115 seconds) while it took beads produced using AAJ and also those fabricated using both ES and AAJ in combination the shortest amount of time to reach the desired level of deformation (average time = 64 seconds).

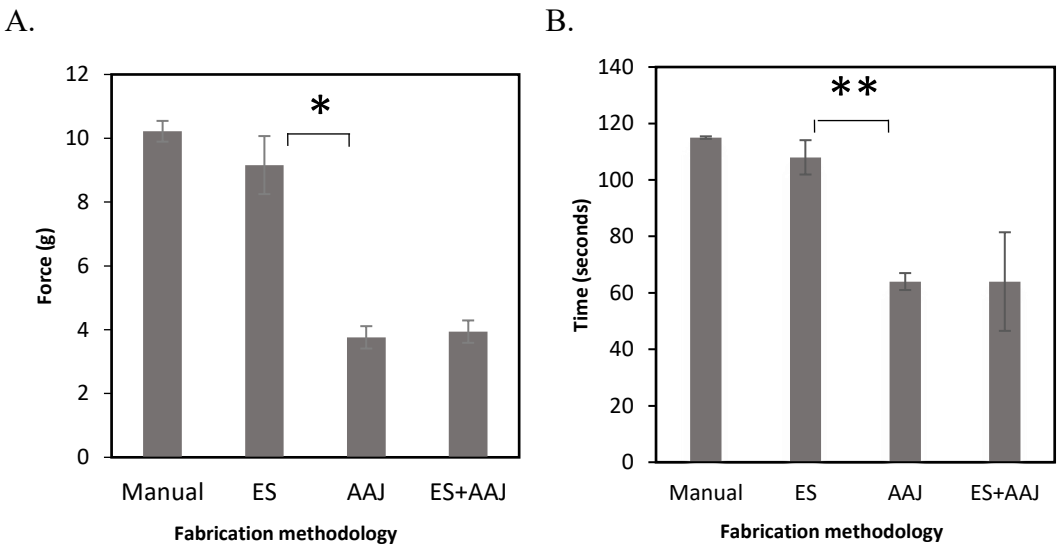

Figure 4-18: *Bar chart showing A) force required to achieve 60% deformation (*p <0.05, n = 5) and B) time required to reach the same level of deformation for microbeads fabricated using four different fabrication methodologies; manual deposition, ES, AAJ and finally ES in combination with AAJ (**p<0.01, n = 5). Average bead size was 2 mm*

An explanation for these findings is that even though the gelling time with cross-linking agent was kept constant, the sizes of microbeads produced using the four methodologies varied as highlighted in figure 4-19. The same trend in mechanical stability was observed when the cross-linking agent was changed from $CaCl_2$ to $SrCl_2$ and $BaCl_2$. Since the range of microbead sizes produced using AAJ can be almost ten times smaller than those produced through electrospraying, it was challenging to keep all the sizes at one constant range. Since the beads needed to be sized before they could be tested for mechanical properties it was deemed suitable to produce a sample with its homogeneity kept intact. The particles were kept as close in size as possible, for this reason only the offspring particles fabricated using AAJ were collected as they tend to be larger in size and could therefore be easily compared to the particles fabricated using ES.

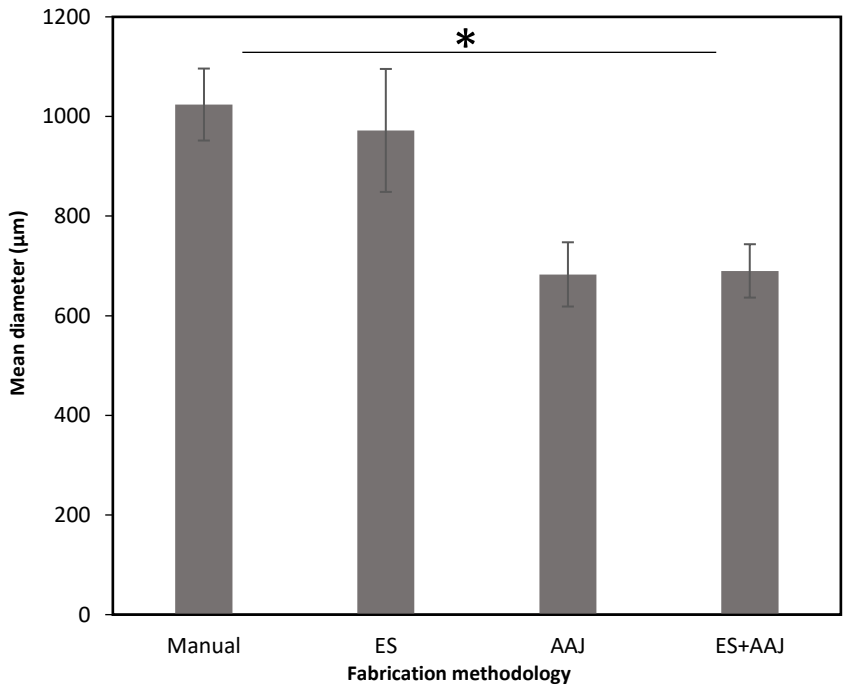

Figure 4-19: *Bar chart highlighting the difference in microbead sizes produced using the four different methodologies assessed. (*p < 0.05, n = 5). Average bead size was 2 mm*

Research shows that increasing the size of bead will also increase the stability of that bead. Since the volume of a bead is a function of its $(radius)^3$, if the radius is halved the volume will be decreased to an eighth. Therefore, an increase in bead size will also increase both the force and time required to reach a certain level of deformation during a compression test (Bhujbal et al. 2014). As can be seen in figure 4-18, an increased microbead size shows an increase in both force and time required, too. An increased microbead size means an increase in the divalent ions that will eventually cross-link the alginate bead core therefore increasing the overall mechanical stability. Therefore, the decreased mechanical stability exhibited by microbeads produced through AAJ and ES in combination with AAJ is a function of their smaller radii as compared to manually deposited or electrosprayed microbeads that were in fact bigger in size.

4.6 Summary

As stated in Section 4.1 the main aim of this chapter was to assess and optimise both ES and AAJ for their ability to fabricate alginate microbeads. An increase in polymer concentration was shown to create more homogenous beads that were also more spherical in shape. Effects of the governing process parameters on the mean bead diameters was also studied. It was concluded that for both fabrication methodologies - an increase in flow rate contributed to an increase in microbead size, too. Whereas, an increase in applied voltage considerably decreased microbead size. As far as applied pressure was concerned, an increase caused a substantial decrease in microbead size for beads fabricated using AAJ.

Operational size maps were produced using MATLAB as seen in figures 4 - 3 and 4 - 4. It was seen that ES possessed the ability to produce microbeads ranging from 250 – 2500 µm while AAJ produced beads ranging from 25 – 60 µm for 2% alginate solution. Moreover, ES and AAJ were seen to produce microbeads ranging from 250 – 2250 µm and 30 – 80 µm respectively, for 2% Alginate and 2% TiO_2 – used as a vaccine stand in for this sizing study.

As the final aim of this chapter, the mechanical stability of microbeads fabricated using ES and AAJ were studied. As seen in Figure 4 – 15, a positive correlation was witnessed between alginate concentration and force applied. 2% alginate solution required a higher amount of force – 10.7g – to reach 60% deformation as compared to beads produced using 0.6% alginate solution, which was seen to require only 3.7g applied force to reach the same exact level of deformation.

It was also seen that microbeads cross-linked with $BaCl_2$ required the most amount of force (average force = 25g) to compress while $SrCl_2$ (average size = 10g) required the least. However, the time required to compress $SrCl_2$ beads (average time = 125 seconds) was found to be slightly higher than that for both $BaCl_2$ and $CaCl_2$ (average time = 110 and 115 seconds, respectively). Therefore, it can be concluded that microbeads cross-linked with $BaCl_2$ were stronger with decreased elasticity while $SrCl_2$ showed the highest elasticity with decreased strength. Fabrication methodologies had negligible influence on microbead mechanical properties.

5. Dissolution testing – observational and in vitro analysis

5.1 Introduction and aims

In order to gain a clearer understanding of the behaviour of a solid dosage form throughout the dissolution test, one of the primary objectives of this chapter was to analyse the dissolution process using optical microscopy as a tool for direct visual observation. The effects of polymer concentration, type of cross-linking solution and fabrication methodologies on microbead dissolution were studied.

Following which the encapsulation ability of alginate microbeads was assessed by analysing their encapsulation efficiencies and dissolution properties. As the principal aim of this research was to characterise alginate microbeads as antigen delivery systems, it was deemed suitable for them to undergo in vitro dissolution testing. This furthers the development of an orally deliverable alginate system possessing the ability to deliver antigens to the distal intestine of A.Salmon while keeping their own integrity intact since successful oral delivery is only possible if the encapsulated antigen is protected from acidic and proteolytic degradation in the gastrointestinal tract of the fish.

Moreover, in order for the encapsulated antigen to elicit an immune response, the antigen must first be able to release from the fabricated microbeads. Therefore, another primary objective of this chapter was to assess the release profiles of BD (Blue dextran) - model antigen - from alginate microbeads through a specifically tailored

dissolution test representative of the environmental conditions faced by A.Salmon particularly temperature as well as intestinal conditions such as pH.

To further the understanding of the link between varying levels of encapsulation efficiencies and therefore release profiles, it was deemed appropriate to analyse the viscosities and molecular weights of the various types of alginates used in this section of the research.

5.2 Dissolution testing - Observational

Dissolution is a process where mass transfer from a solid surface to the liquid phase occurs. Drug dissolution tests are routinely carried out in the pharmaceutical industry in order to provide significant information about drug release, clinical performance and bioavailability. It is employed throughout all phases of product release and stability testing. This is critical for drug release profiles as well as quality control purposes (Lee, Chan et al. 2006). A polymer's behaviour during the process of dissolution can prove to be vital since an ideal drug delivery system will only provide the drug when and where it is needed and also just the minimum dose level required to produce the desired therapeutic effects (Miller-Chou and Koenig 2003).

In order to protect the drug from harmful conditions in the body, it can be dispersed within a polymeric matrix. This system should be able to provide a programmable concentration – time profile that shows optimum therapeutic responses. Research has also shown that not only are polymeric drug carrier systems able to protect otherwise unstable drugs but also help increase residence time at the application site while enhancing the activity duration of drugs with a short half-life. This means that with the help of an ideal polymeric delivery system, compounds that would have otherwise been discarded and deemed useless can now be rendered effective (Miller-Chou and Koenig 2003).

Polymer dissolution involves two transport processes; solvent diffusion and chain disentanglement. When an un-crosslinked amorphous polymer comes into contact with a thermodynamically stable compatible solvent, the solvent itself will diffuse into the polymer. This forms a gel like swollen layer, which is witnessed in the initial

moments of the dissolution process. After some time, the polymer will dissolve. There have also been reported cases where no gel layer is formed instead the polymer cracks (Miller-Chou and Koenig 2003). Mass is lost through ion exchange of calcium which is then followed by the detachment of individual chains, this also results in a loss of mechanical stiffness over time (Augst, Kong et al. 2006). A cross-linked polymer on the other hand comprises of a structure joined in a three-dimensional lattice of polymeric materials through covalent or secondary bonding. The idea behind this approach is to induce the formation of a lattice surrounding drug molecules hence encapsulating them in a matrix (Hoffman 2012). As far as cross-linked matrix systems are concerned, drug release is governed by the process of degradation or swelling.

Noyes and Whitney (1897) were the first to conduct and publish dissolution experiments. They set up glass cylinders submerged in vessels containing water and these cylinders were rotated at constant speed and temperature. In spite of the development of the in vitro dissolution process, the concept was not extensively used until early 1950s. Until then the in vivo availability of the drug was solely assessed through the disintegration of the tablet neglecting the dissolution process. In 1934, the Pharmacopeia Helvetica published the first official disintegration test for tablets. Even though this test was carried out using water at 37 ℃ as the medium and also incorporated periodical shaking, it was still quite modest in terms of procedural elements. A much more sophisticated method of testing was carried out in 1948 (Filleborn 1948) where an artificial stomach was stimulated through in vivo conditions which included peristalsis, pH and the presence of food.

The relationship between oral administration and drug dissolution was first explored by (Edwards 1951) it was suggested that if the drug absorption process from the GI tract was rapid then its appearance in the body can be attributed to the rate of

dissolution of the drug - aspirin - itself. Following this, (Nelson 1957) successfully related blood levels of orally administered theophylline salts to their in vitro dissolution rates. It was then realised that varying product formulations caused differences in the intensity, speed and duration of the drug response. Thus suggesting that drug bioavailability – the degree to which a dose of drug will reach circulation - is affected by the drugs dissolution behaviour. One study that supported this cause-effect relationship was where various Digoxin formulations yielded up to sevenfold differences in serum digoxin levels (Lindenbaum, Mellow et al. 1971). This specific study motivated the FDA to implement comprehensive dissolution studies on various batches of digoxin tablets available in North America during 1972. The studies showed astounding differences in dissolution profiles of the varying digoxin products and concluded that the difference in bioequivalence stemmed from the varying dissolution rates. Similar situations like these lead to the initiation of developing official dissolution tests.

The first USP (United States Pharmacopeia) apparatus 1 (consisting of the basket stirred flask test) was officially accepted as the dissolution test in 1970 - other apparatus' have been developed since then and will be discussed in detail later in the chapter. However, the official guidelines for dissolution testing of solid oral dosage forms were first published in 1981 by the FIP (International Pharmaceutical Federation). These guidelines put forward an established approach to test an API (active pharmaceutical ingredient).

The main aim in mind while designing an orally administered release formulation is for the gastrointestinal environment to have little or no effect on drug release rate. This happens to be quite challenging since the formulation will need to pass through quite a vast array of contrasting mediums throughout the gastro intestine. For example, the

optimum pH for digestive enzymes in the intestine of A. salmon has been reported to be 7.5 – 8.5 (Bucking and Wood 2009), while chyme pH ranges from 6.7 – 7.8 (Usher, Talbot et al. 1990). Even though commercial production of Atlantic salmon has been on-going for the past forty years, gaps regarding the physiological and biochemical characteristics of digestive processes in the intestine still exist (Krogdahl, Sundby et al. 2015).

Observational analysis of the dissolution process helps detect any physical changes in an API. This can help guide the optimization of design and processing conditions as well as drug release from formulations.

Over the years, various experimental techniques have been utilized to characterize polymer dissolution behaviour. Such techniques include gravimetry, interferometry, FT-IR imaging and optical microscopy. All these techniques have their own set of advantages and disadvantages. For example, gravimetry shows highly accurate frequency measurements but the variable viscoelastic properties exhibited by polymers can produce unwanted distortions. FT-IR imaging is able to produce real-time analysis of the dissolution process but since no apertures are used in the set-up, the diffraction effects that normally affect resolution will not come into play using this methodology.

Optical microscopy on the other hand, allows direct visual observation of the dissolution process. Moreover, when a slice of polymer is sandwiched between two glass slides, information about various stages of dissolution (solvent, gel and polymer layers) can also be received (Miller-Chou and Koenig 2003). Even though this method is limited to the micrometre scale, it does not prove as a hindrance in this study since the microbeads assessed here are all in the micrometre range, too. Since optical

microscopy has the ability to provide significant information into the behaviour of polymers in contact with solvents, this methodology was chosen for the assessment of empty alginate microbeads.

The rate of dissolution is dependent on various factors such as; the nature of solvent and solute, particle size, temperature and/or mixing. Therefore, the dissolution study carried out in this part of the research - based around observational findings - was divided into three main objectives; the effect of solution concentration on dissolution rate, the effect of cross-linking agent on dissolution rate, the effect of fabrication methodologies of beads on dissolution.

5.2.1 Effect of solution concentration on microbead dissolution

Increase in the concentration of alginate solution means an increase in the mass of alginate and a decrease in the volume of water present in the solution. The gradual absence of water whilst increasing the mass of polymer in the solution suggests an apparent increase in the viscosity of the solution as well as the overall molecular weight of the bead produced using that solution. For example, 1.6% final concentration of alginate solution will be more viscous than 0.2% due to the increase in mass of alginate in the former solution.

As seen in Figure 5-1 it can clearly be observed that there is a positive correlation between dissolution time and concentration since an increase in concentration of alginate solution increases the dissolution time too. Hence, the higher the mass of alginate possessed by the microbead, an increased interaction takes place between the cross-linking agent and more bonds are formed. This ends up increasing the overall dissolution time as it takes longer to break the increased amount of bonds present.

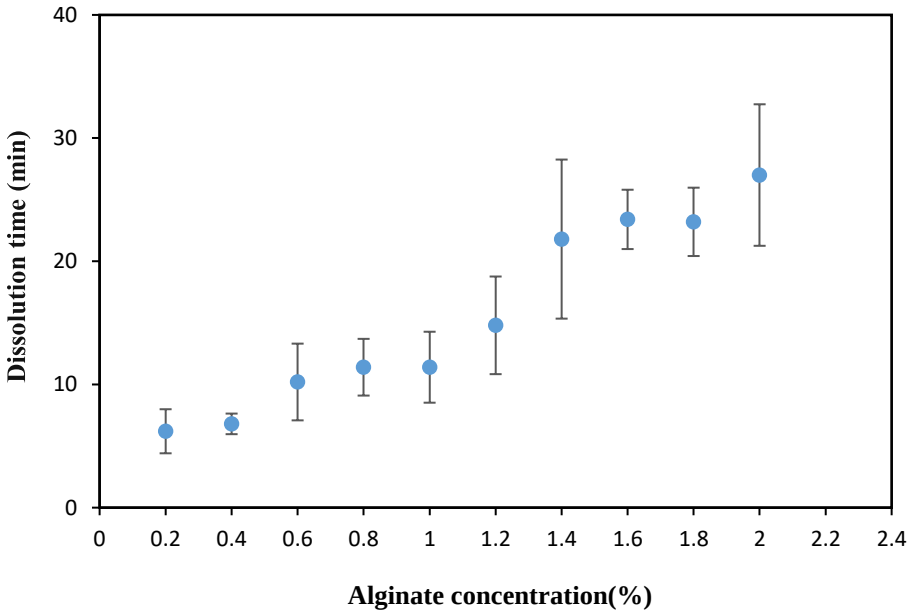

Figure 5-1: *Effect of alginate concentration (%) on dissolution time (mins). Ten different concentrations were assessed; 0.2, 0.4, 0.6, 0.8, 1, 1.2, 1.4, 1.6, 1.8 and 2% (n=5). Microbeads fabricated manually, average size 2 mm*

Figure 5-2 shows that within a set time period i.e. 10 minutes in this case, the bead produced using 0.2% solution completely dissolved. However, within the same time period it was seen that the bead produced using 2% solution was only able to dissolve partially. The complete dissolution of this particular bead took 26 minutes. The same trend was witnessed for microbeads cross-linked using $SrCl_2$ in order to assess whether the trend witnessed was not just constricted to the $CaCl_2$ cross-linker.

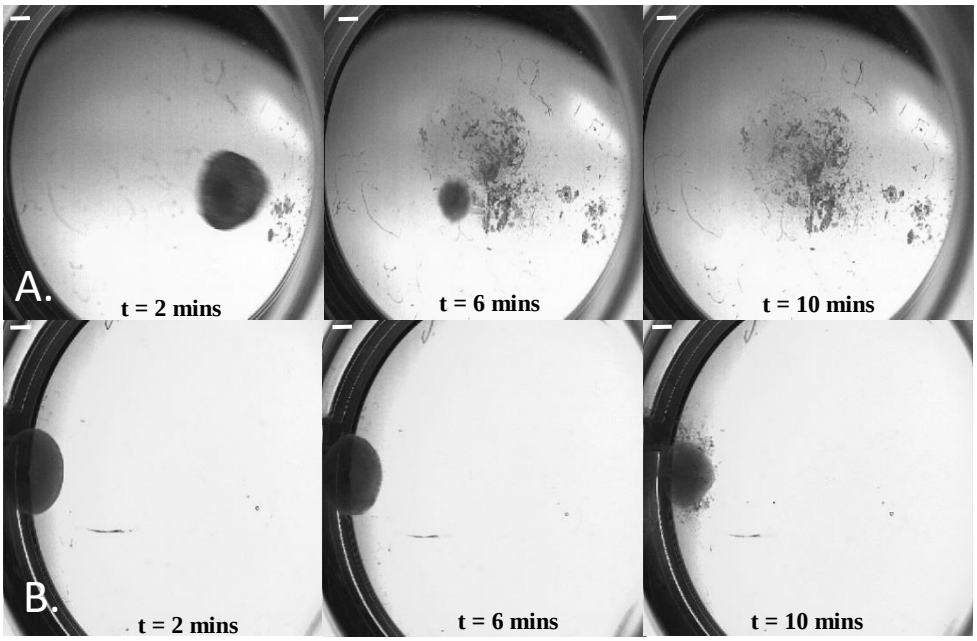

Figure 5-2: *Time lapse images of the dissolution of microbeads produced using A) 0.2% solution and B) 2% polymer solution over the duration of ten minutes, using optical microscopy. Microbeads fabricated manually, average size 2 mm. Scale bar represents 200 μm*

This trend is supported by previous research (Parsonage, Peppas et al. 1987) which suggests that dissolution is a process dictated by chain disentanglement dependent upon polymer molecular weight. Hence, larger molecular weights yield higher levels of disentanglement, which is why it takes a longer time for the dissolution of highly concentrated solutions to occur. Ueberrieter's early work also supported this phenomenon as he also reported a decrease in dissolution rate with increased polymer molecular weight (Ueberrieter., 1968).

Tapia, Ormazabal et al. (2007) analysed the erosion, swelling and dissolution behaviour of diltiazem hydrochloride release matrices based on alginate-gelatin mixtures. It was found that tablets produced using 20% polymer solution (gelatin-alginate) had lower rates of swelling and the disruption of these tablets occurred fairly

quickly too, when compared to tablets produced using 50% polymer solution. These tablets ended up demonstrating a noticeable increase in the degree of swelling. However, the erosion process for these tablets was quite fast too. The high ion concentration present in a 50% polymer solution is responsible for increased water flow into the gel due to osmosis which then results in an increase in swelling. Moreover, research (Brondsted and Kopecek 1992) has suggested another important factor affects gel swelling behaviour: the repulsion of charges present along the polymer chain.

However, as far as using alginate beads as drug carrier systems is concerned, it should be noted that according to previous research, the concentration of both the alginate solution used along with the concentration of the cross-linking agent have an effect on drug release rate. Mandal, Bostanian et al. (2001) concluded that drug release is directly proportional to the polymer concentration used to prepare the bead and an increase in $CaCl_2$ (used as the cross-linking agent) concentration decreased the rate of drug release. Rajinikanth, Sankar et al. (2003) suggested that the rate at which the drug diffuses from the alginate matrix decreases as the concentration of $CaCl_2$ solution increases, since there is greater cross-linking that tends to take place with the alginate.

5.2.2 Effect of cross-linking agent on dissolution

One of the most important features of alginate is its ability to efficiently bind with divalent cations leading to eventual hydrogel formation. Research suggests that the

affinity of alginate towards various divalent ions tends to decrease in the following order; Pb > Cd > Ba > Sr > Ca > Co.

This effect of enhanced aggregation of alginate structure with divalent cations can be attributed to a mechanism known as ‘gel bridging’. In the presence of these cations, alginate will undergo bridging as they form gels. The integrity and efficiency of the gel formed will be dependent on the type of divalent cation present. The divalent cation for which alginate has a higher affinity, will form the gel faster and also allow for enhanced aggregation on a higher level (Chen, Mylon et al. 2007). In order to assess whether the cross-linking agent was the only variable affecting the dissolution rate of microbeads in this study, it was made sure that the gelling time (time spent in contact with cross-linking agent by microbead) was kept constant throughout. This is because during gel formation uronic molecules in alginate will bind to cations and the constitutive uronic molecules in alginate will create junction zones within the gel (Thu, Bruheim et al. 1996). With an increase in gelling time, the number of junction zones present in the gel will increase, too, until saturation of the gel is achieved (Zhang, Daubert et al. 2007).

Results obtained from this study, supported the proposed order to affinity as it was seen that microbeads tend to show complete dissolution when cross-linked with $CaCl_2$, only partial dissolution with $SrCl_2$ and no dissolution at all when cross-linked with $BaCl_2$. As seen in Figure 5-3 it took 25 minutes for a microbead cross-linked using $CaCl_2$ to completely dissolve, but in that same time period the microbead cross-linked using $SrCl_2$ was only able to partially dissolve. Whereas, the microbead cross-linked with $BaCl_2$ showed no dissolution in that time period at all.

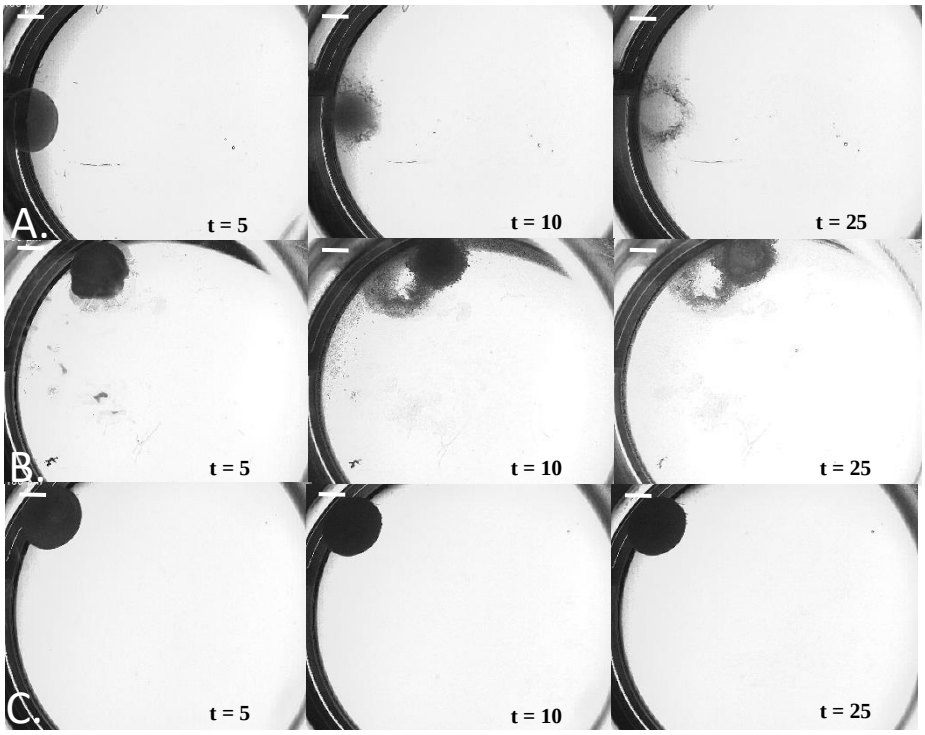

Figure 5-3: *Optical microscopy time lapse images showing microbeads produced using 2% w/v alginate solution and cross-linked with A) $CaCl_2$, B) $SrCl_2$ and C) $BaCl_2$. Images acquired over time points t = 5, 10 and 25 mins. While it took 25 minutes for the microbead cross-linked with $CaCl_2$ to fully dissolve, the microbead cross-linked using $SrCl_2$ was only able to partially dissolve in that time whereas the one cross-linked with $BaCl_2$ showed no dissolution at all. Microbeads fabricated manually, average size 2 mm. Scale bar represents 500 μm*

Binding studies (Morch, Donati et al. 2006) reveal that different block structures in alginate will bind the ions to different extents; Ca^{2+} binds to G- and MG- blocks, Sr^{2+} binds to G blocks solely and Ba^{2+} binds to G – and M- blocks.

(Smidsrod 1973) used both light scattering and viscosity studies to conclude that the stiffness of the chain blocks increased in order of MG<MM<GG. Therefore, it takes longer for beads cross-linked using Ba^{2+} since it binds to both M and G blocks forming

the most stable alginate structure. But Ca^{2+} only tends to bind with G and MG blocks in the entire alginate chemical structure, which is a fairly less efficient junction and therefore can be broken in a much shorter period of time. Since the type of alginate being used will alter the composition and ratio of M:G blocks present and therefore also have an effect on the dissolution rate, it was made sure that only one type of alginate (Protanal LF 10/60, food grade, BioPolymer, AS, Norway) was used throughout this study, in order for the results gained to be consistent and only in response to the type of cross-linking ion used.

The results showed that none of the microbeads assessed using $BaCl_2$ as the cross-linking agent showed any dissolution at all. To confirm the eventual time it might take for an alginate bead cross-linked with $BaCl_2$ to dissolve, a sample was kept under observation for 24 hours. Figure 5 - 4 shows no visible dissolution during the 24 hour time period either, hence supporting research that suggests Barium ions form the strongest gels with alginate. Therefore, it can be said, that the results gained from this study support the theoretical sequence of alginate affinity towards divalent ions i.e. Ba > Sr > Ca.

Figure 5-4: *Optical microscopy time lapse images of microbead produced using 2% w/v alginate solution, cross-linked with $BaCl_2$, showed no dissolution over the 0 – 24 hour observation time period. Microbead fabricated manually, average size 2 mm. Scale bar represents 500 μm*

5.2.3 Effect of microbead fabrication methodologies on dissolution

The final objective set for this observational dissolution study was to assess whether the process employed for the fabrication of the microbead will play a part in its dissolution rate. As seen in Figure 5 - 5, beads fabricated using AAJ and also the ones produced using ES in combination with AAJ had a shorter dissolution time as compared to the other two methodologies used. This can be contributed to the fact that these particular microbeads were also much smaller in size. Microbeads produced were kept at this particular size specifically in order to keep the homogeneity of the sample intact as well as for clear and concise visual dissolution observation.

As seen in the scatter graph (Figure 5-5) below, the purple and red clusters representing samples fabricated using AAJ, and ES in combination with AAJ respectively, are very tight and spread closely. In comparison, beads fabricated manually and through ES were larger in size (almost double) and also had a wider spread. This can be contributed to the dissolution times of the beads and are not necessarily related to the size distribution. For manual and ES fabricated beads the range of dissolution times was larger due to their smaller surface area. It’s important to note that the overall dissolution range remains the same for both groups – ES/manual and AAJ/ES in combination with AAJ, hence suggesting that dissolution was in relation to particle size and not necessarily the fabrication methodology used.

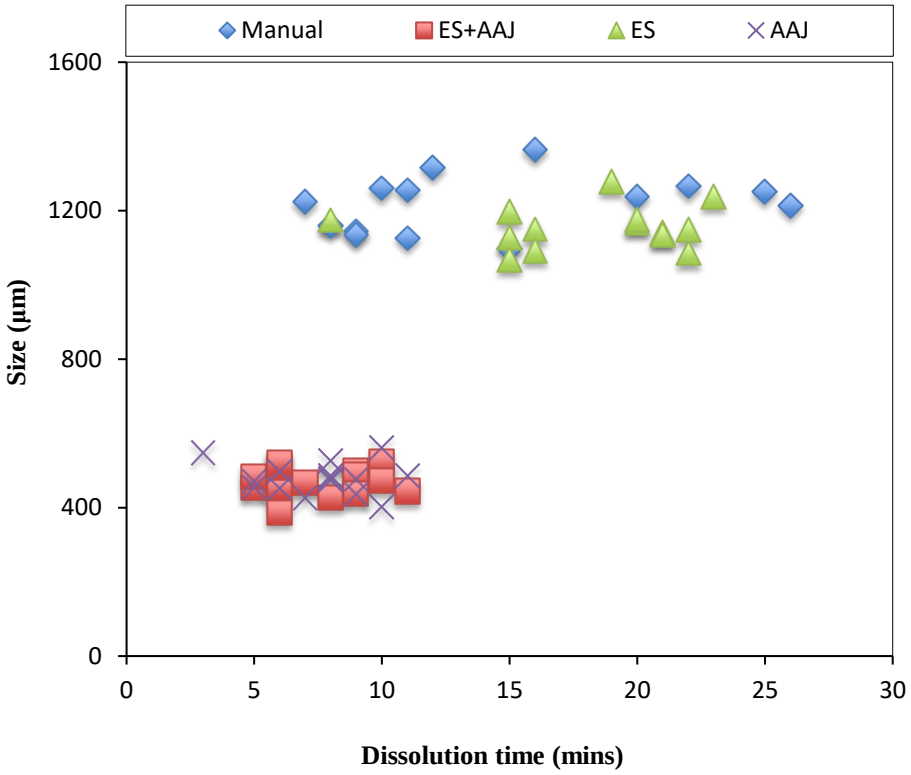

Figure 5-5: *Scatter graph comparing microbeads produced using the four different types of fabrication methodologies, their respective dissolution times (mins) and sizes (µm) (n=5)*

The dissolution times of beads produced using ES in combination with AAJ and the one's produced using AAJ on its own were much shorter in comparison to the microbeads produced using the other two methods. This is due to the fact that beads produced using these methodologies were in fact much smaller - almost half in size. This means that there is almost half the amount of polymer present for the same amount of cross-linking agent to act upon and create disentanglements with. Due to this, it takes less time for the dissolving agent to break the disentanglements formed, hence the shorter dissolution times.

Figure 5-6 shows an electrosprayed bead and a manually deposited one. Both had a similar size range and therefore dissolution time. Whereas Figure 5-7 shows microbeads produced using AAJ followed by ES and AAJ in combination. Both beads were close to each other in size and also dissolution rate. To clearly see the relationship between bead size and dissolution time a bar graph was produced (Figure 5-8).

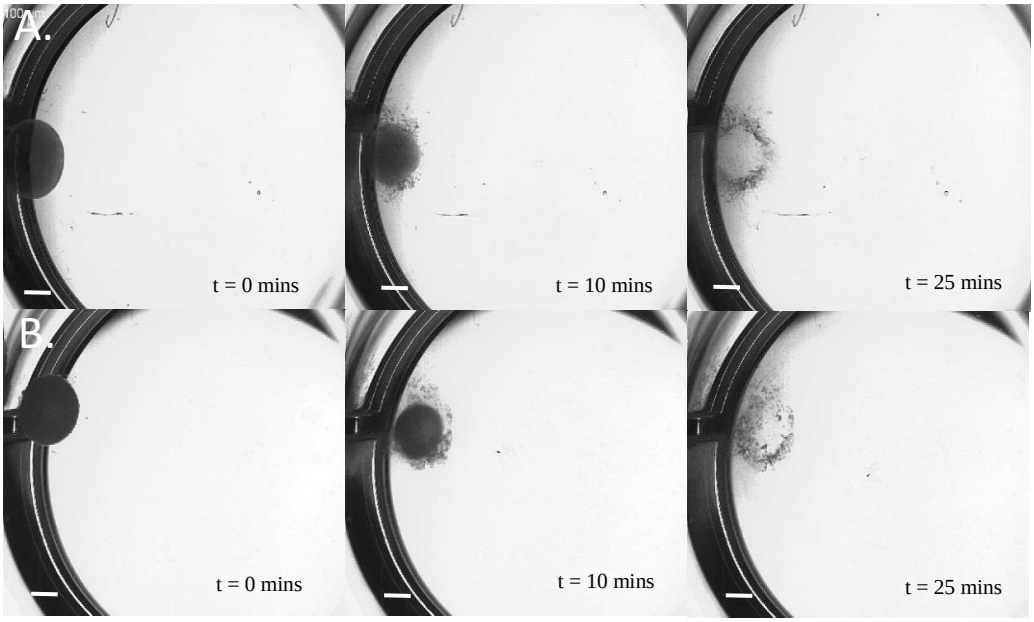

Figure 5-6: *Optical microscopy time lapse images of microbeads (2% w/v alginate) fabricated through A) manual deposition (D = 1290 µm) and B) electrospraying, (D = 1203 µm). Images acquired over time points t = 0, 10 and 25 mins. Scale bar represents 200 µm*

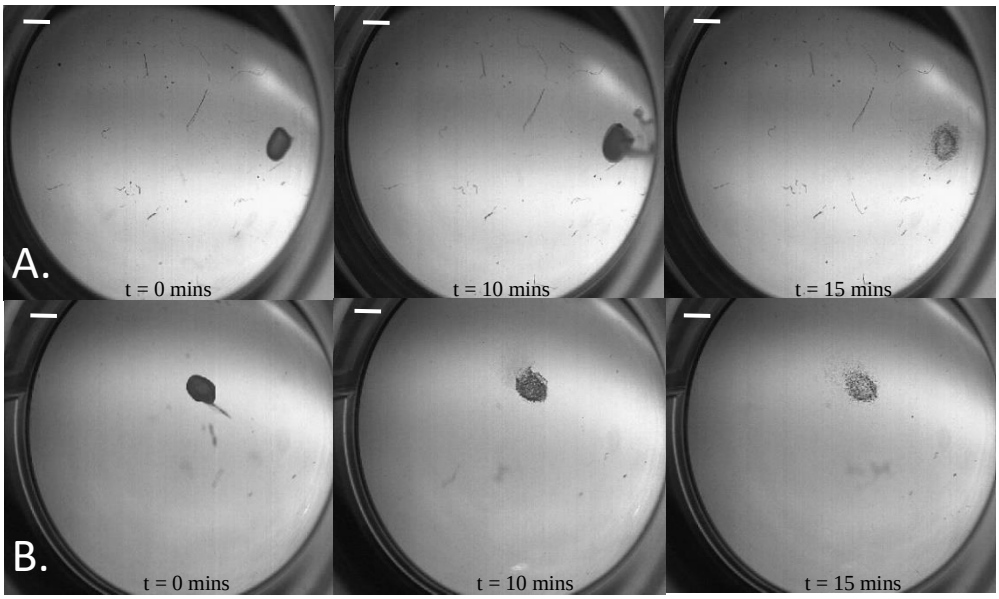

Figure 5-7: *Optical microscopy time lapse images of alginate microbeads (2% w/v) fabricated through A) AAJ and B) ES in combination with AAJ. Scale bar represents 200 μm*

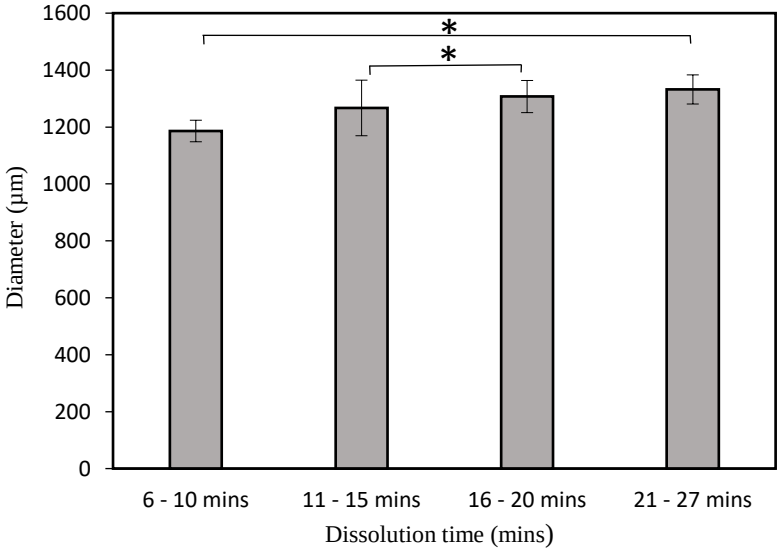

Figure 5-8: *Bar graph highlighting the relationship between microbead size (μm) and dissolution time (mins). It can be seen that with an increase in bead size, the dissolution time increased too (*p < 0.05, n = 5)*

The results did not show any substantial difference in dissolution rates for microbeads produced using the four different methodologies assessed in this study. The higher dissolution times for beads produced using electrospraying and manual deposition can be contributed to the fact that these beads were in fact larger in size, too. Suggesting that size is the most critical factor affecting dissolution rates.

5.3 Viscosity and Molecular weight

To assess and analyse the difference between the molecular properties of different types of alginates, their corresponding viscosities and molecular weights followed by their encapsulation efficiencies as well as their release profiles were studied.

Alginate viscosity is reported to play a role in influencing drug release pattern from alginate matrices (Liew, Chan et al. 2006), their size and also their encapsulation efficiency (Lee, Chan et al. 2006).

Microbeads were produced using five leading grades of sodium alginates; Scogin LDH, MV, Manugel GHB, GMB and DMB – all FDA approved as pharmaceutical excipients. The test was carried out as described in Section 3.2.7 (Chapter 3). The obtained dynamic viscosity values were summarised in the histogram below.

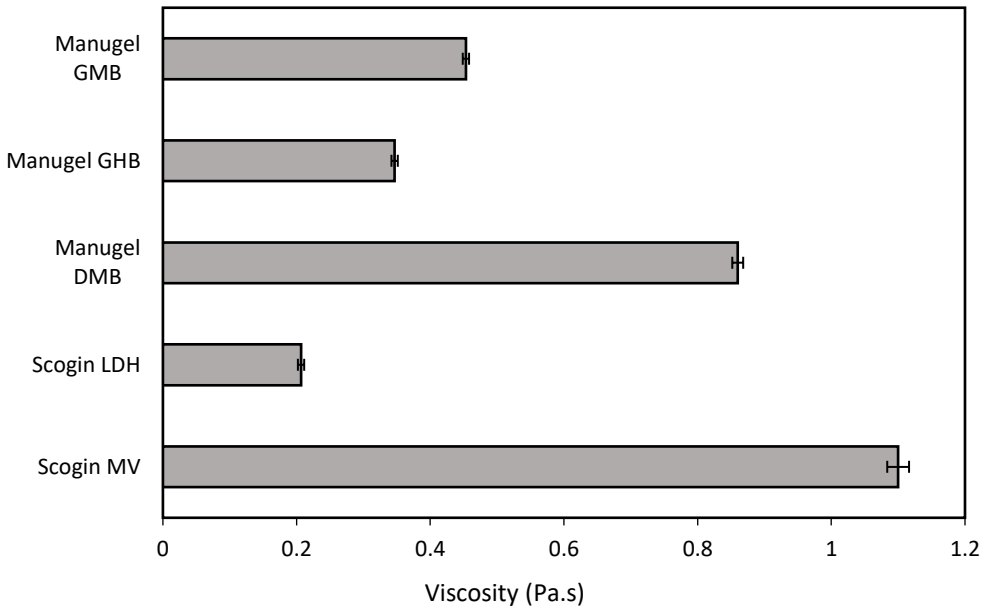

Figure 5-9: *Histogram highlighting the average dynamic viscosity (Pa.s) of all five types of alginates at constant shear rate 101 1/s, with Scogin MV being the most viscous while Scogin LDH being the least (n=5)*

Since the name codes of the alginate types themselves do not signify their viscosity grade, the measurements observed here can help classify them. It was seen that the experimental viscosities reported here correlated with the suggested viscosity trends on the product specification summaries provided by FMC biopolymers; where Scogin MV possesses the highest viscosity followed by Manugel DMB > GMB > GHB > Scogin LDH. These five samples reflect a range of varied viscosities with Scogin MV and Manugel DMB easily placed into the high/medium viscosity grades while Manugel GMB/GHB and Scogin LDH fall into lower viscosity grades.

The extreme difference between viscosity levels found between Scogin MV - 1.1 Pa.s - and Scogin LDH - 0.21 Pa.s - highlights the fact that M:G ratio is perhaps not the only factor affecting viscosity, since both Scogin MV and LDH have an equal 61:39 M:G ratio as seen in table 3-2 (Chapter 3). It should be noted that the solution's viscosity is also heavily dependent upon its molecular weight (King 1994) while the alignment of M and G blocks present along with the polymer chain length contribute too (Rustoen 2015).

It was imperative to understand the differences in sample viscosities in order to interpret their encapsulation efficiencies. Therefore, it was deemed suitable to analyse their molecular weights. Alginate's that possess similar M:G ratios have been found to have significantly different molecular weights (Lee, Chan et al. 2006). Once the dynamic viscosity of the samples was acquired using a rheometer, those values were converted to relative viscosity using;

$$\eta_r = \frac{\eta}{\eta_0} \quad (1)$$

where η_r is the relative viscosity, η is the viscosity of the polymer solution and η_0 is the viscosity of the pure solvent. The intrinsic viscosity can then be determined using the following equation (Haug and Smidsrod 1962);

$$[\eta_{intr}] \equiv \lim_{c \to 0} \frac{(\eta_r - 1)}{C} \equiv \lim_{c \to 0} \ln \frac{\eta_r}{C} \quad (2)$$

where η_r is the viscosity of the solution which is relative to the solvent (and η_r -1 being equal to the intrinsic viscosity) and *C* is the concentration in g (100 mL)$^{-1}$. Once these values were obtained for all samples, (ln η)/*C* values were plotted against concentration. From this plot, the data was extrapolated to zero concentration and the intrinsic viscosity of the solution was estimated.

An estimate of alginate's respective molecular weights (M_{wt}) – approximated to the nearest thousand - were then obtained using the following equation (Smidsrod and Haug 1968) (Smidsrod 1970) (Matsumoto and Mashiko 1990);

$$[\eta] = 2.0\, x\, 10^{-5}\, M_{wt} \quad (3)$$

It should be noted that the relationship between intrinsic viscosity and molecular weight acts as an estimation of the degree of polymerisation since it does not take into account the M:G ratio or block structure of the alginate (Johnson, Craig et al. 1997).

Another reason why it was significant to obtain the molecular weights of these alginates, is for the simple reason that sodium alginate undergoes cross-linking to form insoluble calcium alginate microbeads and for this reason their viscosities should have no direct effect on drug release (Lee, Chan et al. 2006). The influence of viscosity comes into play as far as microbead morphology and/or their sizes are concerned.

Given the structural complexity of alginates, it is quite conducive to obtain information on viscosities and molecular weights that can be helpful for characterisation and comparison between the encapsulation efficiencies and release profiles of the five different sample sets, in order to understand their functionalities as leading products available in industry currently.

Alginate type	Scogin MV	Scogin LDH	Manugel GHB	Manugel GMB	Manugel DMB
Dynamic viscosity (Pa.s)	1.1	0.21	0.35	0.45	0.86
Relative viscosity	3.60	2.70	3.0	3.0	3.40
Intrinsic viscosity (100 ml g^{-1}) (dL/g)	7.20	5.50	5.50	5.70	6.30
Mol. Weight (g/mol) (Da)	360,000	280,000	280,000	290,000	320,000

Table 5-1: *Summary of the values obtained for dynamic, relative and instrinsic viscosity of samples along with their respective estimated molecular weights (M_{wt}). The M_{wt} values can only be regarded as comparative due to the given approximate nature of the method.*

The M_w values obtained here fell into the range specified for the various types of commercially available sodium alginates, which can lie between the range 32,000 - 400,000 g/mol (Lee and Mooney 2012).

5.4 Encapsulation Efficiency

Drug entrapment/encapsulation efficiency acts as a significant index for drug delivery systems. The ability of a drug delivery system to encapsulate an ample amount of a specific therapeutic agent is one of their most sought after properties (Nii and Ishii 2005). Encapsulation efficiency (EE) of a microparticle depends upon various factors. Formulation factors such as calcium cross-linker concentration, alginate type (mannuronic and guluronic acid content) and concentration, drying time and drug to polymer ratio (Acarturk and Takka 1999).

To assess the ability of alginate microbeads to encapsulate proteins, Blue dextran (BD) was used as a suitable API and the encapsulation efficiencies of various types of alginates was studied. EE was calculated based upon data obtained from a microplate reader. The following equation was used to calculate EE;

$$EE\ (\%) = \frac{Total\ amount\ of\ BD\ present}{Total\ amount\ of\ BD\ theoretical} \times 100$$

where the total amount of BD present in microbeads is the amount of BD entrapped in the polymeric microbead while the total amount of BD loaded is the known theoretical BD content added to the microbead. Values were expressed as a percentage. EE was calculated through reference to a standard calibration curve, which was produced for all five alginate types. Values for the coefficient of determination (R^2) were ≥ 0.9856 (Appendix 2).

Standard curves were generated by plotting BD concentrations of nine two-fold serial dilutions (1.0 mg ml^{-1}) against absorbance. All five calibration curves produced were found to be highly reproducible and linear. The full test methodology carried out is highlighted in section 3.2.6 and a schematic representation of the test strategy is highlighted in figure 3-8 (Chapter3).

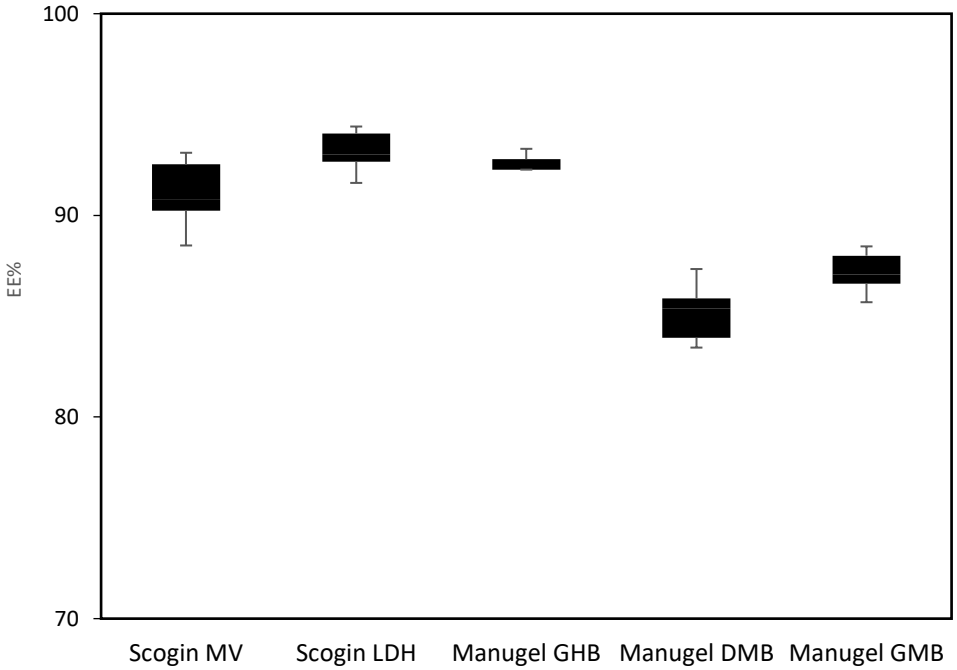

Alginate type	Average EE%
Scogin MV	91.60
Scogin LDH	93.50
Manugel GHB	92.40
Manugel GMB	87
Manugel DMB	84.5

Figure 5-10: *Box plot summarising the encapsulation efficiencies in terms of percentage of the five types of alginates. Error bars represent the SD values. Summary*

of the EE% values reported for all five types of test alginates. Test was carried out in quintuplicates and values were averaged

The EE% values were observed to be high for all five types of alginates, ranging from 84.5(± 1.66) % to 93.50(± 1.19) %. These high EE% values obtained can be explained by the microbead fabrication technique used involving cross-linking. As the surface of the polymer and BD solution comes into contact with $CaCl_2$, the divalent cations Ca^{2+} interact with the alginate's gluronic residues giving rise to spherical gel microbeads instantaneously, while promoting BD to become acutely entrapped into the three-dimensional matrix of the ionically cross-linked alginate (Lee, Chan et al. 2006). Other authors have also reported high EE% of BD in alginate beads (Kim and Lee 1992). The duration of this test can also be held responsible for the high levels of EE% values obtained. The microbeads were left to dissolve over a period of 24 hours which helped assess whether the microbeads are capable of releasing 100% of the encapsulated agent over time.

It was observed that Scogin types tend to have a comparatively higher EE% as compared to Manugels. This could be attributed to Scogin types being rich in mannuronic acid residues which tend to produce softer and less porous microbeads possessing the ability to disintegrate with time eventually. Therefore, lower levels of porosity allow the matrix to hold a higher amount of drug within them. However, on the other hand, alginates that are rich in guluronic acid residues have a higher porosity which can contribute to a lower drug entrapment efficiency as drug leakage into the cross-linking solution can occur (Sankalia, Mashru et al. 2005).

The molecular weight of Scogin MV was found to be 360,000 while Scogin LDH was lower at 280,000. This is paralleled by their EE% as Scogin MV at a higher Mw has a

lower EE% whereas Scogin LDH at a lower Mw has a higher EE%. The same trend was witnessed for Manugels as well where GHB possessed the lowest Mw and the highest EE% while DMB possessed the highest Mw and the lowest EE% suggesting that an increase in molecular weight contributes to a decrease in EE%. Furthermore, it is also to be noted that even though both Scogin LDH and Manugel GHB had varying M:G ratios, their molecular weights happened to be the same and therefore EE% were also found to be quite similar – 93.50% and 92.40% respectively.

These findings were also supported by previous research by (Fu, Ping et al. 2005) who found that molecular weight of the polymer itself also had an effect on the encapsulation efficiency. They concluded that the EE% of PLGA microspheres produced using PLGA 15000, 20000 and 30000 were 62.75, 27.52 and 16.3% respectively. Thus suggesting that an increase in molecular weight leads to a decrease in EE%.

These results happen to be interconnected with both the viscosity and size of the samples as well. An increase in alginate molecular weight can extend the total number of cross-linking sites between the guluronic acid units and Ca^{2+} therefore increasing the viscosity and also microbead size (Lemoine, Wauters et al. 1998).

Other factors have also known to contribute to the EE% of microbeads. (Jeyanthi, Mehta et al. 1997) reported that an increase of polymer concentration contributed to an increased level of EE too. An increase in concentration from 20 to 32.5% caused the EE to increase from 53.1 to 70.9%. This can be explained by the fact that when the polymer exists at a high concentration, it precipitates faster on a superficial level hence stopping drug diffusion (Rafati, Coombes et al. 1997). In addition to this, this phenomenon can also be contributed to the increasing viscosity of the solution which

helps delay drug diffusion within the polymer (Bodmeier and McGinity 1988). Interaction which takes place between the polymer and protein is also reported to make a contribution towards an increased EE value (Boury, Marchais et al. 1997).

5.5 Dissolution testing – In vitro

It was deemed significant to carry out in vitro dissolution testing since it is a vital analytical test that helps identify physical changes in an API (Technical Brief Particles Sciences 2010). The in vitro dissolution test is the only standardised method to analyse and measure how an API is withdrawn out of a solidified dosage form. Data gained from a standardised in vitro dissolution test can help confirm quality control, validate the fabrication process, and ensure that the dosage form does not fail (rupture) during transit and that the API is released in a predicted way.

A suitably accurate dissolution test will not only speed up drug development, but will also curtail the need for avoidable in vivo human/animal tests (Technical Brief Particles Sciences 2010). In vivo drug release in the human body can be measured through testing the urine or plasma concentrations, however, this is clearly not a practical technique that can be employed routinely. The FDA also recommends in vitro dissolution testing as a means to regulate in vitro-in vivo correlation levels (Kytariolos, Dokoumetzidis et al. 2010).

In vitro drug release studies help give an insight into the characteristics of not only the API but the drug delivery mechanism as well. Alginate is non-toxic when administered orally and also offers protection to the mucous membranes of the upper GI tract (Koji, Chiaki et al. 1982). Alginate microbeads are also known to re-swell once dried hence possessing the ability to act as a controlled release system. Such controlled drug delivery systems have the capacity to control the rate of drug delivery, sustain the duration of therapeutic activity and targeting the delivery of drug to a tissue (Utreja,

Jain et al. 2010). A controlled release system will have to deliver a constant supply of the API through continuous release over a certain time period.

In order to take full advantage of what in vitro dissolution testing has to offer, selection of appropriate experimental conditions is deemed crucial. To draw imperative conclusions, in vivo conditions need to be imitated. Therefore, designing a suitable test method will take into account the most significantly appropriate parameters that will eventually help mimic certain in vivo conditions for e.g. temperature, pH, dissolution medium, agitation rate, sampling time points etc.

Cumulative dissolution profiles offer a look into the amount of total drug dissolved from the formulation over time. The amount of volume lost during sample collection is replaced by the same amount throughout so as to avoid a change in total volume present in the vessel and to keep the accuracy of the final release profile intact.

5.5.1 In vitro BD release

BD encapsulated microbeads were prepared as described in Section 3.2.5.2 (Table 3.16). BD concentrations of nine two-fold serial dilutions (1.0 mg ml^{-1}) against absorbance were plotted to generate standard curves. All five calibration curves produced were put together in one graph, the co-efficient of determination for all five sets of samples suggested linear and reproducible results. Values for the coefficient of determination (R^2) were ≥ 0.9992 (Appendix 3).

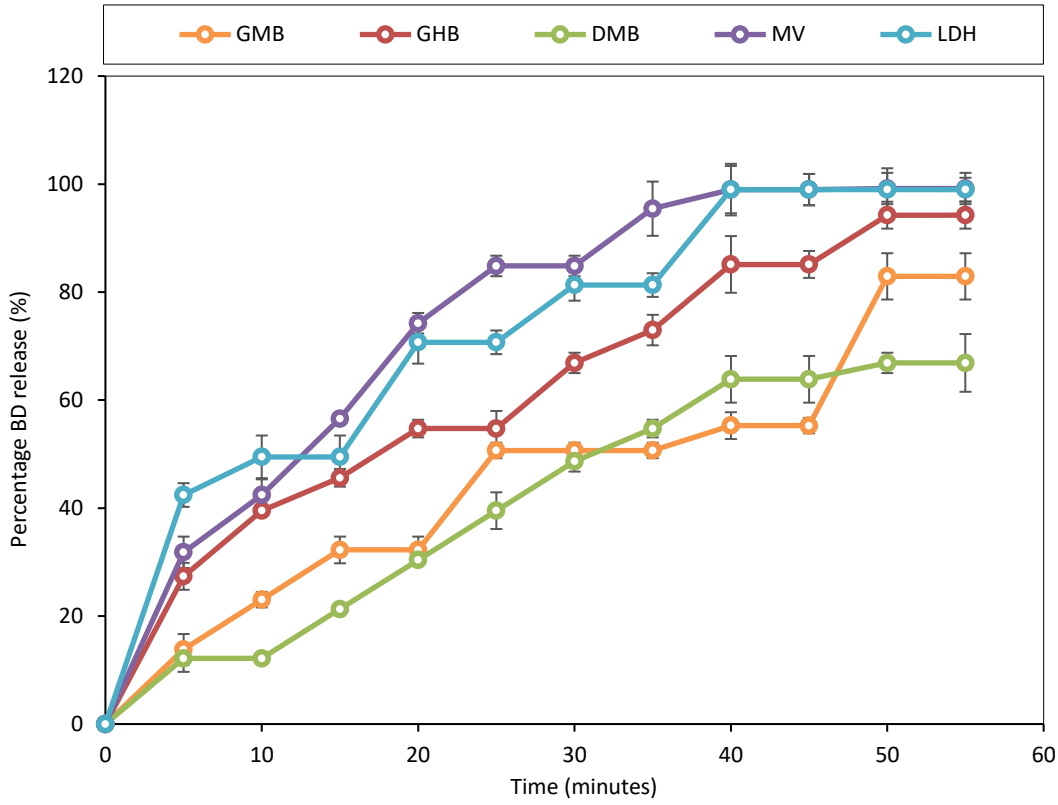

Figure 5-11: *In vitro cumulative BD release profiles shown as mean percentage over time (minutes). Error bars represent standard deviation (SD) (n = 5 for each time point). Average bead size ranged from 3217.5 – 3308.9µm*

The results as shown in Figure 5-10 suggest that the types of alginate used to fabricate microbeads had a significant effect on the release kinetics of BD. While alginate composition (M:G ratio) contributes to the observed trend in a considerable way, their encapsulation efficiency, viscosity and molecular weight - while all interconnected - play a role, too.

Out of the five types tested, for the given time period Manugel DMB showed the least amount of BD release - 66.9% - it is also important to note that DMB also had the lowest encapsulation efficiency - 84.5%. Since the EE for DMB microbeads was quite low to begin with, this correlated with the BD release values as well. On the other hand, the highest BD release was seen for Scogin MV and LDH – 99.2% and 99.0%,

respectively. Akin to their release values, their EE% were also quite similar – 91.60 and 93.50% respectively.

Polymer molecular weight affects polymer degradation and drug release (Kim and Pack 2006). Therefore the trend for BD release can also be explained using their molecular weight values values. A comparatively higher particle porosity suggests a higher quantity of the associated entrapped drug release. This was seen in the increasing BD release values which followed the trend Manugel GHB > GMB > DMB while their increasing Mw's followed the inverse trend DMB> GMB > GHB suggesting that polymers with lower Mw produce more porous particles which in turn causes higher diffusivity and an increased amount of BD release.

It should be noted that the higher the molecular weight, the more increased number of crosslinking points (Kikuchi, Yamada et al. 1996) between the guluronic acid units and calcium are present. Furthermore, a higher molecular weight can also produce microspheres with an increased density (Pepeljnjak, Filipovicgrcic et al. 1994). A microbead produced using a higher molecular weight may also contribute to a slight increase in size as well due to which it may take comparatively longer for alginate microbead erosion to occur. Previous research (Murata, Inose et al. 1993) also found that the release rate of BD from alginate beads fabricated using lower molecular weight happened to be faster as compared to those fabricated using an alginate of a higher molecular weight.

The increased BD release observed for Scogin types in comparison to Manugel types can be explained by their composition; M:G ratio (Table 3 - 2). Scogins are rich in M-type blocks whereas Manugels are high-G type. As far as Manugels are concerned, their guluronic acid conformation helps produce a high degree of coordination of

calcium which gives rise to more rigid gels due to being more calcium ion reactive. Due to this rigidity, they become less prone to erosion. With an increase in the mannuronic content the gel formed will become more elastic and softer in nature and also tend to dissolve more easily (Tonnesen and Karlsen 2002). This is observed in the behaviour of Scogin alginates as they release a higher amount of BD for the same test duration as compared to samples prepared using Manugel alginates. These results show that the M:G composition present in the hydrogel acts as the primary driving force behind microbead dissolution. This is because even though both Scogins; MV and LDH have substantially varying viscosities i.e. 1.1 and 0.21 Pa.s respectively, their release profiles are almost identical, with MV releasing 99.2% and LDH releasing 99.0% for the given test duration. Whereas, Manugel GHB and GMB have a closer viscosity to Scogin LDH – 0.35 and 0.45 Pa.s, their BD release is lower in comparison at 94.2% and 82.9% respectively.

Since BD is dispersed inside the biodegradable alginate matrix, when these encapsulated systems are exposed to a dissolution medium, the drug release is driven by diffusion through matrix swelling and dissolution/erosion at the periphery of the polymeric matrix (Takka, Ocak et al. 1998). As the matrix is composed of both the polymer and drug molecule, the swelling effect is a uniform volume expansion of the bulk polymeric material which causes the pores present throughout the structure of the matrix to open up (Stevenson, Santini et al. 2012).

Since this system was based on sodium alginate cross-linked with calcium chloride, the osmotic pressure gradient existing between the alginate gel and the environment plays a significant role in the swelling process. In the stomach i.e. acidic conditions, the swelling of calcium alginate beads is almost negligible, release is more likely to occur through the insoluble matrix by diffusion. In the intestine i.e. neutral conditions,

the beads will tend to swell and the drug release will be dependent upon the processes of swelling and erosion. The porous nature of these alginate beads allows for diffusion and penetration of water hence promoting its hydrolytic degradation followed by the ensuing release of dye (Schliecker, Schmidt et al. 2003).

The cumulative release profiles developed from this dissolution study highlight that diffusion of the API occurs in two phases; first phase dictated by diffusion while the second phase driven by erosion of the polymeric matrix itself. During the first fifteen minutes of the test in alkaline media, Scogin MV, LDH and Manugel GHB released around 50% of their payload. All three types also encapsulated the highest amount of BD as seen in Table 5 - 9.

The initial rapid release of BD from the beads can be explained by the large surface area of these particles (Soppomath et al., 2001). Moreover, it can also be suggested that the incorporated BD was present close to the particle's surface and hence was solubilized immediately from the particles into the test media. The porous network of the polymer microbead presents itself as a channel where penetration of the dissolution media can occur.

5.6 Summary

Initially, dissolution characteristics of microbeads were analysed through microscopic observation. Effects of solution concentration (0.2% - 2%), type of cross-linking agent ($CaCl_2$, $SrCl_2$ and $BaCl_2$) and fabrication methodology (manual deposition, ES, AAJ and ES in combination with AAJ) were assessed. It was seen that increasing solution concentration also increased the microbead dissolution rate. This rate was also seen to be dependent on the type of cross-linking agent used, which decreased in the following order; $Ba^{2+} > Sr^{2+} > Ca^{2+}$. The fabrication methodologies used for microbeads did not show any substantial difference on their dissolution rates.

Through the analysis of release profiles it was observed that alginates containing high mannuronic content - Scogin LDH and MV - tend to dissolve more easily therefore releasing a higher amount of BD over the given test duration while guluronic acid-rich alginates – Manugel GMB, GHB and DMB – are more rigid and therefore less prone to erosion. This leads to a lower release of BD from the microbeads over the same time duration. In conclusion, the composition of alginate plays a central role in the release of BD from microbeads. Additionally, an array of factors including the alginate's viscosity, molecular weight and encapsulation efficiency have an impact too. It is also important to note that the spherical shape of all microbead samples remained intact throughout the test duration and no bead rupture was observed. This suggests that the methodology applied, successfully fabricated polymeric microbeads which possessed the ability to withstand potential in vivo environmental conditions in A. salmon.

This study lays the platform to study the release of various types of vaccines from microbeads fabricated using ES and how these systems would potentially perform in *in vivo* studies with Atlantic Salmon.

6. Study of immune response to IPNV antigen in Atlantic salmon

6.1 Introduction and aims

The final objective of this research was to assess and analyse the ability of orally administered IPNV antigen encapsulated into alginate microbeads (fabricated using aerodynamically assisted jetting) to immunise Atlantic salmon. Two sets of samples were produced for the trial; the control sample consisted of alginate beads while the experimental group consisted of IPNV antigen-alginate encapsulated beads. The effect of orally administered IPNV antigen-alginate microbeads was estimated by measuring the level of IPNV specific antibodies in plasma after the treatment, and was complemented by profiling the expression of fifteen genes at three time points (day 0, 21 and 57) post the vaccination/immunization treatment. A number of fish exposed to encapsulated viral antigen in their feed showed slightly higher level of IPN-specific antibodies in plasma, measured by ELISA in comparison to the control group that received only alginate. This finding was complemented by qPCR profiling of expression of a number of immune genes in the head kidney, namely those encoding transcription factors; FoxP3, GATA3 and Tbet, T-cell receptor (CD4 and TCRy) and intracellular signalling (STAT6) molecules, cytokines (IL 17A, TGFb, IFNa), antiviral effector proteins of the interferon system (Mx) and antibody effector molecules (IgM and IgT). Results gained from this research suggest that the IPNV encapsulated

alginate microbeads represent a promising venue for further exploration of oral vaccination against IPN in A. salmon.

6.2 Trial specifications

6.2.1 IPNV antigen encapsulation in microbeads

IPN is a disease that usually affects young salmonids, and the pelleted feed was produced in accordance with the small size of fish used in this study. Therefore, the crevices present in the feed pellet were also comparatively smaller. Due to this, an average microbead size of 15 – 25 µm was set to be produced, for successful vacuum packing and eventual oral delivery. The production methodology of IPNV encapsulated alginate microbeads was highlighted in Section 3.2.8.1 (Chapter 3).

The encapsulated antigen (IPNV Ag) was produced by growing a recombinant Sp strain of IPNV, rNVI-15PTA - as previously reported (Chen et al. 2014). Sizes of samples that were produced are recorded in Table 6-1.

Sample batch No.	Mean Diameter (µm)	Standard deviation
1	15	7
2	16	7
3	20	8

Table 6-1: *The average size of IPNV antigen encapsulated microbeads for all three batches of samples prepared using aerodynamically assisted jetting*

Figure 6-1 shows an image taken from one of the experimental sample batches prepared for the trial. All three batches were contained in 1000ml of $CaCl_2$ cross-linking solution – each – and refrigerated until feed preparation.

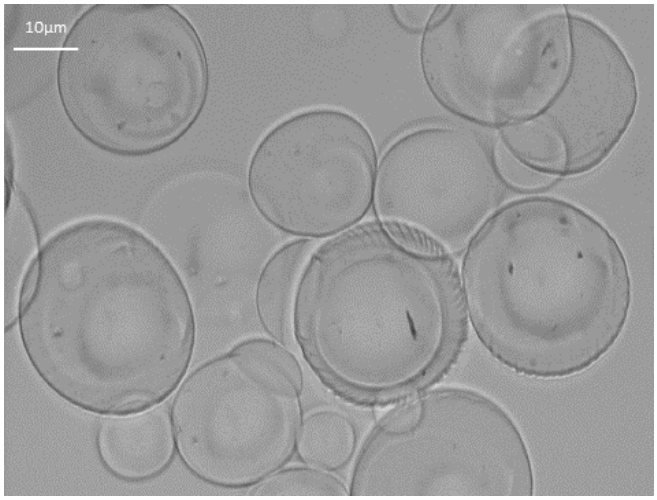

Figure 6-1: *Optical Microscopic image of IPNV encapsulated microbeads (batch 2) taken at x80 magnification. Scale bar represents 10 µm*

6.2.2 Feeding plan

Diets were divided into three different groups. Diet 0 was based on the EWOS Start 1 recipe and it contained neither antigen nor polymer. Diet 1/Ca-alginate contained EWOS Start 1 and empty calcium alginate beads while Diet 2/IPNV Ag consisted of EWOS Start 1 loaded with IPNV antigen encapsulated alginate microbeads. It should be noted that for result analysis (Section 6.2) Diet 0 was used as a control for gene expression data comparison; it was set to 0 on the qPCR data graphs while results from Diet 1 and 2 groups were expressed relative to it. All upregulations and downregulations shown on qPCR graphs were thus relative to the control Diet 0 that contained no beads. The average antigen dose was 10^9 $TCID_{50}$/ml (Chen., 2015).

6.2.3 Trial design

The trial was conducted in the subsequent order of events highlighted in Figure 6-2 below.

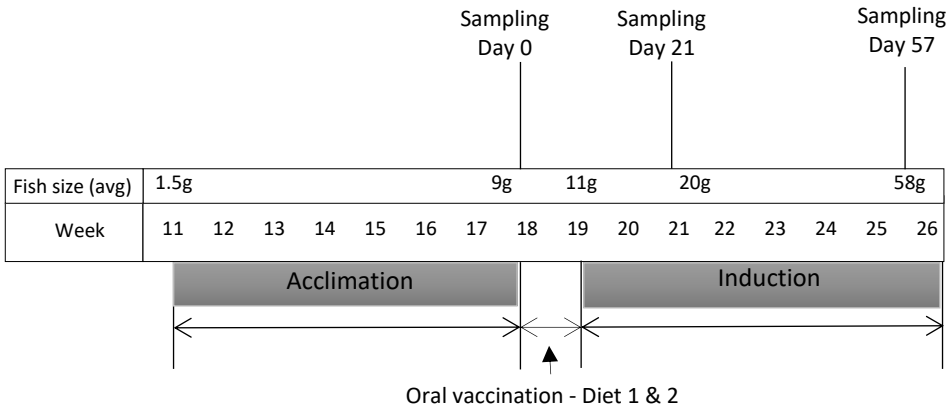

Figure 6-2: *The time line highlighting the fish size and time course of the trial: period of acclimation (7 weeks), first sampling, oral vaccination interval (one week), immune induction (7 weeks) with second sampling in week 21 and third sampling in week 26. The entire trial lasted for a duration of 26 weeks*

Starting point was chosen at week 11 as the fish were quite small prior to that and their immune system was given time to develop. This time point – week 11 – was when fish were moved to tanks in order to begin acclimatisation. Acclimatisation is the process where an organism adjusts to a change in its environment.

Eighty fish were present in each tank and the weight of individual fish from each tank was recorded. Eight circular tanks of 0.2 m^3 volume were used in the trial. This trial was conducted in fresh water supplied from an underground source in Dirdal, Norway. Fresh water was used in order to mimic their natural environment as during this life stage fish are normally present in fresh water. The average flow in each tank was 3

l/h. The oxygen saturation in water happened to be 90% while the temperature was 13.5 °C. Only three sampling points were chosen due to logistical constraints.

Parameter	Quantity
No. of tanks	8
No. of treatments	2
No. of tanks per treatment	4
No. of fish per tank – Start	100
No. of fish per tank – Day 1	85
No. of fish per tank – Day 21	80
No. of fish per tank – Day 57	80
No. of sampling points	3
No. of fish – Sampling Day 0	5
No. of fish per tank – Sampling Day 21	5
No. of fish per tank – Sampling Day 57	10

Table 6-2: *Fish challenge trial parameters*

The vaccination interval took place during week 21. This is because the immune response of salmon can be significantly affected by smoltification. Vaccination should be avoided during this time to ensure maximum immune response. The interval lasted for a week as that is the typical length of exposure for IPNV oral vaccines.

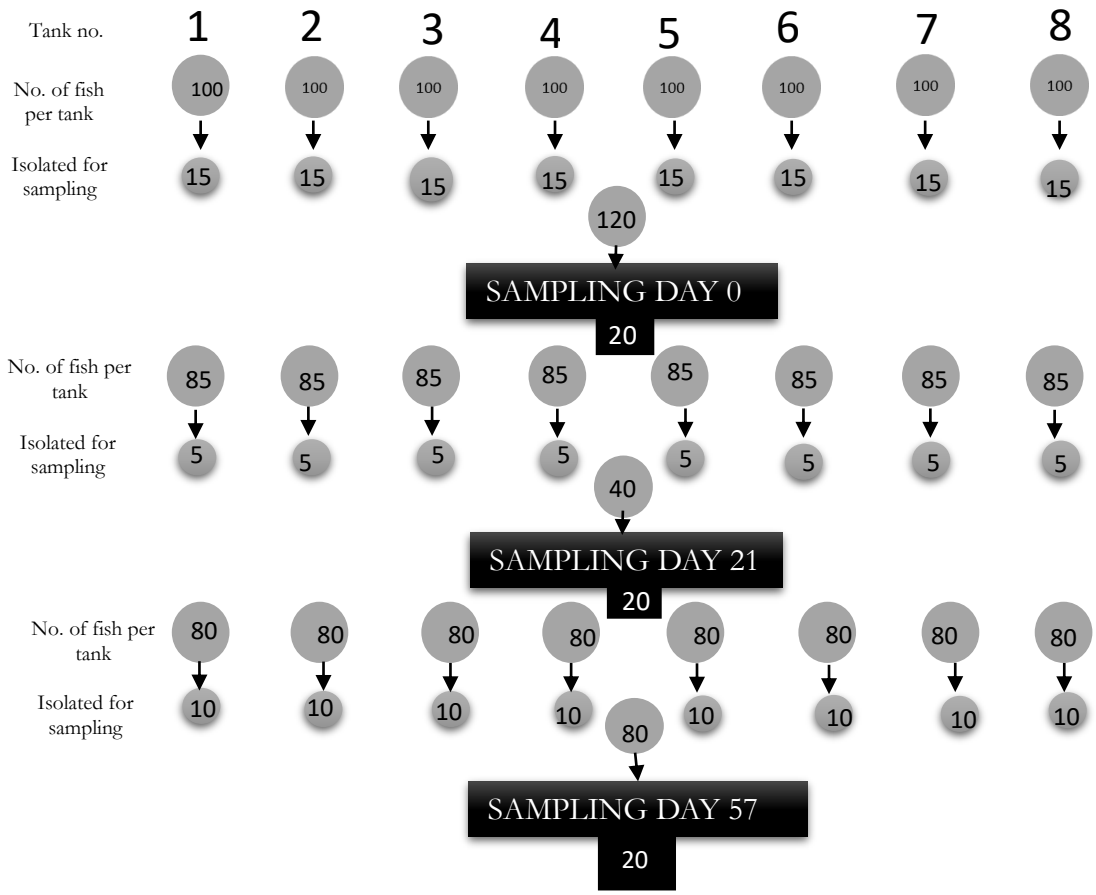

Figure 6-3: *Sampling chart for the trial. For sampling Day 0, 15 fish were removed from each tank and placed in a new tank. Out of which 20 fish were then randomly chosen for sampling. For sampling Day 21, 5 fish were removed from each tank and placed in a separate tank, from which 20 fish were chosen for sampling. On Day 57, 10 fish were removed from each tank out of which 20 were chosen for sampling*

6.3 Gene expression assessment through qPCR

Gene expression profiling has proven itself as a useful tool when studying complex conditions in A. salmon (Skugor et al. 2008) (Johansen et al. 2016) (Alzaid, Martin, and Macqueen 2016). High-throughput approaches (microarray or RNA sequencing technology) are ideally suited for previously unexplored or poorly studied conditions while targeted profiling of a selected number of key genes (e.g. by qPCR) offers an alternative for situations where prior knowledge exists, that is, when one knows which genes are responsive. qPCR is also suitable for screening in pilot studies; it is typically used to help in the refinement of treatments, before resources are spent on more costly high-throughput transcriptomics approaches. In this study, targeted qPCR profiling of the expression of fifteen genes with key roles in immune responses was done on head kidney samples at 3 time points during the study period. This has helped shed more light on the type and dynamics of immune responses which followed upon the test oral vaccine/immunization treatment. As mentioned, targeted approach was suitable for this study as 1) target organ (head kidney) has been selected based on previously described essential roles of this organ in immunity and responses of head kidney T and B cells to vaccination and 2) immune gene sequences exist in Atlantic study and validated primers for these genes are accessible in literature. The selection of head kidney tissue for qPCR screening was based on the fact that it performs key immune functions in fish, represents the systemic compartment as it is one of the main antigen trapping organs for blood-borne antigens in fish (Espenes et al. 1996) and finally, because IPNV has high tropism for head kidney (Munang'andu et al. 2013).

Special focus was given to T and B cell specific markers and other factors that regulate their behaviour. How a naïve T helper (Th) cell develops will largely determine the outcome of the overall immune response that ensues. In order to differentiate into a specialized Th cell, naive Th cell needs to receive cytokine signals from cells that got in contact with antigen and which also present the antigen to Th cells. Based on this stimulation through bound antigen-receptor complexes and cytokines, the Th cell will develop into one of the Th lineages and continue to orchestrate the immune response. Th cells are called helper cells because one of their main roles is to send signals to other types of immune cells. Th cells can be imagined as orchestrators of immune responses which send signals to other immune cell by cytokines. The surface of target cells (e.g. macrophages) express receptors to which these cytokines bind. When cytokine signal is transmitted via the surface receptor into cytoplasm and then by signalling cascade to the nucleus it results in the change of gene expression of the target cell so that its function changes according to Th cell cytokine-mediated instructions. Macrophages, B cells, neutrophils and other immune cells receive these cytokine inputs from Th cells and differentiate highly specialized functions, e.g. a B cell transforms into the antibody producing cell when it receives the cytokine cocktail signal from the Th cell of the Th2 lineage. Antibody-based immunity is based on appropriate signaling of Th2-specific cytokines that are needed for differentiation of B cells into antibody producing cells. More detail description of involved factors can be seen Figure 6-4 which shows cytokines, intracellular signalling cascade molecule and transcription factors involved in the development of naïve Th cell into one of the specific Th lineages (Th1, Th17, Th2, and Treg) (Skugor et al. 2008).

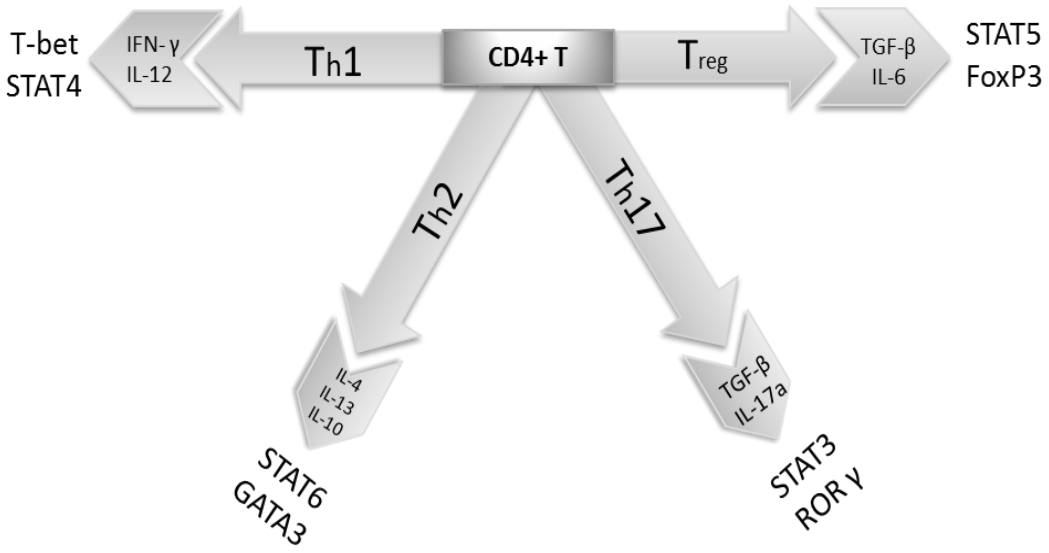

Figure 6-4: *All T helper (Th) cells including the naïve Th cell express CD4. The figure shows T cell pathways with their activator cytokines; Th1 specific (IFNy and IL12), Th17 specific (IL-17, and in some species TGFb), Th2 specific (IL-10 and IL-4/13, which is one gene in fish while in mammals there are two genes, IL-4 and IL-13), and Treg specific (TGFb and IL6), along with transducers of their signals (signalling cascade STAT molecules that transduce the cytokine signals from the surface of target cell to transcription factors with their regulatory factors such as transcription factors (T-bet, RORy, GATA3, FoxP3)*

Once the naïve Th0 cell has differentiated into the Th1 lineage, its function is to respond against intracellular microorganisms such as intracellular bacteria and viruses. Th2 cell lineage on the other hand deals with extracellular pathogens and multicellular parasites, and is required for the stimulation of antibody production by B cells. Th17 is highly pro-inflammatory and deals with extracellular bacteria and fungal microbes; Th17 is also often implicated in autoimmunity (Bedoya et al. 2013). Finally, Treg cells

are anti-inflammatory and are down-regulating immune responses, which can be associated with immune tolerance, or unsuccessful immunization.

Since salmonid fish have genes encoding activator cytokines, signal transducers and transcription factors characteristic of all four Th lineages, targeted analysis of these genes by qPCR allowed investigation of important early process expected to occur during development of an immune response to oral vaccination.

Genes involved in effector functions have also been added to the analysis, including the transcript which encodes Mx protein. Phylogenetic analysis has revealed that Mx genes are present in almost all vertebrate genomes. They are usually active against RNA viruses. Atlantic salmon is known to encode multiple Mx proteins which have the ability to suppress viruses (Verhelst, Hulpiau, and Saelens 2013). IFN-*a* and *b* induce antiviral activity in cells forming an early line of defence against viral infections, they do so by inhibiting the process of IPNV replication. A correlation between the inhibition of IPNV and Mx protein expression has been observed by (Larsen, Rokenes, and Robertsen 2004). This finding adds to the already existing evidence suggesting that antiviral activity is a significant role of Mx proteins.

The expression of Mx genes is controlled by interferons type I (IFNa) or III (IFNλ).

Atlantic salmon IFN (Alpha/beta interferon) has been reported to have an antiviral effect against IPNV in salmon cells, therefore its expression was monitored in this research. Other genes included in the analysis are described in Table 6-3.

Gene symbol and name	Gene function overview	Author/Year
T-bet	Fundamental role in coordinating type I immune responses One of the key transcription factors that control the fate of both innate and adaptive immune cells	(Kumari et al. 2015)
GATA3 – Gata binding protein 3	Transcription factor that is essential for the development of Th2 cell lineage	(Kumari, Bogwald, and Dalmo 2009)
IL-17A - Interleukin 17A	A pro-inflammatory cytokine involved in the development of the Th17 lineage and priming of neutrophils and macrophages around inflamed areas to fight extracellular microbes	(Mutoloki et al. 2010)
IL-4/13 - Interleukin 4/13	Interleukin 4/13 (IL-4/13) plays significant roles in supporting Th2 development through STAT6 signalling cascade and later in immune responses that lead to antibody production in B cells	(Sequeida, Maisey, and Imarai 2017)
STAT1 - Signal transducer and activator of transcription 1	This signal cascade molecule transmits an interferon signalling (IFNy) and is involved in regulation of transcription required for Th1 development	(Sobhkhez et al. 2014)

STAT6 - Signal transducer and activator of transcription 6	This molecule belongs to the Th2 cell signalling cascade that also has the ability to bind directly to DNA and regulate transcription	(Goenka and Kaplan 2011)
TGFb - Transforming growth factor b	This cytokine is an immune response regulator that controls the fate of multiple cell types including Treg cells	(Li and Flavell 2008)
CD4 - T helper cells	This receptor is expressed on naïve T cells and Th cells and is involved in assisting in the communication with antigen-presenting cells Evidence has been gathered over years that supports the existence of at least four CD4 T-cell subsets in fish; Th1, Th2, Th17 and Treg cells	(Zhu and Paul 2008)
IFNa - Interferon type I	IFNa plays a vital role in host defense against viral pathogens, part of Th1 responses	(Skjesol et al. 2010)
Mx	Anti-viral effector protein induced by IFN I, known to provide protection against IPNV infections	(Das et al. 2007)
MHCII - Histocompatibility complex class II	Surface marker of antigen-presenting cells that first come in contact with the antigen and present it in the groove of the MHC proteins to Th cells	(Holling, Schooten, and van Den Elsen 2004)

TCRy - T cell receptor	This receptor is expressed on T cells and is involved in recognition of fragments of antigen peptides bound to MHC molecules. Each T cell expresses TCR receptors which specifically bind antigen/MHC complex during physical contact between T cell and antigen-presenting cell	(Yazawa et al. 2008)
IgM - Immunoglobulin M	Effector antibody molecule, subtype M is the major systemic antibody in teleost fish	(Hordvik 2015)
IgT - Immunoglobulin T	Effector antibody molecule, subtype T is produced in mucosal surfaces in fish	(Tadiso, Lie, and Hordvik 2011)
FOXP3	T-cell specific transcription factor. Plays a significant role in the immune regulatory process and the development of Treg cells	(Zhang et al. 2011)

***Table 6-3**: An overview of genes assessed via qPCR, along with their function*

6.3.1 Gene expression results

The qPCR data on day 0, day 21 and day 57 are presented in Figures 6-4, 6-5 and 6-6, respectively. Expression of fifteen genes was profiled on Day 0 in order to assess the immune status in head kidney prior to exposure to test diets (all fish were exposed to Diet 0 at day 0 for seven weeks (acclimatisation period) but tanks that were later

assigned to test diets were labelled) (Figure 6 - 7). All genes showed regulation within the +1 and -1 ddCt values, which translates to 2-fold up- and down-regulation. Only 2 genes, both with previously described roles in Th2 responses, GATA3 and STAT6, showed significant up-regulation in fish assigned to tanks that would later receive the test diet with alginate and no antigen. At the same time, Th17-specific cytokine IL17A showed down-regulation of approximately 2-fold; however, it was not statistically significant.

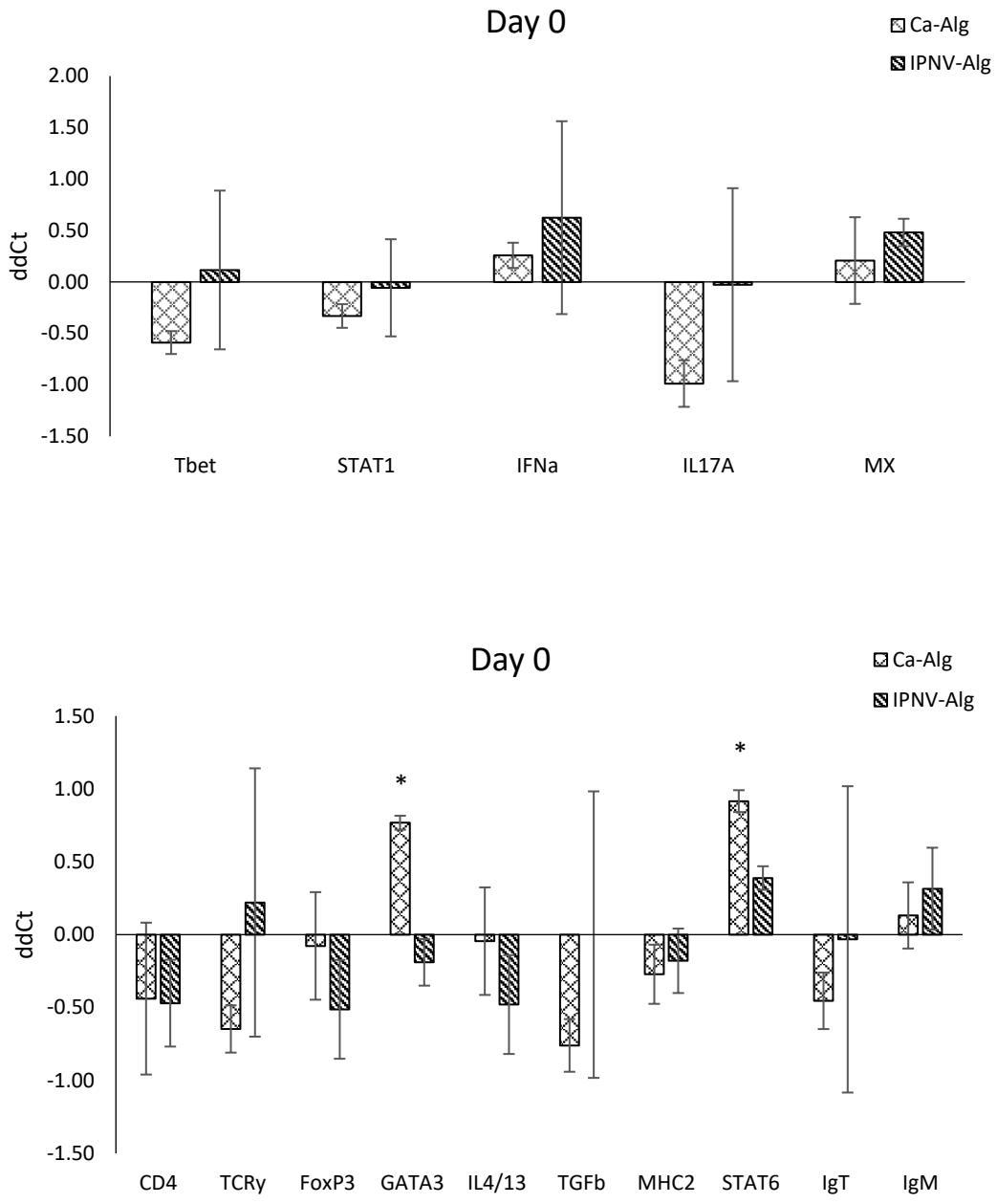

Figure 6-5: *Gene expression using qPCR at sampling Day 0. A differential pattern of up and down-regulation of fifteen genes sampled from A.Salmon head kidney is presented. Mean values of Ca-alg group (Diet 1) and IPNV-alg group (Diet 2) relative to control group (Diet 0) are recorded (n = 20, p <0.05)*

Quite a few genes showed significant upregulation in at least one of the test groups on day 21. At this time point, T-bet induction was highest among all measured genes. The

levels of the transcript encoding T-bet were significantly higher in both test feeds group in comparison to the control diet. Suggesting the onset of Th1 differentiation.

Although differences between test feeds were not large, somewhat higher levels of transcripts were seen for all Th1/17 genes (T-bet, STAT1, IFNa and IL-17A) except for Mx that showed higher level in the alginate-IPNV test group. Of the two measured T cell receptors (CD4 and TCRy) only TCRy was induced by the IPNV antigen test feed; however, this regulation was not significant. In contrast, significant down-regulation of CD4 was observed in the group exposed to IPNV-alg feed. The main mechanism of alginate encapsulated antigens has been proposed to be biased towards the Th2 response.

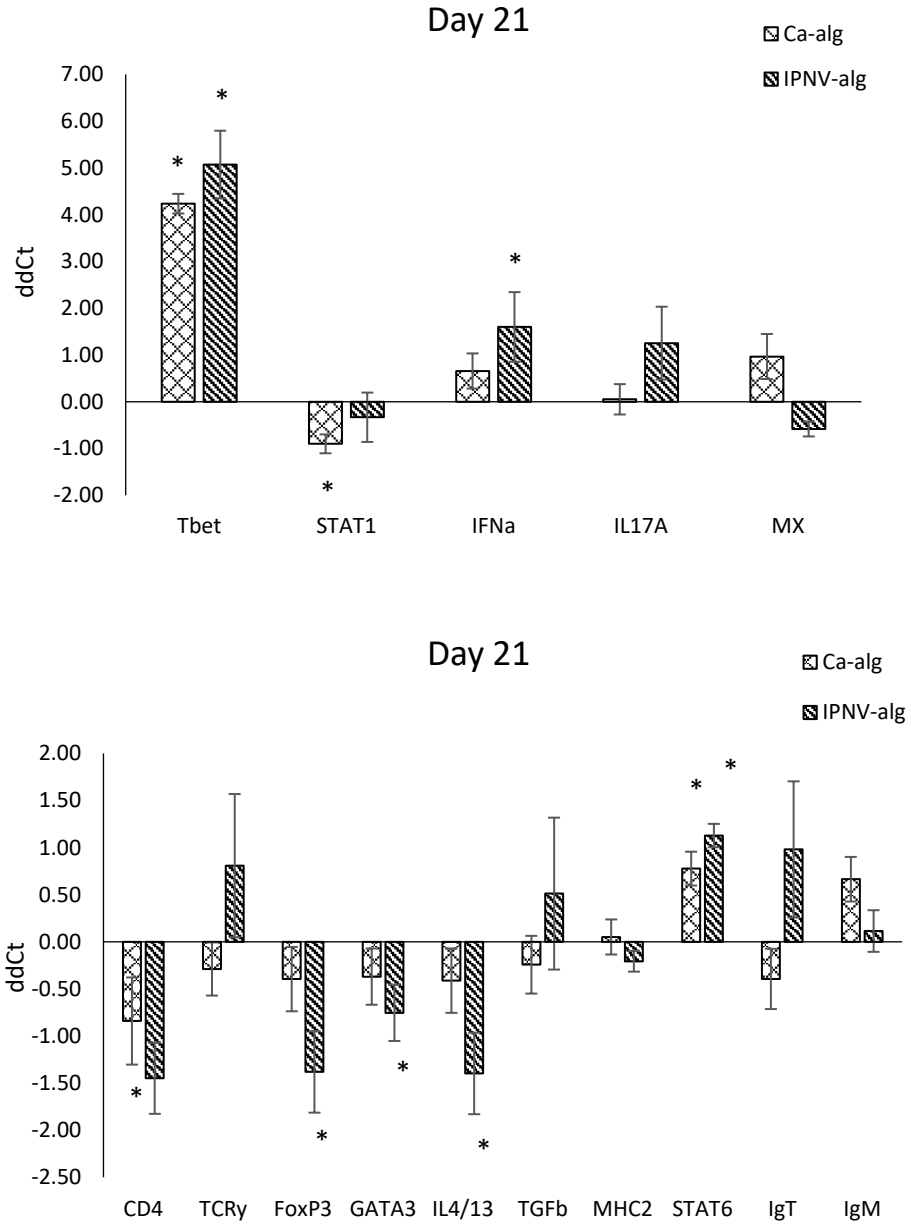

Figure 6-6: *Gene expression using qPCR at sampling Day 21. A differential pattern of up and down-regulation of fifteen genes sampled from A.Salmon head kidney is presented. Mean values of Ca-alg group (Diet 1) and IPNV-alg group (Diet 2) relative to control group (Diet 0) are recorded (n = 20, p <0.05)*

The regulatory transcription factor FOXP3 (usually found in thymus) showed significant downregulation at day 21 only in the group exposed to the antigen. The expression levels of Th2 transcription factor GATA3 and cytokine IL4/13 were also downregulated in this group while STAT6 also implicated in Th2 responses, showed opposite regulation. Increased expression level of around 2-fold of the gene encoding mucosal immunoglobulin IgT was not statistically significant.

Most genes were down-regulated on day 57 in both groups, while differences between the two test diets were negligible. T-bet remained up-regulated, however, there was a drop in the expression of T-bet in comparison to day 21. T cell receptor TCRy was significantly affected in both groups, as were TGFb, STAT6 and IgT. The transcript encoding IgT was found to be most down-regulated at day 57 with an almost 8-fold lower levels in comparison to the control group.

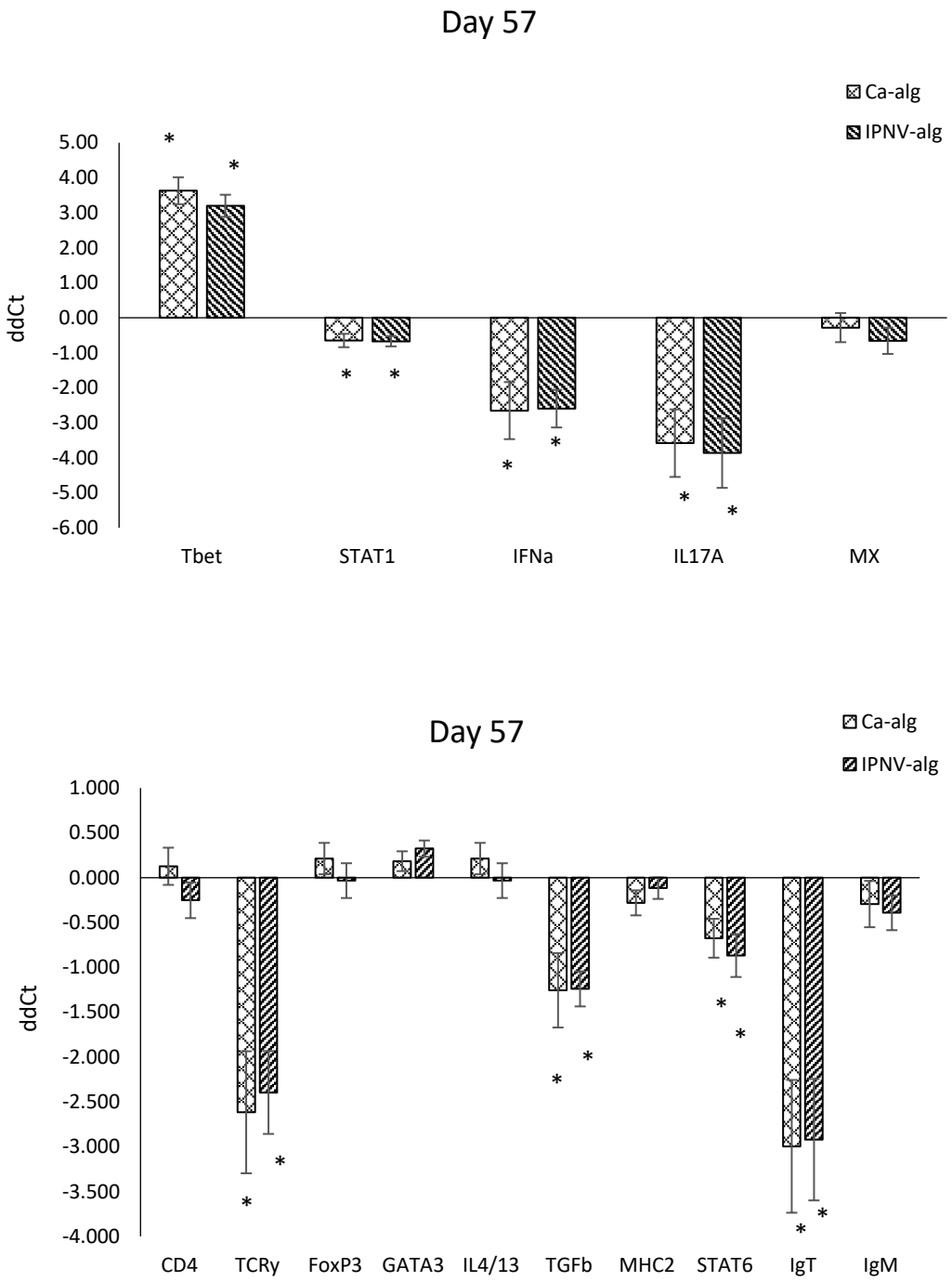

Figure 6-7: *Gene expression using qPCR at sampling Day 57. A differential pattern of up and down-regulation of fifteen genes sampled from A.Salmon head kidney is presented. Mean values of Ca-alg group (Diet 1) and IPNV-alg group (Diet 2) relative to control group (Diet 0) are recorded (n = 20, p <0.05)*

6.4 Assessment of immune responses through ELISA

Immunoglobulin (Ig) (also referred to as antibody) is part of the humoral defence which plays a critical role in parasitic, bacterial and viral infections (Choudhury and Prasad 2011). As mentioned earlier, IgM is the major systemic antibody found in teleost fish, including salmonids (Hordvik., 2015). IgM was the first immunoglobulin to appear in evolution (Magnadottir 1998). IgM levels have previously been used as an indicator of fish health and ELISA is widely used as the principal technique for the quantification of IgM in the serum of fish (Choudhury and Prasad 2011). The methodology followed for ELISA analysis is described in Section 3.2.8.3 (Chapter 3). The ELISA assay in the present study quantified IgM that specifically binds to the IPNV antigen used for oral vaccination.

The assay revealed slightly higher values in fish that received antigen with alginate in their diet (blue), irrespective of the OD used (Figure 6-8). It is recommended that the output of the ELISA assay developed for the IPNV antigen-specific IgM is measured at two OD values (Branas and Estepa 1994). Absorption spectrum at two maxima: 450 and 490 nm offers a higher assay sensitivity i.e. boosting the ability to detect differences present. Both measurements showed high correlation at the individual sample level.

It could be noted that this mostly occurred in tanks 1 and 6 (Figure 6-8). The result was, however, not significant. Differences related to the plate were minor, while all fish that exhibited higher IgM level belonged to the group which consisted of large fish (Figure 6-9).

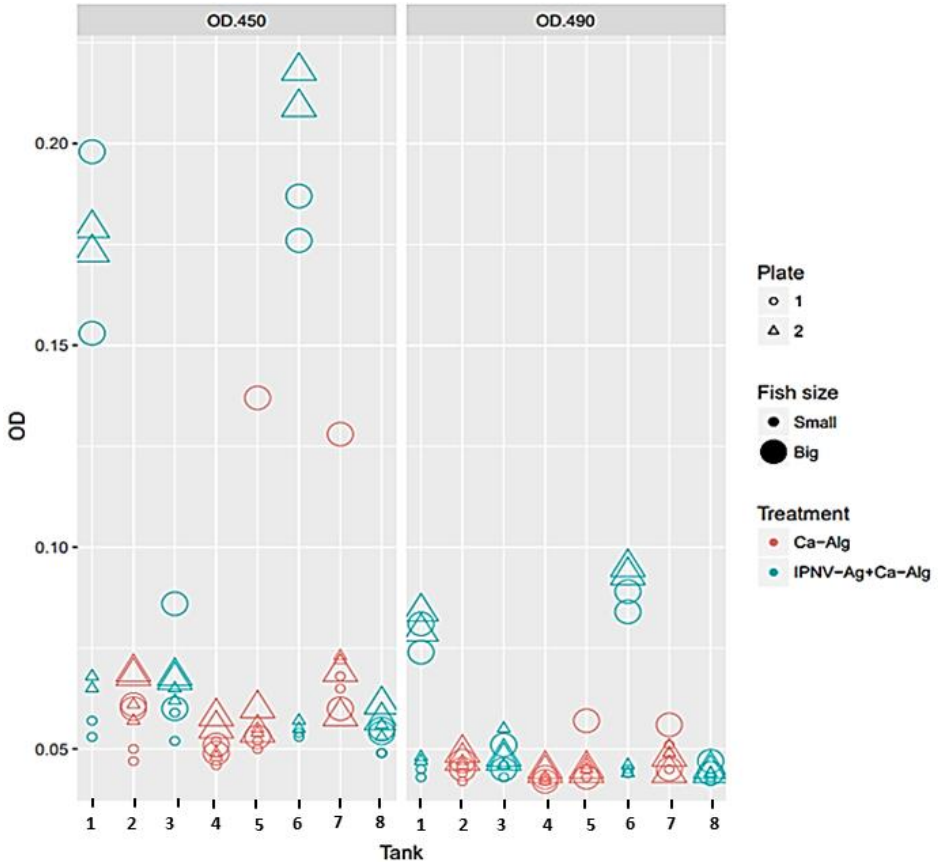

Figure 6-8: *ELISA results of IPNV antigen-specific immunoglobulin IgM in plasma of A. salmon at day 57 post oral vaccination. Values of two OD measurements (450 and 490 nm) in relation to the eight tanks shown. The ELISA samples were n = 8 per tank, are represented by shapes, with the smaller circles denoting smaller fish while bigger circles denote bigger fish. Red shapes represented the unencapsulated sample while blue represented IPNV encapsulated samples*

It would be fair to suggest that the IPN antigen encapsulated in polymeric microbeads survived through the encapsulation/feed preparation process as higher IgM levels can generally be detected in tanks containing IPNV-alg feed.

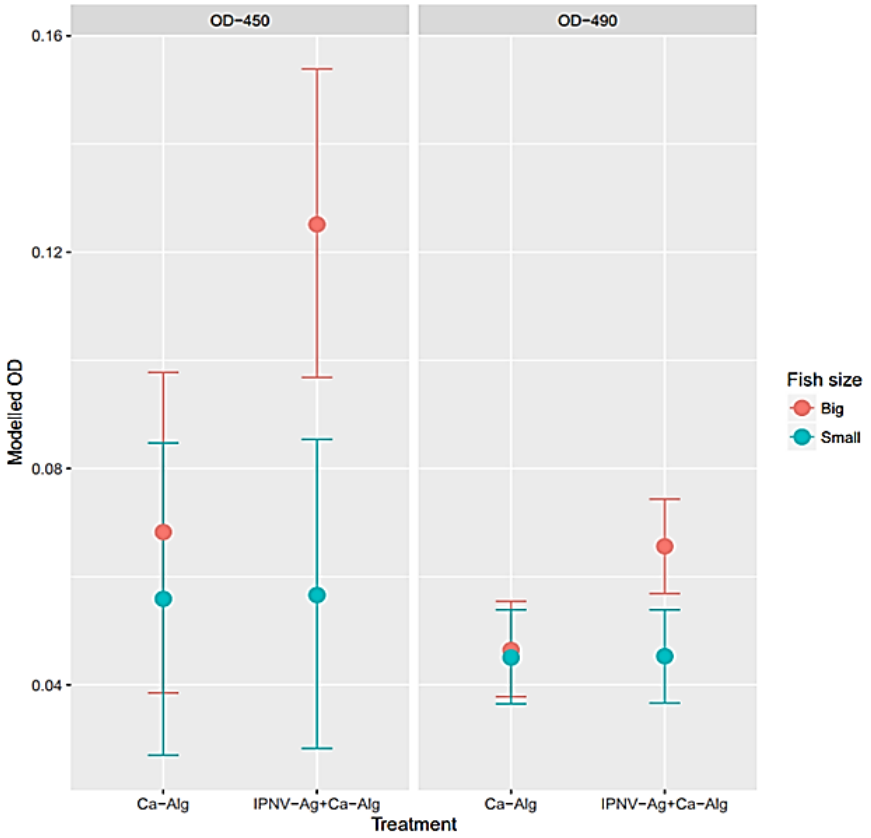

Figure 6-9: *ELISA results of IPNV antigen-specific immunoglobulin IgM in plasma of A. salmon at day 57 post oral vaccination. Values of two OD measurements (450 and 490 nm) are shown (n = 16 per diet)*

6.5 Discussion

6.5.1 Gene expression data through qPCR

Sampling at Day 0 was carried out to assess whether there were any significant differences between the fish in tanks that would be assigned to test treatments. Not too many substantial differences were observed – they were mainly below +1 and -1 ddCt. However, as judged by the profiled genes in this particular study, it could be said that there was a slightly higher level of genes implicated in Th2 immunity in the group later assigned to the alginate only diet.

At day 21, the effect of dietary treatments was evident in both groups. Judged by the similarity of observed responses in two dietary groups, it could be concluded that any prior activation of Th2 immune responses in the group which received only alginate did not play a major role in responses that occurred at day 21. The marker of Th cells CD4 was found down-regulated while the TCR-γ showed higher expression in vaccinated fish (although not significant). Together, this could mean that the population of T cells in head kidneys of vaccinated fish contained more cytotoxic T-cells expressing TCR-γ (Goodman and Lefrancois 1988) than CD4 positive T cells.

The expression profile of T-bet suggested that alginate by itself influences expression of immune related genes, and possibly skews immunity towards Th1 responses. Addition of IPNV antigen and alginate in the diet slightly increased induction of T-bet compared to the alginate only group. An additional proof for more pronounced Th1 responses in the vaccinated antigen-alginate group was the expression profile of the anti-viral cytokine IFNa, which was significantly induced in comparison to the

control feed. Master regulator FoxP3 that is required for the development of Treg cells in mammals (Weaver et al. 2007) and very likely in fish too, showed lower expression profile in the vaccinated fish. Treg cells are immunosuppressive towards pro-inflammatory Th-mediated responses, which suggested that vaccinated fish had an improved chance of mounting the immune response. Furthermore, T-bet is known to inhibit development of the Th2 lineage by suppressing the production of Th2 cytokines and GATA3 in mammals (Weaver et al. 2007) which were indeed more markedly downregulated in the vaccinated group.

Thus, the low expression profile of both GATA3 and IL4/13 could be an evidence that the vaccinated group at day 21 showed more pronounced anti-viral immune responses and somewhat downplayed Th2 responses. However, STAT6 that transduces Th2 signals and transcript encoding IgT were also among the genes that showed higher expression profiles in vaccinated than in fish that received only alginate. Although considered a Th1 cytokine, T-bet has also been shown to be involved in improved antibody-mediated clearance of malaria in humans (Oakley et al, 2014), while Sun et al, 2011 showed that predominant expression of intraglomerular T-bet expression correlated with antibody-mediated rejection in humans.

6.5.2 Immune response through ELISA

ELISA analysis showed that a number of fish managed to produce IPNV antigen specific IgM antibodies.

The responses were weak, but were seen to be tank specific as tank 1 and 6 showed higher IgM levels for both OD values analysed. The fish located in these tanks were

fed samples containing the IPNV antigen encapsulated microbeads. This could mean that one or more unknown factors present in tanks 1 and 6 and absent in tanks 2, 4 and 8 greatly contribute to the effect of oral vaccination.

Interestingly, it was also noted that fish bigger in size displayed the highest levels of IgM whereas smaller fish possessed half as much. Perhaps fish larger in size consumed more feed per fish weight as compared to smaller fish or were able to absorb the antigen more effectively, which resulted in a larger dose of the antigen in immune tissues resulting in the better response to oral vaccination.

The low levels of IgM detected (Figure 6-8) can certainly be contributed to a significant factor which was that samples were only exposed to a small dose of antigen and not a real virus following the process of immunisation. After coming into contact with the viral infection, the fish exposed to the IPN antigen would perhaps be quicker in mounting an increased immune response.

The detection of IgM however suggests that the fish samples had been primed. The amount of circulating B cells was increased. These B cells then successfully produced IgM which possesses the ability to bind to the IPN antigen. In the case of exposure to the IPN virus in future, these fish samples will be able to produce IgM more rapidly which will neutralise the virus in the initial stages of onset.

6.4 Limitations

Even though IPNV is known to have an increased tropism for head kidney, the spleen is another major organ that is acknowledged as the region where antibodies are produced. Viral antigens can also be detected in the liver and pancreas too. Hence, in a future challenge trial it would be ideal to include samples taken from the spleen, liver, pancreas and hindgut as well.

Another critical limitation of this trial was the amount of time points considered throughout the duration of the experiment. Since samples were taken all of three times through a period of 57 days, the intervals were in fact quite long for sampling. It is therefore possible that many interesting dynamics regarding gene expression were overlooked. However, the reason why these time points were initially chosen were due to the fact that oral vaccine is not expected to show a quick response, specifically with regards to fish it takes approximately two weeks for adaptive immunity to kick in.

6.5 Summary

The evolutionary relationship which exists between host immune defences and viral counter attacks are important to analyse since a better understanding only beneficially aids the aquaculture industry as a whole. An enhanced knowledge of host-pathogen synergy provides additional input for an improved viral infection survival rates during high susceptibility periods where farmed fish especially Atlantic salmon are concerned.

7. Conclusions and Future work

7.1 Summary and conclusions

This chapter offers an overview of the principal conclusions established throughout this thesis. In Chapter 1, a series of objectives were set out in order to achieve the overall aim of this research study. These objectives followed a sequential order as outlined in Figure 7-1 below.

The optimisation of two novel microbead fabrication techniques: ES and AAJ resulted in microbeads ranging from 25 – 2500 μm (Figure 4-10 and 4-11). This size range promotes the promising application of microbeads to serve as oral drug delivery mechanisms through the encapsulation of an API, since this size range is ideal for easy and effective incorporation within the feed pellet for oral intake. In terms of the wider implications of this work, the operational maps produced offer a distinct look into the size range of microbeads that can potentially be fabricated using ES and AAJ methodologies for every appropriate combination of flow rate and applied voltage/pressure possible for a given concentration of alginate.

Furthermore, mechanical testing revealed that fabrication methodologies had negligible influence on the microbeads' mechanical properties. The mechanical properties of microbeads fabricated through ES and AAJ were also conclusively associated with polymer concentration and type of cross-linking solution. The novelty of these methodologies lies in the simplicity of control they have to offer since homogenous microbeads of a vast size range are produced through the adjustment of basic process parameters, which is a substantial drawback where other conventional synthesis techniques are concerned.

An in vitro dissolution test methodology specifically tailored to mimic the in vivo environment of A. salmon was established. This study helps lay a platform for the analysis of biologically active compound release from the Ca-alg matrix. Furthermore, it provides an insight into the potential performance of these release systems in vivo.

Since the primary aim of this research is to characterise alginate microbeads as antigen delivery systems, Chapter 4 was solely dedicated to the assessment and analysis of Ca-alg microbeads' dissolution profiles and encapsulation efficiencies. The approach applied for the encapsulation of a potential API (BD) promises an efficient, continuous single-step process, possessing the ability to fabricate monodisperse BD encapsulated microbeads with high encapsulation efficiency (>84.5 – 93.50%) for all five types of commercially leading alginates tested. While the release profiles obtained concluded potential API release of up to 66.9 - 99% under simulated A. salmon in vivo conditions, for a test duration of 55 minutes under pH 3.0 and 8.0, as the antigen is significantly inclined to be released in the mid/distal intestine – consisting of an acidic environment leading to an alkaline one - where the antigen can be absorbed.

As the final principal aim of this research, the absorbed antigen is tested for its ability to induce a specific immune response in A. salmon. Results gained from an IPNV challenge trial indicated that the absorbed antigen was able to induce an immune response in A. salmon. ELISA analysis highlighted a slight increase in levels of IPN specific antibodies in the blood plasma of the experimental group exposed to encapsulated viral antigen in Ca-alg microbeads as compared to the control group fed un-encapsulated Ca-alg microbeads. Results gained from qPCR gene analysis supported these findings as upregulation in specific immune genes in the experimental group consisting of fish fed with encapsulated IPNV-alg microbeads was observed over the sampling time period.

Additionally, another imperative observation established by the analysis of data gained through qPCR and ELISA was the stability of IPNV antigen through the challenge trial. Indication of the presence of IPNV antigen at the final stage of sampling (day 57) of the trial suggests its survival through the process of storage – highlighting long shelf-life, the process of feed production – highlighting robustness and finally the process of antigen incorporated pellet uptake by the A.Salmon – highlighting successful crossing through the epithelial layers present in the intestine.

7.2 Recommendations for future research

Section 7.1 emphasized the outcomes achieved diligently through the course of this research. This section presents further suggestions for possible future work that can help build on the platform initiated at present through this thesis. Given the constraints in resources available in terms of variables such as risk, time and especially cost, further exploration of various areas of interest associated with this research were hindered. Some of the suggestions are as follows;

- In Chapter 4, an additional operational size map study should be performed using a biologically active compound such as the IPNV antigen itself. This can offer a more specific outlook on the size range of microbeads that can be produced through ES and AAJ. Even though the stand in used in our studies consisted of particles small enough in size in comparison to alginate chains, the incorporation of an active macromolecule may make a contribution to the final fabricated microbeads' size
- Mechanical testing can be further branched out by performing compression testing on the same five alginate types as those used during dissolution testing so as to present a more comprehensive outlook into these specific types of alginates. This will also help further the understanding of the effect their chemical structures may have on their mechanical stability
- The approach for optimisation of microbead fabrication methodologies; ES and AAJ can be extended towards the exploration of various other polymer/drug combinations

- In chapter 5, the model API (BD) for in vitro dissolution testing can be replaced with the relevant antigen itself. This can perhaps offer a more definitive result of the effect of the encapsulated compound on the dissolution behaviour of Ca-alg microbeads
- In Chapter 6, the challenge trial carried out has the potential to be carried out more systematically with the addition of many more sampling points and collecting sample's from more than one organ
- Furthermore, in addition to the ELISA and qPCR techniques, the immune response can be analysed through protionics. Since qPCR is a more targeted approach, it might be useful to look into protein expression to gain a closer understating of the immune response
- A challenge trial that assesses mortality rate could also prove useful. The trial carried out in this thesis analysed the effect of vaccination itself. The fish samples were exposed to a small dose of antigen. A new approach for a trial could expose the samples to a real virus after the process of immunisation and assess levels of success by looking at mortality rates

References

Alzaid, A., S. A. Martin, and D. J. Macqueen. 2016. 'The complete salmonid IGF-IR gene repertoire and its transcriptional response to disease', Sci Rep, 6: 34806.

Acarturk, F. and S. Takka (1999). "Calcium alginate microparticles for oral administration: II. Effect of formulation factors on drug release and drug entrapment efficiency." J Microencapsul 16(3): 291-301.

Augst, A. D., H. J. Kong and D. J. Mooney (2006). "Alginate hydrogels as biomaterials." Macromolecular Bioscience 6(8): 623-633.

Ahmed, E. M. 2015. 'Hydrogel: Preparation, characterization, and applications: A review', Journal of Advanced Research, 6: 105-21.

Almeria, B., W. W. Deng, T. M. Fahmy, and A. Gomez. 2010. 'Controlling the morphology of electrospray-generated PLGA microparticles for drug delivery', Journal of Colloid and Interface Science, 343: 125-33.

Arumuganathar, S., S. Irvine, J. R. McEwan, and S. N. Jayasinghe. 2007. 'Aerodynamically assisted bio-jets: the development of a novel and direct non-electric field-driven methodology for engineering living organisms', Biomedical Materials, 2: 158-68.

Abad, M. E., F. M. Binkhorst, M. T. Elbal, and J. H. Rombout. 1987. 'A comparative immunocytochemical study of the gastro-entero-pancreatic (GEP) endocrine system in a stomachless and a stomach-containing teleost', Gen Comp Endocrinol, 66: 123-36.

Ahmed, E. M. 2015. 'Hydrogel: Preparation, characterization, and applications: A review', Journal of Advanced Research, 6: 105-21.

Aldrin, M., B. Storvik, A. B. Kristoffersen, and P. A. Jansen. 2013. 'Space-time modelling of the spread of salmon lice between and within Norwegian marine salmon farms', Plos One, 8: e64039.

Arumuganathar, S., S. Irvine, J. R. McEwan, and S. N. Jayasinghe. 2007. 'Aerodynamically assisted bio-jets: the development of a novel and direct non-electric field-driven methodology for engineering living organisms', Biomedical Materials, 2: 158-68.

Azad, I. S., K. M. Shankar, C. V. Mohan, and B. Kalita. 2000. 'Uptake and processing of biofilm and free-cell vaccines of Aeromonas hydrophila in Indian major carps and common carp following oral vaccination - antigen localization by a monoclonal antibody', Diseases of Aquatic Organisms, 43: 103-08.

Aas, I. B., L. Austbo, K. Falk, I. Hordvik, and E. O. Koppang. 2017. 'The interbranchial lymphoid tissue likely contributes to immune tolerance and defense in the gills of Atlantic salmon', Dev Comp Immunol, 76: 247-54.

Ballesteros, N. A., S. S. Saint-Jean, P. A. Encinas, S. I. Perez-Prieto, and J. M. Coll. 2012. 'Oral immunization of rainbow trout to infectious pancreatic necrosis virus (Ipnv) induces different immune gene expression profiles in head kidney and pyloric ceca', *Fish Shellfish Immunol*, 33: 174-85.

Banerjee, S., and S. Mazumdar. 2012. 'Electrospray Ionization Mass Spectrometry: A Technique to Access the Information beyond the Molecular Weight of the Analyte', *International Journal of Analytical Chemistry*.

Baras, B., M. A. Benoit, O. Poulain-Godefroy, A. M. Schacht, A. Capron, J. Gillard, and G. Riveau. 2000. 'Vaccine properties of antigens entrapped in microparticles produced by spray-drying technique and using various polyester polymers', *Vaccine*, 18: 1495-505.

Barua, S., J. W. Yoo, P. Kolhar, A. Wakankar, Y. R. Gokarn, and S. Mitragotri. 2013. 'Particle shape enhances specificity of antibody-displaying nanoparticles', Proceedings of the National Academy of Sciences of the United States of America, 110: 3270-75.

Branas, M.V. and Estepa. A. 1994. 'A sandwich ELISA to detect VHSV and IPNV in turbot', *Aquaculture International*, 2: 206 – 217

Bedoya, S. K., B. Lam, K. Lau, and J. Larkin, 3rd. 2013. 'Th17 cells in immunity and autoimmunity', Clin Dev Immunol, 2013: 986789

Bodmeier, R. and J. W. McGinity (1988). "Polylactic acid microspheres containing quinidine base and quinidine sulphate prepared by the solvent evaporation method. III. Morphology of the microspheres during dissolution studies." J Microencapsul 5(4): 325-330.

Boury, F., H. Marchais, J. P. Benoit and J. E. Proust (1997). "Surface characterization of poly(alpha-hydroxy acid) microspheres prepared by a solvent evaporation/extraction process." Biomaterials 18(2): 125-136.

Brondsted, H. and J. Kopecek (1992). "Hydrogels for site-specific drug delivery to the colon: in vitro and in vivo degradation." Pharm Res 9(12): 1540-1545.

Bhujbal, S. V., G. A. Paredes-Juarez, S. P. Niclou, and P. de Vos. 2014. 'Factors influencing the mechanical stability of alginate beads applicable for immunoisolation of mammalian cells', Journal of the Mechanical Behavior of Biomedical Materials, 37: 196-208.

Bock, N., M. A. Woodruff, D. W. Hutmacher, and T. R. Dargaville. 2011. 'Electrospraying, a Reproducible Method for Production of Polymeric Microspheres for Biomedical Applications', Polymers, 3: 131-49.

Bruslind, L. D., and P. W. Reno. 2000. 'Virulence comparison of three buhl-subtype isolates of infectious pancreatic necrosis virus in brook trout fry', Journal of Aquatic Animal Health, 12: 301-15.

Bucking, C., and C. M. Wood. 2009. 'The effect of postprandial changes in pH along the gastrointestinal tract on the distribution of ions between the solid and fluid phases of chyme in rainbow trout', Aquaculture Nutrition, 15: 282-96.

Bhattarai, N., J. Gunn, and M. Zhang. 2010. 'Chitosan-based hydrogels for controlled, localized drug delivery', Adv Drug Deliv Rev, 62: 83-99.

Bootland, L. M., P. Dobos, and R. M. W. Stevenson. 1990. 'Fry Age and Size Effects on Immersion Immunization of Brook Trout, Salvelinus-Fontinalis Mitchell, against Infectious Pancreatic Necrosis Virus', Journal of Fish Diseases, 13: 113-25.

Brudeseth, B. E., R. Wiulsrod, B. N. Fredriksen, K. Lindmo, K. E. Lokling, M. Bordevik, N. Steine, A. Klevan, and K. Gravningen. 2013. 'Status and future perspectives of vaccines for industrialised fin-fish farming', Fish Shellfish Immunol, 35: 1759-68.

Choudhury, M. and K.P. Prasad. 2011. 'Isolation and characterization of immunoglobulin M of Asian sea bass, Lates calcarifer and its level in serum'. Cent Eur J Biology, 6: 180 – 187

Chen, K. L., S. E. Mylon and M. Elimelech (2007). "Enhanced aggregation of alginate-coated iron oxide (hematite) nanoparticles in the presence of calcium, strontium, and barium cations." Langmuir 23(11): 5920-5928.

Chen, L., G. Klaric, S. Wadsworth, S. Jayasinghe, T. Y. Kuo, O. Evensen, and S. Mutoloki. 2014. 'Augmentation of the antibody response of Atlantic salmon by oral administration of alginate-encapsulated IPNV antigens', Plos One, 9: e109337

Chan, E. S., B. B. Lee, P. Ravindra, and D. Poncelet. 2009. 'Prediction models for shape and size of ca-alginate macrobeads produced through extrusion-dripping method', Journal of Colloid and Interface Science, 338: 63-72.

Canepa, C., J. C. Imperiale, C. A. Berini, M. Lewicki, A. Sosnik, and M. M. Biglione. 2017. 'Development of a Drug Delivery System Based on Chitosan Nanoparticles for Oral Administration of Interferon-alpha', Biomacromolecules, 18: 3302-09.

Caputo, A., E. Brocca-Cofano, A. Castaldello, R. Voltan, R. Gavioli, I. K. Srivastava, S. W. Barnett, A. Cafaro, and B. Ensoli. 2008. 'Characterization of immune responses elicited in mice by intranasal co-immunization with HIV-1 Tat, gp 140 Delta V2Env and/or SIV Gag proteins and the nontoxicogenic heat-labile Escherichia coli enterotoxin', Vaccine, 26: 1214-27.

Caruffo, M., C. Maturana, S. Kambalapally, J. Larenas, and J. A. Tobar. 2016. 'Protective oral vaccination against infectious salmon anaemia virus in Salmo salar', Fish Shellfish Immunol, 54: 54-9.

Castro-Sanchez, P., and J. M. Martin-Villa. 2013. 'Gut immune system and oral tolerance', Br J Nutr, 109 Suppl 2: S3-11.

Chen, L., G. Klaric, S. Wadsworth, S. Jayasinghe, T. Y. Kuo, O. Evensen, and S. Mutoloki. 2014. 'Augmentation of the antibody response of Atlantic salmon by oral administration of alginate-encapsulated IPNV antigens', Plos One, 9: e109337.

Chen, W., W. Jin, N. Hardegen, K. J. Lei, L. Li, N. Marinos, G. McGrady, and S. M. Wahl. 2003. 'Conversion of peripheral CD4+CD25- naive T cells to CD4+CD25+

regulatory T cells by TGF-beta induction of transcription factor Foxp3', J Exp Med, 198: 1875-86.

Coelho, J. F., P. C. Ferreira, P. Alves, R. Cordeiro, A. C. Fonseca, J. R. Gois, and M. H. Gil. 2010. 'Drug delivery systems: Advanced technologies potentially applicable in personalized treatments', EPMA J, 1: 164-209.

Coelho. J. 2013. 'Drug delivery systems: advanced technologies potentially applicable in personalised treatment.

Collet, B. 2014. 'Innate immune responses of salmonid fish to viral infections', Dev Comp Immunol, 43: 160-73.

Crane, M., and A. Hyatt. 2011. 'Viruses of fish: an overview of significant pathogens', Viruses, 3: 2025-46.

Das, B. K., K. K. Nayak, M. Fourrier, B. Collet, M. Snow, and A. E. Ellis. 2007. 'Expression of Mx protein in tissues of Atlantic salmon post-smolts--an immunohistochemical study', Fish Shellfish Immunol, 23: 1209-17.

DeVos, P., B. DeHaan, J. Pater, and R. VanSchilfgaarde. 1996. 'Association between capsule diameter, adequacy of encapsulation, and survival of microencapsulated rat islet allografts', Transplantation, 62: 893-99.

Dalla Valle, A. Z., M. Iriti, F. Faoro, C. Berti, and S. Ciappellano. 2008. 'In vivo prion protein intestinal uptake in fish', APMIS, 116: 173-80.

de las Heras, A. I., S. R. Saint-Jean, and S. I. Perez-Prieto. 2010. 'Immunogenic and protective effects of an oral DNA vaccine against infectious pancreatic necrosis virus in fish', Fish & Shellfish Immunology, 28: 562-70.

Dhandayuthapani, B., Y. Yoshida, T. Maekawa, and D. S. Kumar. 2011. 'Polymeric Scaffolds in Tissue Engineering Application: A Review', International Journal of Polymer Science.

Dhar, A. K., S. K. Manna, and F. C. Thomas Allnutt. 2014. 'Viral vaccines for farmed finfish', Virusdisease, 25: 1-17.

Dorak, M. T. 2007. 'Role of natural killer cells and killer immunoglobulin-like receptor polymorphisms: association of HLA and KIRs', Methods Mol Med, 134: 123-44.

Dreifus, M., T. Herben, D. Lim, and O. Wichterle. 1960. '[Tolerance of orbital implants made of hydrocolloid acrylate]', Sb Lek, 62: 212-8.

Duff, D. C. B. 1942. 'The oral immunization of trout against Bacterium salmonicida', *Journal of Immunology*, 44: 87-94.

Dunn, A. J. 1989. 'Psychoneuroimmunology for the psychoneuroendocrinologist: a review of animal studies of nervous system-immune system interactions', Psychoneuroendocrinology, 14: 251-74.

Devi. N., Chandana. M, Sindhura. A, Ratnavali. G and Kavitha. R. 2010. ‘Comparative evaluation of alginate beads prepared by ionotropic gelation technique’, Pharmacophore, 1: 196 – 213

Dobos. 1995. ‘Advances in virus research’. Elsevier Academic Press, 62: 119

Desmettre. P.H, and Martinod. S. 1997. ‘Research and development in veterinary vaccinology’. Amsterdam, Netherlands: Elsevier

DFO. 2017. ‘Residual infectious pancreatic necrosis (IPN) transmission risk from arctic char transfers into British Columbia’. DFO Can Sci Advis Sci Resp: 041: 1 – 34

Espenes, A., C. M. Press, L. J. Reitan, and T. Landsverk. 1996. 'The trapping of intravenously injected extracellular products from Aeromonas salmonicida in head kidney and spleen of vaccinated and nonvaccinated Atlantic salmon, Salmo salar L', Fish & Shellfish Immunology, 6: 413-26.

Edwards, L. J. (1951). "The Dissolution and Diffusion of Aspirin in Aqueous Media." Transactions of the Faraday Society 47(11): 1191-1210.

Eisenberg, E., and E. Y. Levanon. 2003. 'Human housekeeping genes are compact', Trends in Genetics, 19: 362-65.

Embregts, C. W., and M. Forlenza. 2016. 'Oral vaccination of fish: Lessons from humans and veterinary species', Dev Comp Immunol, 64: 118-37.

FAO (Food and agriculture organisation of the United Nations). 2017. ‘Globefish – analysis and information on world fish trade’. Available from: http://www.fao.org/docrep/x5738e/x5738e02.htm

Filleborn, V. M. (1948). "A new approach to tablet disintegration testing." Am J Pharm Sci Support Public Health 120(7): 233-255.

Fu, X., Q. Ping and Y. Gao (2005). "Effects of formulation factors on encapsulation efficiency and release behaviour in vitro of huperzine A-PLGA microspheres." J Microencapsul 22(7): 705-714.

Egidius, E., R. Wiik, K. Andersen, K. A. Hoff, and B. Hjeltnes. 1986. 'Vibrio-Salmonicida Sp-Nov, a New Fish Pathogen', International Journal of Systematic Bacteriology, 36: 518-20.

Elisseeff, J. 2008. 'Hydrogels: structure starts to gel', *Nat Mater*, 7: 271-3.

Embregts, C. W., and M. Forlenza. 2016. 'Oral vaccination of fish: Lessons from humans and veterinary species', Dev Comp Immunol, 64: 118-37.

Enayati, M., M. W. Chang, F. Bragman, M. Edirisinghe, and E. Stride. 2011. 'Electrohydrodynamic preparation of particles, capsules and bubbles for biomedical engineering applications', Colloids and Surfaces a-Physicochemical and Engineering Aspects, 382: 154-64.

Furtmann, B., J. Tang, S. Kramer, T. Eickner, F. Luderer, G. Fricker, A. Gomez, B. Heemskerk, and P. S. Jahn. 2017. 'Electrospray Synthesis of Poly(lactide-co-

glycolide) Nanoparticles Encapsulating Peptides to Enhance Proliferation of Antigen-Specific CD8(+) T Cells', J Pharm Sci, 106: 3316-27.

Feng, L., J. A. Ward, S. K. Li, G. Tolia, J. Hao, and D. I. Choo. 2014. 'Assessment of PLGA-PEG-PLGA copolymer hydrogel for sustained drug delivery in the ear', Curr Drug Deliv, 11: 279-86.

Fenn, J. B. 2002. 'Electrospray ionization mass spectrometry: How it all began', J Biomol Tech, 13: 101-18.

Frohlich, E. 2012. 'The role of surface charge in cellular uptake and cytotoxicity of medical nanoparticles', International Journal of Nanomedicine, 7: 5577-91.

Gallovic, M. D., K. L. Schully, M. G. Bell, M. A. Elberson, J. R. Palmer, C. A. Darko, E. M. Bachelder, B. E. Wyslouzil, A. M. Keane-Myers, and K. M. Ainslie. 2016. 'Acetalated Dextran Microparticulate Vaccine Formulated via Coaxial Electrospray Preserves Toxin Neutralization and Enhances Murine Survival Following Inhalational Bacillus Anthracis Exposure', Adv Healthc Mater, 5: 2617-27.

Geven, E. J. W., and P. H. M. Klaren. 2017. 'The teleost head kidney: Integrating thyroid and immune signalling', *Dev Comp Immunol,* 66: 73-83.

Griessinger, E., S. N. Jayasinghe, and D. Bonnet. 2012. 'Aerodynamically assisted bio-jetting of hematopoietic stem cells', Analyst, 137: 1329-33.

Gudding, R., and W. B. Van Muiswinkel. 2013. 'A history of fish vaccination Science-based disease prevention in aquaculture', Fish & Shellfish Immunology, 35: 1683-88.

Grasdalen, H., B. Larsen, and O. Smidsrod. 1981. 'C-13-Nmr Studies of Monomeric Composition and Sequence in Alginate', Carbohydrate Research, 89: 179-91.

Goenka, S., and M. H. Kaplan. 2011. 'Transcriptional regulation by STAT6', Immunol Res, 50: 87-96.

Goodman, T., and L. Lefrancois. 1988. 'Expression of the gamma-delta T-cell receptor on intestinal CD8+ intraepithelial lymphocytes', Nature, 333: 855-8.

Ganan-Calvo, A. M., and A. Barrero. 1999. 'A novel pneumatic technique to generate steady capillary microjets', Journal of Aerosol Science, 30: 117-25.

Gomez, A., and K. Q. Tang. 1994. 'Charge and Fission of Droplets in Electrostatic Sprays', Physics of Fluids, 6: 404-14.

Gawde, S and Agrawal. S. 2012. ‘Design and characterization of Eudragit coated Chitosan microspheres of Deflazacort for colon targeting’, Journal of pharmacy research, 5: 4867 – 4870

GOAL (Global outlook on aquaculture leadership). 2016. China. Available from:

Harder. W. 1975. ‘The digestive tract. Anatomy of fishes. Part 1’, Stuttgart:E. Schweizerbart'sche Verlagsbuchhandlung: 128–186.

Haug, A. and O. Smidsrod (1962). "Determination of Intrinsic Viscosity of Alginates." Acta Chemica Scandinavica 16(7): 1569-&.

Hoffman, A. S. (2012). "Hydrogels for biomedical applications." Advanced Drug Delivery Reviews 64: 18-23.

Hamidi, M., A. Azadi, and P. Rafiei. 2008. 'Hydrogel nanoparticles in drug delivery', Adv Drug Deliv Rev, 60: 1638-49.

Hartman, R. P. A., D. J. Brunner, D. M. A. Camelot, J. C. M. Marijnissen, and B. Scarlett. 1999. 'Electrohydrodynamic atomization in the cone-jet mode physical modeling of the liquid cone and jet', Journal of Aerosol Science, 30: 823-49.

Holling, T. M., E. Schooten, and P. J. van Den Elsen. 2004. 'Function and regulation of MHC class II molecules in T-lymphocytes: of mice and men', Hum Immunol, 65: 282-90.

Hordvik, I. 2015. 'Immunoglobulin isotypes in Atlantic salmon, Salmo salar', Biomolecules, 5: 166-77.

Haugland, O., A. B. Mikalsen, P. Nilsen, K. Lindmo, B. J. Thu, T. M. Eliassen, N. Roos, M. Rode, and O. Evensen. 2011. 'Cardiomyopathy syndrome of atlantic salmon (Salmo salar L.) is caused by a double-stranded RNA virus of the Totiviridae family', J Virol, 85: 5275-86.

Herath, T. K., J. E. Bron, K. D. Thompson, J. B. Taggart, A. Adams, J. H. Ireland, and R. H. Richards. 2012. 'Transcriptomic analysis of the host response to early stage salmonid alphavirus (SAV-1) infection in Atlantic salmon Salmo salar L', Fish Shellfish Immunol, 32: 796-807.

Holopainen, R., A. M. Eriksson-Kallio, and T. Gadd. 2017. 'Molecular characterisation of infectious pancreatic necrosis viruses isolated from farmed fish in Finland', Arch Virol, 162: 3459-71.

Hordvik, I. 2015. 'Immunoglobulin isotypes in Atlantic salmon, Salmo salar', Biomolecules, 5: 166-77.

Hori, S., T. Nomura, and S. Sakaguchi. 2003. 'Control of regulatory T cell development by the transcription factor Foxp3', Science, 299: 1057-61.

Horter, D., and J. B. Dressman. 2001. 'Influence of physicochemical properties on dissolution of drugs in the gastrointestinal tract', Advanced Drug Delivery Reviews, 46: 75-87.

Hu, W., and C. Pasare. 2013. 'Location, location, location: tissue-specific regulation of immune responses', J Leukoc Biol, 94: 409-21.

Irie, T., S. Watarai, T. Iwasaki, and H. Kodama. 2005. 'Protection against experimental Aeromonas salmonicida infection in carp by oral immunisation with bacterial antigen entrapped liposomes', Fish & Shellfish Immunology, 18: 235-42.

Irvine, S., S. Arumuganathar, J. R. McEwan, and S. N. Jayasinghe. 2007. 'Coaxial aerodynamically assisted bio-jets: A versatile paradigm for directly engineering living primary organisms', Engineering in Life Sciences, 7: 599-610.

Johansen, L. H., M. K. Dahle, O. Wessel, G. Timmerhaus, M. Lovoll, M. Rosaeg, S. M. Jorgensen, E. Rimstad, and A. Krasnov. 2016. 'Differences in gene expression in Atlantic salmon parr and smolt after challenge with Piscine orthoreovirus (PRV)', Mol Immunol, 73: 138-50.

Jensen, L. B., T. Wahli, C. McGurk, T. B. Eriksen, A. Obach, R. Waagbo, A. Handler and C. Tafalla (2015). "Effect of temperature and diet on wound healing in Atlantic salmon (Salmo salar L.)." Fish Physiol Biochem 41(6): 1527-1543.

Jeyanthi, R., R. C. Mehta, B. C. Thanoo and P. P. DeLuca (1997). "Effect of processing parameters on the properties of peptide-containing PLGA microspheres." J Microencapsul 14(2): 163-174.

Johnson, F. A., D. Q. Craig and A. D. Mercer (1997). "Characterization of the block structure and molecular weight of sodium alginates." J Pharm Pharmacol 49(7): 639-643.

Juarez. G. 2014. Immunological and technical considerations in application of alginate-based microencapsulation systems. Frontiers in bioengineering and biotechnology. Volume 2, Issue 26

Jain, S., W. T. Yap, and D. J. Irvine. 2005. 'Synthesis of protein-loaded hydrogel particles in an aqueous two-phase system for coincident antigen and CpG oligonucleotide delivery to antigen-presenting cells', Biomacromolecules, 6: 2590-600.

Jaworek, A. 2007. 'Electrospray droplet sources for thin film deposition', Journal of Materials Science, 42: 266-97.

Jaworek, A., and A. Krupa. 1999. 'Classification of the modes of EHD spraying', Journal of Aerosol Science, 30: 873-93.

Jayasinghe, S. N., and A. C. Sullivan. 2006. 'Electrohydrodynamic atomization: An approach to growing continuous self-supporting polymeric fibers', Journal of Physical Chemistry B, 110: 2522-28.

Jayasinghe, S. N., and N. Suter. 2006. 'Aerodynamically assisted jetting: a pressure driven approach for processing nanomaterials', Micro & Nano Letters, 1: 35-38.

Jayasinghe. S.N and Suter. N. 2006. ‘Aerodynamically assisted jetting: a pressure driven approach for processing nanaomaterials’. Micro and Nano letters. Vol1, Issue 1, pages 35 – 38

Joosten, P. H. M., E. Tiemersma, A. Threels, C. CaumartinDhieux, and J. H. W. M. Rombout. 1997. 'Oral vaccination of fish against Vibrio anguillarum using alginate microparticles', Fish & Shellfish Immunology, 7: 471-85.

Kapoor, B. G., H. Smit, and I. A. Verighina. 1975. 'Alimentary Canal and Digestion in Teleosts', Advances in Marine Biology, 13: 109-239.

Kendall, M. R., Bardin, D., Shih, R. et al. 2012. Scaled-up production of monodisperse, dual layer microbubbles using multi-array microfluidic module for medical imaging and drug delivery. Bubble Science, Engineering and technology, 4: 12 - 20

Kongtorp, R. T., A. Kjerstad, T. Taksdal, A. Guttvik, and K. Falk. 2004. 'Heart and skeletal muscle inflammation in Atlantic salmon, Salmo salar L: a new infectious disease', J Fish Dis, 27: 351-8.

Kreuter, J. 1996. 'Nanoparticles and microparticles for drug and vaccine delivery', J Anat, 189 (Pt 3): 503-5.

Kumari, J., J. Bogwald, and R. A. Dalmo. 2009. 'Transcription factor GATA-3 in Atlantic salmon (Salmo salar): molecular characterization, promoter activity and expression analysis', Mol Immunol, 46: 3099-107.

Kumari, J., Z. Zhang, T. Swain, H. Chi, C. Niu, J. Bogwald, and R. A. Dalmo. 2015. 'Transcription Factor T-Bet in Atlantic Salmon: Characterization and Gene Expression in Mucosal Tissues during Aeromonas Salmonicida Infection', Front Immunol, 6: 345.

Koji, D., Mamabu. Y., Chiaki, Y (1982). “Pharmacological studies of sodium alginate. IV. Erythrocyte aggregation by sodium alginate.” Yakugaku Zasshi 102: 573 – 578

Kikuchi, T., H. Yamada and M. Shimmei (1996). "Effect of high molecular weight hyaluronan on cartilage degeneration in a rabbit model of osteoarthritis." Osteoarthritis Cartilage 4(2): 99-110.

Kim, C. K. and E. J. Lee (1992). "The Controlled Release of Blue Dextran from Alginate Beads." International Journal of Pharmaceutics 79(1): 11-19.

King, K. (1994). "Changes in the Functional-Properties and Molecular-Weight of Sodium Alignate Following Gamma-Irradiation." Food Hydrocolloids 8(2): 83-96.

Krogdahl, A., A. Sundby and H. Holm (2015). "Characteristics of digestive processes in Atlantic salmon (Salmo salar). Enzyme pH optima, chyme pH, and enzyme activities." Aquaculture 449: 27-36.

Kytariolos, J., A. Dokoumetzidis and P. Macheras (2010). "Power law IVIVC: An application of fractional kinetics for drug release and absorption." European Journal of Pharmaceutical Sciences 41(2): 299-304.

Kim, K., X. Y. Liu, Y. Zhang, J. Cheng, X. Yu Wu, and Y. Sun. 2009. 'Elastic and viscoelastic characterization of microcapsules for drug delivery using a force-feedback MEMS microgripper', Biomedical Microdevices, 11: 421-27.

Kwok, A., S. Arumuganathar, S. Irvine, J. R. McEwan, and S. N. Jayasinghe. 2008. 'A hybrid bio-jetting approach for directly engineering living cells', Biomedical Materials, 3.

Klaric, G. 2015. ‘Oral delivery of protein antigens to atlantic salmon’. Thesis Doctor of Philosophy. UCL, Dept Mech Eng

Kim. K., Pack. D. 2006. ‘Microspheres for drug delivery’. BioMEMS and Biomedical Nanotechnology. 19 – 50

Kaklamani, G., D. Cheneler, L. M. Grover, M. J. Adams, and J. Bowen. 2014. 'Mechanical properties of alginate hydrogels manufactured using external gelation', Journal of the Mechanical Behavior of Biomedical Materials, 36: 135-42.

Kim, K., and Pack. D. 2006. ‘Microspheres for drug delivery’. BioMEMS and Biomedical nanotechnology. Springer: I

Liew, C. V., L. W. Chan, A. L. Ching, and P. W. S. Heng. 2006. 'Evaluation of sodium alginate as drug release modifier in matrix tablets', International Journal of Pharmaceutics, 309: 25-37.

Livak, K. J., and T. D. Schmittgen. 2001. 'Analysis of relative gene expression data using real-time quantitative PCR and the 2(-Delta Delta C(T)) Method', Methods, 25: 402-8.

Larsen, R., T. P. Rokenes, and B. Robertsen. 2004. 'Inhibition of infectious pancreatic necrosis virus replication by atlantic salmon Mx1 protein', J Virol, 78: 7938-44.

LeBlanc, F., J. R. Arseneau, S. Leadbeater, B. Glebe, M. Laflamme, and N. Gagne. 2012. 'Transcriptional response of Atlantic salmon (Salmo salar) after primary versus secondary exposure to infectious salmon anemia virus (ISAV)', Mol Immunol, 51: 197-209.

Li, M. O., and R. A. Flavell. 2008. 'TGF-beta: a master of all T cell trades', Cell, 134: 392-404.

Lighvani, A. A., D. M. Frucht, D. Jankovic, H. Yamane, J. Aliberti, B. D. Hissong, B. V. Nguyen, M. Gadina, A. Sher, W. E. Paul, and J. J. O'Shea. 2001. 'T-bet is rapidly induced by interferon-gamma in lymphoid and myeloid cells', Proc Natl Acad Sci U S A, 98: 15137-42.

Lim, F., and A. M. Sun. 1980. 'Microencapsulated islets as bioartificial endocrine pancreas', Science, 210: 908-10.

Lorenzen, N., and S. E. LaPatra. 2005. 'DNA vaccines for aquacultured fish', Rev Sci Tech, 24: 201-13.

Lowrie, D.B, and Whalen. R. 2000. ‘DNA vaccines – methods and protocols’. Methods in molecular medicine series: Humana Press 29

Liew, C. V., L. W. Chan, A. L. Ching and P. W. S. Heng (2006). "Evaluation of sodium alginate as drug release modifier in matrix tablets." International Journal of Pharmaceutics 309(1-2): 25-37.

Lindenbaum, J., M. H. Mellow, M. O. Blackstone and V. P. Butler, Jr. (1971). "Variation in biologic availability of digoxin from four preparations." N Engl J Med 285(24): 1344-1347.

Lee, H. Y., L. W. Chan, A. V. Dolzhenko and P. W. Heng (2006). "Influence of viscosity and uronic acid composition of alginates on the properties of alginate films and microspheres produced by emulsification." J Microencapsul 23(8): 912-927.

Lee, K. Y. and D. J. Mooney (2012). "Alginate: properties and biomedical applications." Prog Polym Sci 37(1): 106-126.

Lemoine, D., F. Wauters, S. Bouchend'homme and V. Preat (1998). "Preparation and characterization of alginate microspheres containing a model antigen." International Journal of Pharmaceutics 176(1): 9-19.

Larsen, R., T. P. Rokenes, and B. Robertsen. 2004. 'Inhibition of infectious pancreatic necrosis virus replication by atlantic salmon Mx1 protein', J Virol, 78: 7938-44.

Li, M. O., and R. A. Flavell. 2008. 'TGF-beta: a master of all T cell trades', Cell, 134: 392-404.

Motwani, S. K., S. Chopra, S. Talegaonkar, K. Kohli, F. J. Ahmad, and R. K. Khar. 2008. 'Chitosan-sodium alginate nanoparticles as submicroscopic reservoirs for ocular delivery: formulation, optimisation and in vitro characterisation', European Journal of Pharmaceutics and Biopharmaceutics, 68: 513-25.

Morch, Y. A., I. Donati, B. L. Strand, and G. Skjak-Braek. 2006. 'Effect of Ca2+, Ba2+, and Sr2+ on alginate microbeads', Biomacromolecules, 7: 1471-80.

Mody. N., Sharma. R. 2017. Chapter 14 – Microparticles for vaccine delivery. Micro and nanotechnology in vaccine development. Pages 259 – 278

Madsen, S. S., J. H. Olesen, K. Bedal, M. B. Engelund, Y. M. Velasco-Santamaria, and C. K. Tipsmark. 2011. 'Functional characterization of water transport and cellular localization of three aquaporin paralogs in the salmonid intestine', Frontiers in Physiology, 2.

Martinez-Sanz, M., A. Lopez-Rubio, and J. M. Lagaron. 2012. 'Optimization of the dispersion of unmodified bacterial cellulose nanowhiskers into polylactide via melt compounding to significantly enhance barrier and mechanical properties', Biomacromolecules, 13: 3887-99.

Munang'andu, H. M., B. N. Fredriksen, S. Mutoloki, B. Brudeseth, T. Y. Kuo, I. S. Marjara, R. A. Dalmo, and O. Evensen. 2012. 'Comparison of vaccine efficacy for different antigen delivery systems for infectious pancreatic necrosis virus vaccines in Atlantic salmon (Salmo salar L.) in a cohabitation challenge model', Vaccine, 30: 4007-16.

Munang'andu, H. M., B. N. Fredriksen, S. Mutoloki, R. A. Dalmo, and O. Evensen. 2013. 'Antigen dose and humoral immune response correspond with protection for inactivated infectious pancreatic necrosis virus vaccines in Atlantic salmon (Salmo salar L)', Vet Res, 44: 7.

Mutoloki, S., G. A. Cooper, I. S. Marjara, B. F. Koop, and O. Evensen. 2010. 'High gene expression of inflammatory markers and IL-17A correlates with severity of injection site reactions of Atlantic salmon vaccinated with oil-adjuvanted vaccines',

BMC Genomics, 11: 336.

Magnadottir, B. 1998. ‘Comparison of immunoglobulin (IgM) from four fish species’, Icel Agr Sci, 12: 47 – 59

Mandal, T. K., L. A. Bostanian, R. A. Graves, S. R. Chapman and T. U. Idodo (2001). "Porous biodegradable microparticles for delivery of pentamidine." European Journal of Pharmaceutics and Biopharmaceutics 52(1): 91-96.

Matsumoto, T. and K. Mashiko (1990). "Viscoelastic Properties of Alginate Aqueous-Solutions in the Presence of Salts." Biopolymers 29(14): 1707-1713.

Miller-Chou, B. A. and J. L. Koenig (2003). "A review of polymer dissolution." Progress in Polymer Science 28(8): 1223-1270.

Morch, Y. A., I. Donati, B. L. Strand and G. Skjak-Braek (2006). "Effect of Ca2+, Ba2+, and Sr2+ on alginate microbeads." Biomacromolecules 7(5): 1471-1480.

Murata, K., T. Inose, T. Hisano, S. Abe, Y. Yonemoto, T. Yamashita, M. Takagi, K. Sakaguchi, A. Kimura and T. Imanaka (1993). "Bacterial Alginate Lyase - Enzymology, Genetics and Application." Journal of Fermentation and Bioengineering 76(5): 427-437.

Maurice, S., A. Nussinovitch, N. Jaffe, O. Shoseyov, and A. Gertler. 2004. 'Oral immunization of Carassius auratus with modified recombinant A-layer proteins entrapped in alginate beads', Vaccine, 23: 450-59.

Moisan, J., R. Grenningloh, E. Bettelli, M. Oukka, and I. C. Ho. 2007. 'Ets-1 is a negative regulator of Th17 differentiation', J Exp Med, 204: 2825-35.

Morch, Y. A., I. Donati, B. L. Strand, and G. Skjak-Braek. 2006. 'Effect of Ca2+, Ba2+, and Sr2+ on alginate microbeads', Biomacromolecules, 7: 1471-80.

Munday, B. L., J. Kwang, and N. Moody. 2002. 'Betanodavirus infections of teleost fish: a review', Journal of Fish Diseases, 25: 127-42.

Munir, K., and F. S. B. Kibenge. 2004. 'Detection of infectious salmon anaemia virus by real-time RT-PCR', Journal of Virological Methods, 117: 37-47.

Murillo, M., C. Gamazo, M. M. Goni, J. M. Irache, and M. J. Blanco-Prieto. 2002. 'Development of microparticles prepared by spray-drying as a vaccine delivery system against brucellosis', International Journal of Pharmaceutics, 242: 341-44.

McGonigle. R.H. 1941. ‘Acute catarrhal enteritis of salmonid fingerlings. Trans Am Fish Soc, 70: 297

Nakanishi, T., and M. Ototake. 1997. 'Antigen uptake and immune responses after immersion vaccination', Dev Biol Stand, 90: 59-68.

Neutra, M. R., and P. A. Kozlowski. 2006. 'Mucosal vaccines: the promise and the challenge', Nat Rev Immunol, 6: 148-58.

Nguyen, D. N., C. Clasen, and G. Van den Mooter. 2016. 'Pharmaceutical Applications of Electrospraying', J Pharm Sci, 105: 2601-20.

Nidhi, M. Rashid, V. Kaur, S. S. Hallan, S. Sharma, and N. Mishra. 2016. 'Microparticles as controlled drug delivery carrier for the treatment of ulcerative colitis: A brief review', Saudi Pharm J, 24: 458-72.

Nelson, E. (1957). "Solution rate of theophylline salts and effects from oral administration." J Am Pharm Assoc Am Pharm Assoc 46(10): 607-614.

Nii, T. and F. Ishii (2005). "Encapsulation efficiency of water-soluble and insoluble drugs in liposomes prepared by the microencapsulation vesicle method." Int J Pharm 298(1): 198-205.

Oh, C. M., Q. Y. Guo, P. W. S. Heng, and L. W. Chan. 2014. 'Spray-congealed microparticles for drug delivery - an overview of factors influencing their production and characteristics', Expert Opinion on Drug Delivery, 11: 1047-60.

Olesen, N. J., and P. E. V. Jorgensen. 1986. 'Quantification of Serum Immunoglobulin in Rainbow-Trout Salmo-Gairdneri under Various Environmental-Conditions', Diseases of Aquatic Organisms, 1: 183-89.

Oyewumi, M. O., A. Kumar, and Z. R. Cui. 2010. 'Nano-microparticles as immune adjuvants: correlating particle sizes and the resultant immune responses', Expert Review of Vaccines, 9: 1095-107.

Peppas, N. A., J. Z. Hilt, A. Khademhosseini, and R. Langer. 2006. 'Hydrogels in biology and medicine: From molecular principles to bionanotechnology', Advanced Materials, 18: 1345-60.

Pakes, N. K., S. N. Jayasinghe, and R. S. Williams. 2011. 'Bio-electrospraying and aerodynamically assisted bio-jetting the model eukaryotic Dictyostelium discoideum: assessing stress and developmental competency post treatment', J R Soc Interface, 8: 1185-91.

Paleos. 2012. ‘Properties of chemically cross-linked hydrogels – Functional Biopolymers’. Springer series on polymer and composite materials. Chapter 5, 303

Prang, P., R. Muller, A. Eljaouhari, K. Heckmann, W. Kunz, T. Weber, C. Faber, M. Vroemen, U. Bogdahn, and N. Weidner. 2006. 'The promotion of oriented axonal regrowth in the injured spinal cord by alginate-based anisotropic capillary hydrogels', Biomaterials, 27: 3560-9.

Preis, I., and R. S. Langer. 1979. 'A single-step immunization by sustained antigen release', J Immunol Methods, 28: 193-7.

Pancholi, K., E. Stride, and M. Edirisinghe. 2008. 'Generation of microbubbles for diagnostic and therapeutic applications using a novel device', Journal of Drug Targeting, 16: 494-501.

Pepeljnjak, S., J. Filipovicgrcic and V. Jalsenjak (1994). "Alginate Microspheres of Microbial Spores and Viable Cells of Bacillus-Subtilis." Pharmazie 49(6): 436-437.

Parsonage, E. E., N. A. Peppas and P. I. Lee (1987). "Properties of Positive Resists .2. Dissolution Characteristics of Irradiated Poly(Methyl Methacrylate) and Poly(Methyl

Methacrylate-Co-Maleic Anhydride)." Journal of Vacuum Science & Technology B 5(2): 538-545.

Rustoen, T.L (2015). “Efficiency of chitosan and alginate compared with a chemical precipitating agent in treating drilling fluids produced from road construction – a laboratory experiment.” Norwegian University of life sciences. MSc thesis.

Rafati, H., A. G. A. Coombes, J. Adler, J. Holland and S. S. Davis (1997). "Protein-loaded poly(DL-lactide-co-glycolide) microparticles for oral administration: Formulation, structural and release characteristics." Journal of Controlled Release 43(1): 89-102.

Rajinikanth, P. S., C. Sankar and B. Mishra (2003). "Sodium alginate microspheres of metoprolol tartrate for intranasal systemic delivery: Development and evaluation." Drug Delivery 10(1): 21-28.

Rajeshkumar, S., C. Venkatesan, M. Sarathi, V. Sarathbabu, J. Thomas, K. A. Basha, and A. S. S. Hameed. 2009. 'Oral delivery of DNA construct using chitosan nanoparticles to protect the shrimp from white spot syndrome virus (WSSV)', Fish & Shellfish Immunology, 26: 429-37.

Ramos, E. A., J. L. Relucio, and C. A. Torres-Villanueva. 2005. 'Gene expression in tilapia following oral delivery of chitosan-encapsulated plasmid DNA incorporated into fish feeds', Mar Biotechnol (NY), 7: 89-94.

Rice-Ficht, A. C., A. M. Arenas-Gamboa, M. M. Kahl-McDonagh, and T. A. Ficht. 2010. 'Polymeric particles in vaccine delivery', Curr Opin Microbiol, 13: 106-12.

Ronen, A., A. Perelberg, J. Abramowitz, M. Hutoran, S. Tinman, I. Bejerano, M. Steinitz, and M. Kotler. 2003. 'Efficient vaccine against the virus causing a lethal disease in cultured Cyprinus carpio', Vaccine, 21: 4677-84.

Rijcken. C.J.F, and Holthuis. J. J. M. 2016. ‘Vaccination composition’. US Application: US20160030348A1

Ruma (Responsible use of medicines in agriculture alliance) Guidelines. 2006. [cited 2017 04/09/2017]; Responsible use of vaccines and vaccination in fish production. Available from: http://www.ruma.org.uk/wp-content/uploads/2014/09/fish-vaccine-long.pdf

Sankalia, M. G., R. C. Mashru, J. M. Sankalia and V. B. Sutariya (2005). "Papain entrapment in alginate beads for stability improvement and site-specific delivery: physicochemical characterization and factorial optimization using neural network modeling." AAPS PharmSciTech 6(2): E209-222.

Schliecker, G., C. Schmidt, S. Fuchs, R. Wombacher and T. Kissel (2003). "Hydrolytic degradation of poly(lactide-co-glycolide) films: effect of oligomers on degradation rate and crystallinity." Int J Pharm 266(1-2): 39-49.

Siewert, M., J. Dressman, C. K. Brown, V. P. Shah, Fip and Aaps (2003). "FIP/AAPS guidelines to dissolution/in vitro release testing of novel/special dosage forms." AAPS PharmSciTech 4(1): E7.

Smidsrod, O. (1970). "Solution Properties of Alginate." Carbohydrate Research 13(3): 359-&.

Smidsrod, O. (1973). "Relative Extension of Alginates Having Different Chemical Composition." Carbohydrate Research 27(1): 107-118.

Smidsrod, O. and A. Haug (1968). "Dependence Upon Uronic Acid Composition of Some Ion-Exchange Properties of Alginates." Acta Chemica Scandinavica 22(6): 1989-&.

Stevenson, C. L., J. T. Santini, Jr. and R. Langer (2012). "Reservoir-based drug delivery systems utilizing microtechnology." Adv Drug Deliv Rev 64(14): 1590-1602.

Szalai, A. J., J. E. Bly and L. W. Clem (1992). "Chelation affects the conformation, lability and aggregation of channel catfish (Ictalurus punctatus) phosphorylcholine-reactive protein (PRP)." Comp Biochem Physiol B 102(3): 545-550.

Smrdel, P., M. Bogataj, A. Zega, O. Planinsek, and A. Mrhar. 2008. 'Shape optimization and characterization of polysaccharide beads prepared by ionotropic gelation', Journal of Microencapsulation, 25: 90-105.

Stabler, C., K. Wilks, A. Sambanis, and I. Constantinidis. 2001. 'The effects of alginate composition on encapsulated beta TC3 cells', Biomaterials, 22: 1301-10.

Stokke, B. T., O. Smidsrod, P. Bruheim, and G. Skjakbraek. 1991. 'Distribution of Uronate Residues in Alginate Chains in Relation to Alginate Gelling Properties', Macromolecules, 24: 4637-45.

Sequeida, A., K. Maisey, and M. Imarai. 2017. 'Interleukin 4/13 receptors: An overview of genes, expression and functional role in teleost fish', Cytokine & Growth Factor Reviews, 38: 66-72.

Skjesol, A., T. Hansen, C. Y. Shi, H. L. Thim, and J. B. Jorgensen. 2010. 'Structural and functional studies of STAT1 from Atlantic salmon (Salmo salar)', BMC Immunol, 11: 17.

Skugor, S., K. A. Glover, F. Nilsen, and A. Krasnov. 2008. 'Local and systemic gene expression responses of Atlantic salmon (Salmo salar L.) to infection with the salmon louse (Lepeophtheirus salmonis)', BMC Genomics, 9: 498.

Sobhkhez, M., A. Skjesol, E. Thomassen, L. G. Tollersrud, D. B. Iliev, B. Sun, B. Robertsen, and J. B. Jorgensen. 2014. 'Structural and functional characterization of salmon STAT1, STAT2 and IRF9 homologs sheds light on interferon signaling in teleosts', Febs Open Bio, 4: 858-71.

Smidsrod, O. 1973. 'Relative Extension of Alginates Having Different Chemical Composition', Carbohydrate Research, 27: 107-18.

Stabentheiner, E., A. Zankel, and P. Polt. 2010. 'Environmental scanning electron microscopy (ESEM)-a versatile tool in studying plants', Protoplasma, 246: 89-99.

Savale, S. K. 2016. 'Formulation and evaluation of Aceclofenac sustained released tablet', World Journal of Pharmacy and Pharmaceutical Sciences, 5: 1394 – 1405

Saha, K., S. T. Kim, B. Yan, O. R. Miranda, F. S. Alfonso, D. Shlosman, and V. M. Rotello. 2013. 'Surface Functionality of Nanoparticles Determines Cellular Uptake Mechanisms in Mammalian Cells', Small, 9: 300-05.

Sahlmann, C., J. Gu, T. M. Kortner, I. Lein, A. Krogdahl, and A. M. Bakke. 2015. 'Ontogeny of the Digestive System of Atlantic Salmon (Salmo salar L.) and Effects of Soybean Meal from Start-Feeding', Plos One, 10.

Scheerlinck, J. P., and D. L. Greenwood. 2008. 'Virus-sized vaccine delivery systems', Drug Discov Today, 13: 882-7.

Shang, L., K. Nienhaus, and G. U. Nienhaus. 2014. 'Engineered nanoparticles interacting with cells: size matters', Journal of Nanobiotechnology, 12.

Shen, F., and S. L. Gaffen. 2008. 'Structure-function relationships in the IL-17 receptor: implications for signal transduction and therapy', Cytokine, 41: 92-104.

Sinha, V. R., K. Bansal, R. Kaushik, R. Kumria, and A. Trehan. 2004. 'Poly-epsilon-caprolactone microspheres and nanospheres: an overview', International Journal of Pharmaceutics, 278: 1-23.

Skugor, S., K. A. Glover, F. Nilsen, and A. Krasnov. 2008. 'Local and systemic gene expression responses of Atlantic salmon (Salmo salar L.) to infection with the salmon louse (Lepeophtheirus salmonis)', BMC Genomics, 9: 498.

Snieszko, S. F. 1975. 'History and present status of fish diseases', J Wildl Dis, 11: 446-59.

Sommerset, I., B. Krossoy, E. Biering, and P. Frost. 2005. 'Vaccines for fish in aquaculture', Expert Review of Vaccines, 4: 89-101.

Song, H., N. Santi, O. Evensen, and V. N. Vakharia. 2005. 'Molecular determinants of infectious pancreatic necrosis virus virulence and cell culture adaptation', J Virol, 79: 10289-99.

Sonmez, M., B. Sonmez, N. Eren, M. Yilmaz, S. S. Karti, and E. Ovali. 2004. 'Effects of interferon-alpha-2a on Th3 cytokine response in multiple myeloma patients', Tumori, 90: 387-9.

Storni, T., T. M. Kundig, G. Senti, and P. Johansen. 2005. 'Immunity in response to particulate antigen-delivery systems', Adv Drug Deliv Rev, 57: 333-55.

Strober, W., and R. L. Coffman. 1997. 'Tolerance and immunity in the mucosal immune system. Introduction', Res Immunol, 148: 489-599.

Sun, B., I. Skjaeveland, T. Svingerud, J. Zou, J. Jorgensen, and B. Robertsen. 2011. 'Antiviral activity of salmonid gamma interferon against infectious pancreatic necrosis

virus and salmonid alphavirus and its dependency on type I interferon', J Virol, 85: 9188-98.

Tadiso, T. M., K. K. Lie, and I. Hordvik. 2011. 'Molecular cloning of IgT from Atlantic salmon, and analysis of the relative expression of tau, mu, and delta in different tissues', Vet Immunol Immunopathol, 139: 17-26.

Taghavian, O. 2013. Expression and characterisation of infectious Bursal disease virus protein for poultry vaccine development and application in nanotechnology. PhD Thesis.

Takizawa, F., E. O. Koppang, M. Ohtani, T. Nakanishi, K. Hashimoto, U. Fischer, and J. M. Dijkstra. 2011. 'Constitutive high expression of interleukin-4/13A and GATA-3 in gill and skin of salmonid fishes suggests that these tissues form Th2-skewed immune environments', Mol Immunol, 48: 1360-8.

Taksdal, T., A. B. Olsen, I. Bjerkas, M. J. Hjortaas, B. H. Dannevig, D. A. Graham, and M. F. McLoughlin. 2007. 'Pancreas disease in farmed Atlantic salmon, Salmo salar L., and rainbow trout, Oncorhynchus mykiss (Walbaum), in Norway', J Fish Dis, 30: 545-58.

Thinh, N. H., T. Y. Kuo, L. T. Hung, T. H. Loc, S. C. Chen, O. Evensen, and H. J. Schuurman. 2009. 'Combined immersion and oral vaccination of Vietnamese catfish (Pangasianodon hypophthalmus) confers protection against mortality caused by Edwardsiella ictaluri', Fish Shellfish Immunol, 27: 773-6.

Tobar, J. A., S. Jerez, M. Caruffo, C. Bravo, F. Contreras, S. A. Bucarey, and M. Harel. 2011. 'Oral vaccination of Atlantic salmon (Salmo salar) against salmonid rickettsial septicaemia', Vaccine, 29: 2336-40.

Torres-Giner, S., A. Martinez-Abad, M. J. Ocio, and J. M. Lagaron. 2010. 'Stabilization of a nutraceutical omega-3 fatty acid by encapsulation in ultrathin electrosprayed zein prolamine', J Food Sci, 75: N69-79.

Thanos, C. G., B. E. Bintz, and D. F. Emerich. 2007. 'Stability of alginate-polyornithine microcapsules is profoundly dependent on the site of transplantation', Journal of Biomedical Materials Research Part A, 81a: 1-11.

Titgemeyer, E. C., C. K. Armendariz, D. J. Bindel, R. H. Greenwood, and C. A. Loest. 2001. 'Evaluation of titanium dioxide as a digestibility marker for cattle', Journal of Animal Science, 79: 1059-63.

Takka, S., O. H. Ocak and F. Acarturk (1998). "Formulation and investigation of nicardipine HCl-alginate gel beads with factorial design-based studies." Eur J Pharm Sci 6(3): 241-246.

Tapia, C., V. Ormazabal, E. Costa and M. Yazdani-Pedram (2007). "Study of dissolution behavior of matrices tablets based on alginate-gelatin mixtures as prolonged diltiazem hydrochloride release systems." Drug Development and Industrial Pharmacy 33(6): 585-593.

Thu, B., P. Bruheim, T. Espevik, O. Smidsrod, P. SoonShiong and G. SkjakBraek (1996). "Alginate polycation microcapsules .2. Some functional properties." Biomaterials 17(11): 1069-1079.

Technical Brief. (2010). “In vitro dissolution testing for solid oral dosage forms.” Particles sciences 5

Tonnesen, H. H. and J. Karlsen (2002). "Alginate in drug delivery systems." Drug Dev Ind Pharm 28(6): 621-630.

Trivedi, N., M. Keegan, G. M. Steil, J. Hollister-Lock, W. M. Hasenkamp, C. K. Colton, S. Bonner-Weir, and G. C. Weir. 2001. 'Islets in alginate macrobeads reverse diabetes despite minimal acute insulin secretory responses', Transplantation, 71: 203-11.

Tadiso, T. M., K. K. Lie, and I. Hordvik. 2011. 'Molecular cloning of IgT from Atlantic salmon, and analysis of the relative expression of tau, mu, and delta in different tissues', Vet Immunol Immunopathol, 139: 17-26.

Ueberreiter, K. 1968. The Solution Process. In Diffusion in Polymers. Eds.; Academic Press: New York, 1968

Usher, M. L., C. Talbot and F. B. Eddy (1990). "Effects of Transfer to Seawater on Digestion and Gut Function in Atlantic Salmon Smolts (Salmo-Salar L)." Aquaculture 90(1): 85-96.

Utreja, P., S. Jain and A. K. Tiwary (2010). "Novel drug delivery systems for sustained and targeted delivery of anti- cancer drugs: current status and future prospects." Curr Drug Deliv 7(2): 152-161.

USDA (National Agricultural Statistics Service). 2014. ‘Vaccines for aquaculture’. Available from: https://www.ams.usda.gov/sites/default/files/media/Vaccines%20%28Biologics%29%20report.pdf

Vaithilingam, V., G. Kollarikova, M. R. G. Qi, I. Lacik, J. Oberholzer, G. J. Guillemin, and B. E. Tuch. 2011. 'Effect of prolonged gelling time on the intrinsic properties of barium alginate microcapsules and its biocompatibility', Journal of Microencapsulation, 28: 499-507.

Venkatesan, J., I. Bhatnagar, P. Manivasagan, K. H. Kang, and S. K. Kim. 2015. 'Alginate composites for bone tissue engineering: a review', Int J Biol Macromol, 72: 269-81.

Verhelst, J., P. Hulpiau, and X. Saelens. 2013. 'Mx proteins: antiviral gatekeepers that restrain the uninvited', Microbiol Mol Biol Rev, 77: 551-66.

Valo, H., L. Peltonen, S. Vehvilainen, M. Karjalainen, R. Kostiainen, T. Laaksonen, and J. Hirvonen. 2009. 'Electrospray Encapsulation of Hydrophilic and Hydrophobic Drugs in Poly(L-lactic acid) Nanoparticles', Small, 5: 1791-98.

Wang, T., and M. Husain. 2014. 'The expanding repertoire of the IL-12 cytokine family in teleost fish: Identification of three paralogues each of the p35 and p40 genes in salmonids, and comparative analysis of their expression and modulation in Atlantic salmon Salmo salar', Dev Comp Immunol, 46: 194-207.

Wang, Y. S., M. K. Tan, D. B. Go, and H. C. Chang. 2012. 'Electrospray cone-jet breakup and droplet production for electrolyte solutions', Epl, 99.

Ward, M. A., and T. K. Georgiou. 2011. 'Thermoresponsive Polymers for Biomedical Applications', Polymers, 3: 1215-42.

Weaver, C. T., L. E. Harrington, P. R. Mangan, M. Gavrieli, and K. M. Murphy. 2006. 'Th17: an effector CD4 T cell lineage with regulatory T cell ties', Immunity, 24: 677-88.

Weiner, H. L., A. P. da Cunha, F. Quintana, and H. Wu. 2011. 'Oral tolerance', Immunol Rev, 241: 241-59.

Whitmire, J. K. 2014. 'Editorial: Not all roads to T cell memory go through STAT4 and T-bet', Journal of Leukocyte Biology, 95: 699-701.

Williams, L. M., and A. Y. Rudensky. 2007. 'Maintenance of the Foxp3-dependent developmental program in mature regulatory T cells requires continued expression of Foxp3', Nat Immunol, 8: 277-84.

Wolf, K., S. F. Snieszko, C. E. Dunbar, and E. Pyle. 1960. 'Virus Nature of Infectious Pancreatic Necrosis in Trout', Proceedings of the Society for Experimental Biology and Medicine, 104: 105-08.

Workenhe, S. T., M. L. Rise, M. J. T. Kibenge, and F. S. B. Kibenge. 2010. 'The fight between the teleost fish immune response and aquatic viruses', Molecular Immunology, 47: 2525-36.

Xiao, Y. H., and S. N. Isaacs. 2012. 'Enzyme-linked immunosorbent assay (ELISA) and blocking with bovine serum albumin (BSA)-not all BSAs are alike', Journal of Immunological Methods, 384: 148-51.

Xie, J. W., J. C. M. Marijnissen, and C. H. Wang. 2006. 'Microparticles developed by electrohyd ro dynamic atomization for the local delivery of anticancer drug to treat C6 glioma in vitro', Biomaterials, 27: 3321-32.

Xie, J. W., and C. H. Wang. 2007. 'Encapsulation of proteins in biodegradable polymeric microparticles using electrospray in the Taylor Cone-Jet mode', Biotechnology and Bioengineering, 97: 1278-90.

Wee, S., and W. R. Gombotz. 1998. 'Protein release from alginate matrices', Adv Drug Deliv Rev, 31: 267-85.

Weaver, C. T., R. D. Hatton, P. R. Mangan, and L. E. Harrington. 2007. 'IL-17 family cytokines and the expanding diversity of effector T cell lineages', Annu Rev Immunol, 25: 821-52.

Wu, Y. Q., S. J. Kennedy, and R. L. Clark. 2009. 'Polymeric Particle Formation Through Electrospraying at Low Atmospheric Pressure', Journal of Biomedical Materials Research Part B-Applied Biomaterials, 90b: 381-87.

Xiang, S. D., A. Scholzen, G. Minigo, C. David, V. Apostolopoulos, P. L. Mottram, and M. Plebanski. 2006. 'Pathogen recognition and development of particulate vaccines: Does size matter?', Methods, 40: 1-9.

Yadav, A. V., and H. H. Mote. 2008. 'Development of Biodegradable Starch Microspheres for Intranasal Delivery', Indian Journal of Pharmaceutical Sciences, 70: 170-74.

Yannas IV. 2004. ‘Classes of materials used in medicine: natural materials’. Biomaterials Sci – an introduction to materials in medicine. Elsevier academic press

Yang, Y. Y., T. S. Chung, X. L. Bai, and W. K. Chan. 2000. 'Effect of preparation conditions on morphology and release profiles of biodegradable polymeric microspheres containing protein fabricated by double-emulsion method', Chemical Engineering Science, 55: 2223-36.

Yurteri, C. U., R. P. A. Hartman, and J. C. M. Marijnissen. 2010. 'Producing Pharmaceutical Particles via Electrospraying with an Emphasis on Nano and Nano Structured Particles - A Review', Kona Powder and Particle Journal: 91-115.

Yazawa, R., G. A. Cooper, M. Beetz-Sargent, A. Robb, L. McKinnel, W. S. Davidson, and B. F. Koop. 2008. 'Functional adaptive diversity of the Atlantic salmon T-cell receptor gamma locus', Mol Immunol, 45: 2150-7.

Yeo, Y. and K. Park (2004). "Control of encapsulation efficiency and initial burst in polymeric microparticle systems." Arch Pharm Res 27(1): 1-12.

Zhang, J. H., C. R. Daubert and E. A. Foegeding (2007). "A proposed strain-hardening mechanism for alginate gels." Journal of Food Engineering 80(1): 157-165.

Zeleny, J. 1914. 'The electrical discharge from liquid points, and a hydrostatic method of measuring the electric intensity at their surfaces.', Physical Review, 3: 69-91.

Zhang, M., K. Sun, and L. Sun. 2008. 'Regulation of autoinducer 2 production and luxS expression in a pathogenic Edwardsiella tarda strain', Microbiology, 154: 2060-9.

Zhang, S., J. Ermann, M. D. Succi, A. Zhou, M. J. Hamilton, B. Cao, J. R. Korzenik, J. N. Glickman, P. K. Vemula, L. H. Glimcher, G. Traverso, R. Langer, and J. M. Karp. 2015. 'An inflammation-targeting hydrogel for local drug delivery in inflammatory bowel disease', Sci Transl Med, 7: 300ra128.

Zhang, Z., H. Chi, C. Niu, J. Bogwald, and R. A. Dalmo. 2011. 'Molecular cloning and characterization of Foxp3 in Atlantic salmon (Salmo salar)', Fish Shellfish Immunol, 30: 902-9.

Zargham, S., S. Bazgir, A. Tavakoli, A. S. Rashidi, and R. Damerchely. 2012. 'The Effect of Flow Rate on Morphology and Deposition Area of Electrospun Nylon 6 Nanofiber', Journal of Engineered Fibers and Fabrics, 7: 42-49.

Zhang, J. H., C. R. Daubert, and E. A. Foegeding. 2007. 'A proposed strain-hardening mechanism for alginate gels', Journal of Food Engineering, 80: 157-65.

Zhu, J., and W. E. Paul. 2008. 'CD4 T cells: fates, functions, and faults', Blood, 112:

1557-6

Appendices

	Manugel GMB		Manugel GHB		Manugel DMB	
Time (min)	% BD release	SD	% BD release	SD	% BD release	SD
5	13.82	4.04	27.36	6.67	12.16	2.67
10	23.03	5.05	39.52	8.67	12.16	2.67
15	32.24	7.07	45.6	10	21.28	4.67
20	32.24	7.07	54.72	12	30.40	6.67
25	50.67	11.11	54.72	12	39.52	8.67
30	50.67	11.11	66.88	14.67	48.64	10.67
35	50.67	11.11	72.96	16	54.72	12
40	55.27	12.12	85.12	18.67	63.84	14
45	55.27	12.12	85.12	18.67	63.84	14
50	82.91	18.18	94.24	20.67	66.88	14.67
55	82.91	18.18	94.24	20.67	66.88	14.67

	Scogin MV		Scogin LDH	
Time (min)	% BD release	SD	% BD release	SD
5	31.81	6.98	42.42	10.85
10	42.42	9.30	49.49	10.85
15	56.56	12.40	49.49	10.85
20	74.23	16.28	70.70	15.50
25	84.85	18.60	70.70	15.50
30	84.85	18.60	81.30	17.83
35	95.44	20.93	81.30	17.83
40	98.98	21.71	98.98	21.71
45	98.98	21.71	98.98	21.71
50	99.18	21.75	98.98	21.71
55	99.18	21.75	98.98	24.03

Appendix 1: *Average percentage BD release (mean) and standard deviation (SD) of all five different alginate types at 11 ºC, following USP test method 1 at 100 rpm agitation rate*

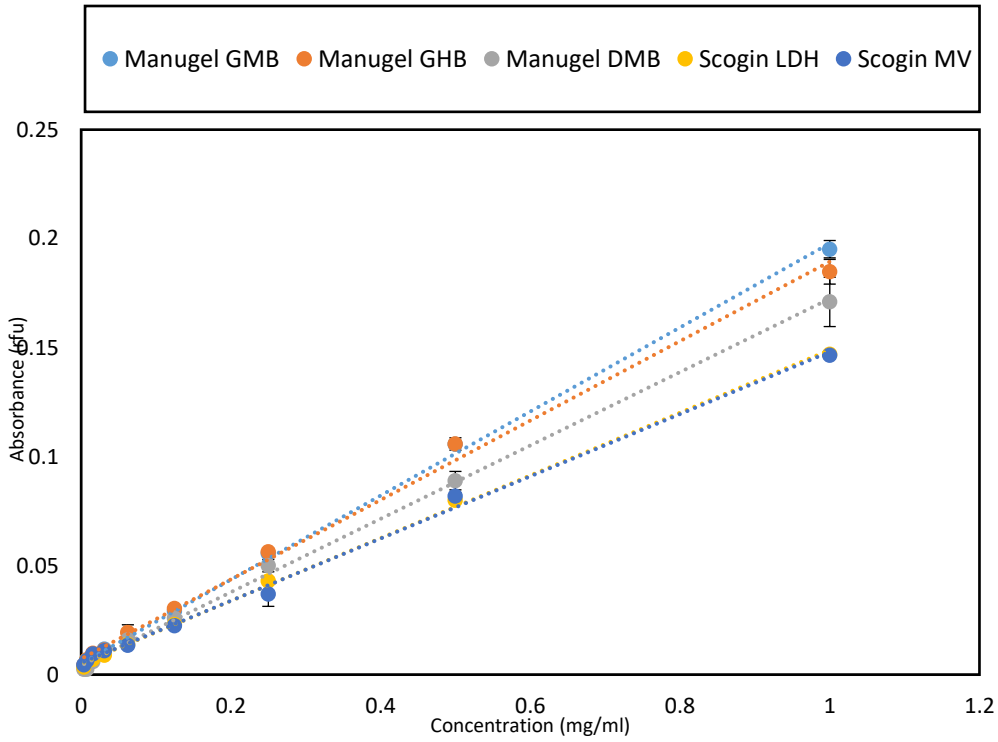

Alginate type	Calibration curve	R^2
Scogin MV	y = 0.1427x + 0.0053	0.997
Scogin LDH	y = 0.1438x + 0.0051	0.9988
Manugel DMB	y = 0.1683x + 0.0042	0.9986
Manugel GHB	y = 0.1822x + 0.0073	0.9963
Manugel GMB	y = 0.1928x + 0.005	0.9988

Appendix 2: *Standard calibration curves along with equation and R^2 values for the five types of alginates used, during the encapsulation efficiency test*

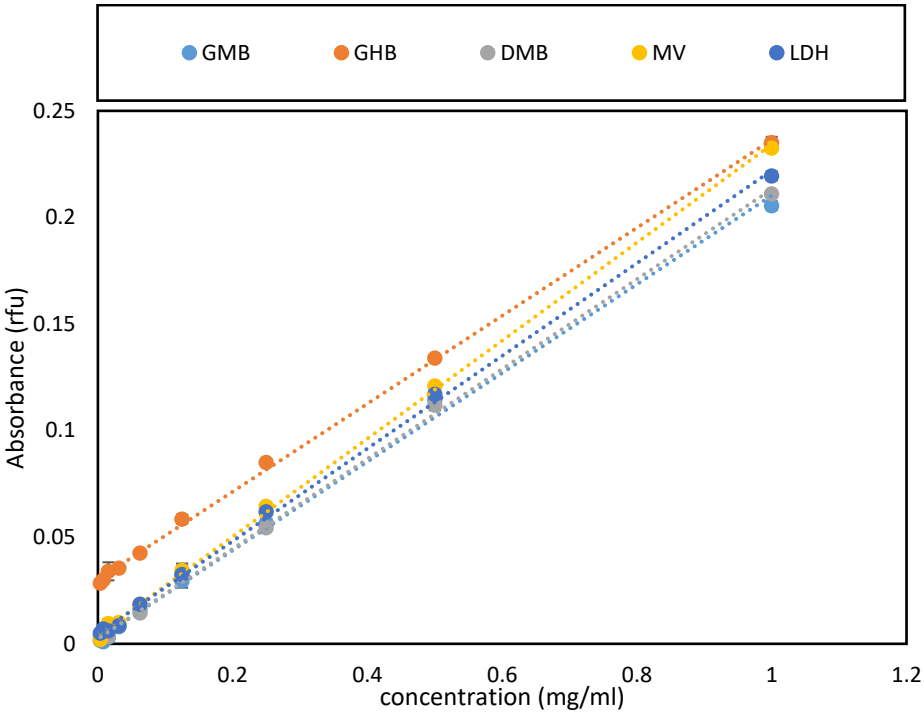

Alginate type	Calibration curve	R^2
Scogin MV	y = 0.208x + 0.0022	0.997
Scogin LDH	y = 0.2063x + 0.0301	0.9992
Manugel DMB	y = 0.2108x + 0.0024	0.9999
Manugel GHB	y = 0.2299x + 0.0043	0.9993
Manugel GMB	y = 0.2174x + 0.0047	0.999

Appendix 3: *Standard calibration curves along with equation and R^2 values for the five types of alginates used, during the dissolution test*